DEVELOPMENT AND VERIFICATION OF SEISMIC CAPACITY AND DUCTILITY DEMAND ESTIMATION PROCEDURES FOR COUPLED CORE WALL SYSTEMS

by

Eren Vuran

B.S., Civil Engineering, Istanbul Technical University, 2006

M. Sc., Earthquake Engineering, Universita degli Studi di Pavia, University of Patras, 2007

Submitted to the Kandilli Observatory and
Earthquake Research Institute in partial fulfillment of
the requirements for the degree of
Doctor of Philosophy

Graduate Program in Earthquake Engineering
Boğaziçi University
2014

DEVELOPMENT AND VERIFICATION OF SEISMIC CAPACITY AND DUCTILITY DEMAND ESTIMATION PROCEDURES FOR COUPLED CORE WALL SYSTEMS

APPROVED BY:

Prof. Dr. Erdal ŞAFAK ……
(Thesis Supervisor)

Prof. Dr. Mehmet Nuray AYDINOĞLU ……
(Thesis Co-supervisor)

Prof. Dr. Eser ÇAKTI ……

Assoc. Prof. Dr. Kutay ORAKÇAL ……

Prof. Dr. Konuralp GİRGİN ……
(ITU, Faculty of Civil Engineering)

Assoc. Prof. Dr. Ercan YÜKSEL ……
(ITU, Faculty of Civil Engineering)

DATE OF APPROVAL: ……

ACKNOWLEDGEMENTS

I would like to express my deepest gratitude to Prof. M. Nuray Aydınoğlu for his continual guidance and support during my study. From our initial meeting until the final sentence of this thesis was written, he continuously displayed great enthusiasm and patience that made this study possible. His teaching was not limited to technical guidance on this research. The moments that we shared talking about history, music, science and most importantly his life experiences are of as much value to me as the time that we spent discussing earthquake engineering. It was an absolute honor to work with him, and for the rest of my life, I will feel lucky to have had this experience.

I also would like to express my sincere appreciation to Prof. Mustafa Erdik and Prof. Erdal Şafak for their support and encouragement during my graduate program. My thanks also go to Dr. Şeref Polat and Assoc. Prof. Kutay Orakçal for their guidance throughout this study.

I am sincerely thankful to my dear wife, Mum and Dad for their continuous support and patience. I could not have completed this study without the endless strength they provided me.

Finally, many thanks to my beloved son, Ediz Zeki Vuran, for being the most recent motivation to complete this study. I hope that he will always appreciate me for my decisions and achievements.

ABSTRACT

Performance-based seismic design of tall buildings is of great importance as demands are increasing for incorporating structural safety in such challenging structures. Although a number of design guidelines and consensus documents have been published in the last few years regarding performance-based seismic design of tall buildings, there are still several issues need to be resolved.

Coupled core wall systems composed of flanged (U, T, E or I shaped) walls coupled by *coupling beams*, represent the most commonly used structural system in tall buildings. Although experimental and analytical research is available regarding the behavior of coupled wall systems with rectangular walls, such systems are not representative of the current design practice. Efforts are necessary not only for a clear understanding of the behavior of coupled core walls both at the component and system levels, but at the same time for the implementation of research results into performance-based seismic design methodologies.

In this study, capacity and ductility demand estimation procedures are developed for preliminary seismic design of coupled core wall systems. These procedures may be considered complementary to *capacity design principles* to be implemented during the preliminary design stage. Effective design parameters controlling the behavior of coupled core wall systems and relative importance of each design parameter are identified through verification studies of the proposed capacity and ductility demand estimation procedures as well as nonlinear response history analyses.

ÖZET

Yüksek binaların deprem etkisi altında performansa dayalı tasarımı yapısal güvenliğin sağlanması açısından oldukça önemlidir. Her ne kadar yüksek binaların deprem etkisi altında performansa dayalı tasarımıyla ilgili birkaç tasarım klavuzu ve uzlaşı raporu yayınlanmış olsa da, hala çözülmesi gereken pek çok konu vardır.

Bağ kirişleri ile birbirine bağlanan başlıklı (U, T, E veya I şeklinde) taşıyıcı duvarlardan (perdelerden) oluşan *bağ kirişli çekirdek perde sistemleri* yüksek binalarda en sık kullanılan taşıyıcı sistemdir. Dikdörtgen perdelerden oluşan bağ kirişli perde sistemleri üzerine çok sayıda deneysel ve analitik araştırma olsa da, bu sistemler mevcut yüksek bina tasarım uygulamalarını temsil etmemektedirler. Sadece bağ kirişli çekirdek perde sistemlerinin hem eleman hem de sistem düzeyinde davranışını anlamak değil, aynı zamanda bunun sonuçlarını performansa dayalı tasarım yöntemlerine de uyarlamak gerekir.

Bu çalışmada, bağ kirişli çekirdek perde sistemleri için kapasite ve süneklik istemi tahmin yöntemleri geliştirilmiştir. Bu yöntemler *kapasite tasarımı ilkelerinin* ön tasarım aşamasında uygulanmasını tamamlayıcı niteliktedir. Bağ kirişli çekirdek perde sistemlerinin davranışında etkin tasarım parametreleri ve bu parametrelerin göreli etkinlikleri, önerilen kapasite ve süneklik istemi tahmin yöntemleri ve zaman tanım alanında doğrusal olmayan analizlerle belirlenmiştir.

TABLE OF CONTENTS

LIST OF FIGURES

LIST OF TABLES

1. INTRODUCTION

Tall building seismic design has evolved during the last decade to become a major area of application of performance-based earthquake engineering. This development has opened a new door to structural design engineers who were struggling to overcome the structural restrictions imposed on tall buildings by traditional prescriptive seismic design codes. In a broader sense, performance-based earthquake engineering has brought new dimensions to tall building design, leading to a major transformation from the linear strength-based design to a nonlinear deformation-based design practice. In line with this development, special seismic design recommendations/guidelines and consensus documents for tall buildings based on performance-based design principles have been developed and published in the last decade by several institutions. In this respect, over the last decade Los Angeles Tall Buildings Structural Design Council – LATBSDC [8] has published and continuously updated a series of *consensus documents* (2005, 2008, 2011, 2013, 2014), reflecting the progress achieved in the state of practice of performance-based seismic design of tall buildings. In 2007 Structural Engineers Association of Northern California – SEAONC Tall Buildings Task Group [9] published its first recommendations on tall building seismic design, which is adopted in 2008 and later updated by San Francisco Department of Building Inspection – SFDBI [12]. On the other hand Council on Tall Buildings and Urban Habitat – CTBUH published in 2008 its design recommendations prepared by Seismic Working Group [7]. As a parallel development, a draft version of a tall building design code was prepared in 2008 for the Istanbul Metropolitan Municipality by the Kandilli Observatory and Earthquake Research Institute [13, 14] at the time when tall building construction started booming in Istanbul. In the meantime Pacific Earthquake Engineering Research Center (PEER) conducted a multi-year collaborative effort, called Tall Buildings Initiative (TBI), to develop more comprehensive performance-based seismic design guidelines for tall buildings [10] along with a supporting document on modeling and acceptance criteria for nonlinear response [11].

Current tall building seismic design guidelines / consensus documents [8, 10, 12] are all based on the same design methodology, starting with a preliminary design followed by two *performance evaluation* stages. In the preliminary design, tall building structural

system is preliminarily proportioned and reinforced on the basis of linear analyses and *capacity design principles*. San Francisco practice [12] treats the preliminary design as a *code-level evaluation* stage where selected *prescriptive* provisions including minimum base-shear requirement of the San Francisco Building Code are applied while a number of exceptions are allowed such removal of force amplification (over-strength) and reliability/redundancy factors, etc. Thus, SFDBI [12] effectively applies a three-stage procedure, while other guidelines [8, 10] insist on a *non-prescriptive* two-stage scheme by completely eliminating the prescriptive code provisions.

The two-stage *performance evaluation* procedure following the preliminary design includes a *serviceability evaluation* stage under the so-called *service earthquake* and a *collapse level evaluation* stage under the so-called *maximum credible earthquake*, corresponding to 43 and 2475 year return periods, respectively. The *serviceability evaluation* stage requires the tall building structural system remains essentially elastic (or nearly elastic with almost negligible nonlinear behavior) under frequently occurring small earthquakes. The *collapse level evaluation* considers the worst-case scenario, where the structure is evaluated under the *maximum credible earthquake* with a performance objective aiming at a *reasonably low risk of partial or total collapse*, which corresponds to an acceptable level of damage in terms of ductile response quantities while at the same time all other brittle response quantities, e.g., internal forces are kept below their strength capacities, thus preserving the gravity load carrying capacity of the structural system.

Preliminary design represents the critical phase of the tall building design where all structural elements need to be preliminarily proportioned and reinforced for the subsequent performance evaluation stages. Here the problem lies with the fact that designer has no reliable analysis tools at this phase other than linear response analysis and application of capacity design principles, which in fact may not provide any guarantee for an acceptable nonlinear response under the maximum credible earthquake. It means that the preliminary design may need to be revised according to the results of the nonlinear performance evaluation. In other words, the so-called *performance evaluation stage* should not be considered only as an evaluation stage, but at the same time as a *design improvement stage*.

Here particular emphasis will be given to the preliminary design of *coupled core wall systems* as typical examples, and a simple but novel capacity estimation procedure as well as a simple ductility demand estimation procedure will be presented. In addition, unique shear response of coupled walls involving *shear amplification* and *shear migration* will be presented briefly.

2. SEISMIC RESPONSE OF COUPLED CORE WALL SYSTEMS

2.1. Behavior of Coupled Core Wall Systems

Reinforced concrete (RC) structural walls have been crucial and indispensable components of tall buildings as they possess substantial lateral stiffness and strength, leading to considerably reduced lateral deformations against wind and/or seismic loads. Beside their efficiency in satisfying structural requirements, reinforced concrete structural walls also serve to fulfill functional requirements simultaneously, as in the case of core walls encasing elevator shafts and stairwells. Today, most of the tall buildings rise up with reinforced concrete structural walls, forming a core at the middle of building plan.

Since cores are used for elevator shafts and stairwells, there must be some openings for circulation of people. In other words, cores are formed by adjoining structural walls linked with beams above the openings. Since mid-1960's these structural walls and beams are referred as *coupled walls* and *coupling beams*, respectively [20]. Major part of the lateral load on a building can be resisted by efficiently designed *coupled core wall systems* and relieve other structural components, which only need to carry gravity loads. An example of a coupled core wall system is shown in Figure 2.1.

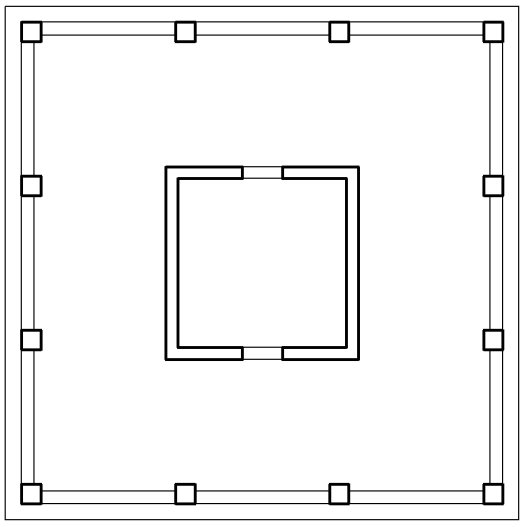

Figure 2.1. Coupled core wall system.

Coupled core wall systems (CCWS) have been widely used as indispensable elements for seismic resistant design of tall buildings, since major part of the lateral load could be resisted by such systems. In other words, coupled walls and coupling beams are relied upon entirely for the lateral stability and strength of the building emphasizing the need of understanding their behavior. Indeed, behavior of coupled walls and coupling beams has not been completely understood until recently because of inadequate capacity of computers, absence of proper structural analysis tools and limited experimental facilities.

In coupled core wall systems, overturning moment induced by lateral loads is resisted by bending moments at each pier (M_1, M_2) and moment provided by axial force couple equal to the sum of seismic shear forces (T) developed in coupling beams (Figure 2.2).

$$M_{\text{tot}} = M_1 + M_2 + Tc \tag{2.1}$$

A commonly used term, *degree of coupling* (A), has been defined as the ratio of moment provided by axial force couple developed through the coupling beams to total overturning moment:

$$A = \frac{Tc}{M_{\text{tot}}} = \frac{Tc}{M_1 + M_2 + Tc} \tag{2.2}$$

With increasing degree of coupling, the whole coupled core wall system tends to behave as a single cantilever. On the contrary, with decreasing degree of coupling, each pier tends to behave as an individual cantilever. Between these two extreme cases, coupling beams effectively provide a back-up system expected from the moment resisting frames of dual systems with cantilever walls [15].

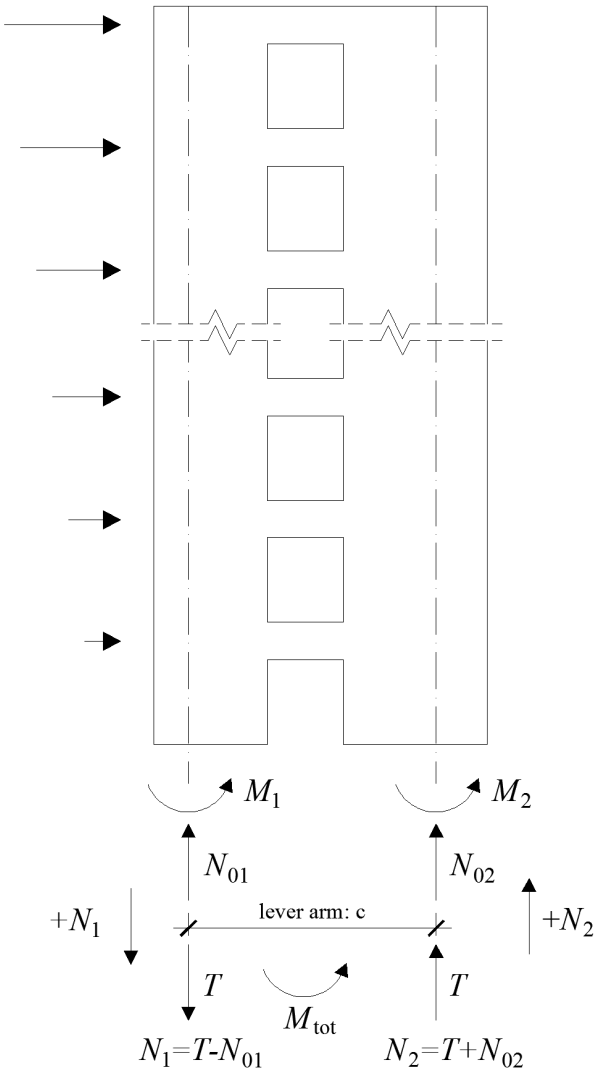

Figure 2.2. Schematic representation of equivalent seismic loads and base reactions of a coupled wall system.

Seismic design codes, such as New Zealand Seismic Code [1], Eurocode 8 [4], National Building Code of Canada [2, 3] and Turkish Seismic Design Code [5], define limits for degree of coupling as a design basis for coupled wall systems. Ductility capacity of buildings with coupled wall systems is assumed to increase with increasing degree of coupling, thus elastic seismic loads are divided by a higher reduction factor than that used for solid structural walls. Normally degree of coupling is calculated as a *demand parameter* in an early stage of design by means of *linear elastic analysis* under reduced seismic loads. However, neither coupling beams nor coupled walls remain in the elastic range; therefore, actually realized degree of coupling based on capacities of coupling beams and coupled walls would be different than those calculated based on elastic demand.

In other words, degree of coupling is a meaningful parameter only if it is calculated based on the *capacities of coupling beams and walls*, hence, strength is a more representative parameter compared to stiffness, considering the actual behavior of coupling beams and coupled walls. Note that actually realized degree of coupling for coupled walls with U, T, I or E shaped flanged wall sections is considerably higher due to larger lever arm between the centroids of compression and tension walls compared to that of the coupled walls with rectangular sections. Thus, even with moderate levels of coupling shear capacity, contribution of coupling effect on total overturning moment capacity could be very high.

Since moment capacity of walls depends on axial force, initial state of axial compression force is as important as the axial tension and compression forces transmitted by coupling beams. Considering the interaction of axial force and bending in each wall member, axial forces transmitted by coupling beams would decrease the initial axial compression stresses hence reducing bending capacity of the so-called *tension wall*, and on the contrary, they would increase the axial compression stresses hence increasing bending capacity of the other wall, the so-called *compression wall*. Eventually, depending on the initial axial compression stress caused by gravity loading and axial forces transmitted by coupling beams, moment capacity of each pier could change significantly. Thus it can be concluded that coupling beam strength and initial state of axial compression forces on walls are two essential parameters playing a crucial role on the behavior of coupled wall system.

Dynamic shear amplification and dynamic shear migration are two critical phenomena, which are particularly important for shear design of structural walls. The notable aspect of such phenomena is that they can never be captured by linear analysis. They can be obtained only from the nonlinear response-history analysis or multi-modal adaptive pushover analysis [15].

Dynamic shear amplification phenomenon is always encountered in an isolated single cantilever wall. Following the formation of a moment hinge at the base of the wall, the higher mode shear effects, notably participation of the second mode is significantly amplified due to a significant modification of seismic load distribution [22]. Although this

is a well-known phenomenon [19], it has been hardly implemented in code-based seismic design practice except in Eurocode 8 [4].

On the other hand, dynamic shear migration is another shear related phenomenon that could occur not only in walls, but more generally in all yielding structural elements and systems. In the particular case of walls, it essentially represents the transfer of shear from yielded wall(s) to non-yielded wall(s). For example it may occur between non-simultaneously yielding cantilever walls [19]. In particular for a coupled core wall system it is an inevitable case where the shear in yielded tension wall partially or even fully migrates to the non-yielded compression wall.

An ongoing challenge in the analytical research is to improve the modeling techniques for coupled wall systems. Almost all of the early analytical research has been based on an equivalent plane frame idealization, using one dimensional line elements to represent walls and coupling beams. In this approach, line elements pass through centroids of walls and coupling beams, and rigid link elements were used for connecting walls and coupling beams at each story level. Concentrated plastic hinges with hysteretic behavior were assumed to develop at the ends of coupling beams and walls. Also, frame elements assigned for walls were divided into sub-elements in order to represent the distribution of plasticity within the walls. However, defining hysteretic behavior especially for walls is not an easy task since hysteretic behavior should actually incorporate axial-shear-flexure interaction effects. On the other hand, axial forces on coupled walls continuously change during the earthquake excitation. Since bending stiffness and strength strongly depend on axial forces on the section, there is no doubt that assuming constant bending stiffness for wall sections would lead to an error. Walls should be able to make axial deformations along with the flexural deformations.

On the other hand, axial stresses on coupled walls can significantly change the shear capacity of walls. Also, shear and bending do exist simultaneously on a section, and contribution of shear and bending to the overall deformation of the member could change considerably, depending on the modeling technique and member characteristics. In other words, depending on the modeling technique and the member aspect ratio, the share of shear and bending deformations would be different.

Rigid diaphragm modeling is a common assumption for three dimensional building models with the aim of reducing the number of degrees of freedom. However, coupling beams tend to elongate due to plastic deformations, leading to differences in lateral displacements of tension and compression walls. Therefore, restricting elongation of the coupling beams creates axial compression, which could increase the moment capacity of the coupling beam. Some attempts have been made to take into account the effects of slabs both in terms of axial stiffness and contribution to moment capacity of coupling beam by modeling the coupling beams as flanged sections with effective slab width and contributing slab reinforcement.

2.2. Literature Review

Research on behavior of coupling beams and coupled wall systems has started in the beginning of 1960's [23-24-25]. Since inadequacy of elastic analysis methods for solving this nonlinear problem have been initially recognized, earlier attempts were made to understand the inelastic behavior both experimentally by testing either full scale coupling beams or small scale coupled wall systems and analytically by creating new methods for nonlinear solution of the problem. As the analytical methods and tools became sufficiently capable of reflecting the characteristics of coupled wall system behavior, more parametric analytical studies were performed in parallel to more comprehensive experiments. Only key research will be reviewed here that led to an innovative development of the subject.

Several attempts were made to develop analytical methods at the beginning of 1960's to understand the behavior of coupled wall systems, including continuum methods such as laminar analysis with several approaches. Although, these elastic analysis methods are still in use, they are not in the scope of this study. Details of these methods can be found in the literature [20].

An experimental research program was performed at the University of Canterbury, New Zealand at the end of 1960's and the beginning of 1970's. Program started with tests of coupling beams performed by Thomas Paulay [20], including twelve approximately ¾ full size relatively deep reinforced concrete coupling beams, with various aspect ratios and web reinforcement contents. Medium and deep coupling beams, having span to depth ratio of 1.29 and 1.02 respectively, were tested under static one-way and near-ultimate cyclic loading. Concluding remarks are as following;

- A shear failure mechanism is observed with diagonal cracks of which major diagonal crack divided the beam into two triangular halves. For beams under-reinforced against shear force, this failure mechanism would yield to *diagonal splitting* of these two triangular halves. This observation was going to lead the idea of using diagonal reinforcement in sufficiently deep coupling beams. Even in case of adequate shear reinforcement, *sliding shear failure* is most probable failure type for conventionally

reinforced deep coupling beams due to rapid degradation of concrete frictional shear resistance because of opening and closure of cracks between two stirrups.

- Considering shear resisting mechanism, contributions of arch action, dowel forces and aggregate interlock forces became unavailable during cyclic loading just after a few number of high intensity reversals. Also, the strength of stirrups in beams which did not have web reinforcement, diminished rapidly during cyclic loading.
- Entire spans of both top and bottom reinforcement were exposed to tensile stress. Since, both flexural top and bottom reinforcements were subjected to tension over the entire span, beams elongated and beneficial effect of the compression reinforcement on ductility could not be mentioned.
- Shear deformations governed the behavior of coupling beams, causing increase in degradation of stiffness after cracking. Loss of stiffness caused by diagonal cracking was about 80% which is considerably more than pronounced for flexure dominated beams.

In addition to experiments, a step by step *ultimate load analysis* procedure was developed by Paulay in scope of this study. Actions and deformations of coupled wall systems could be determined up to a collapse mechanism, based on the assumption that coupling beams would reach their ultimate capacity prior to yielding of coupled walls. Bilinear elastic-plastic behavior was defined for both coupling beams and coupled walls. This attempt was useful to put forward the understanding of significant difference in attained global ductility and component ductility.

As a second step, Binney and Paulay [26-27] introduced the concept of diagonally reinforced coupling beams. Four beams were tested with three varying parameters;

- Reinforcement type; conventionally reinforced vs. diagonally reinforced.
- Diagonal reinforcement cage; with or without confining ties.
- Span to depth ratio of 1.29 an 1.02 with diagonal reinforcement having confining ties.

These tests showed that, with diagonally reinforced coupling beams larger ductility capacities could be achieved with less degradation of load capacity than available in

conventionally reinforced coupling beams under repeated cyclic loading. However, larger ductility demands are associated with higher inter-story drifts which must be paid attention. All diagonally reinforced coupling beams failed because of stability failure, such as buckling of diagonal reinforcement, instead of a material failure. Therefore, buckling problem should be prevented by taking several precautions such as; protecting concrete from high bond and bearing stress, designing coupling beam having a reasonable width controlling concrete core size, arranging diagonal bars with sufficient distance in order to increase buckling resistance and using confining ties. Since vertical components of the diagonal strut and tie forces generate the shear forces at the ends of coupling beam, effectiveness of diagonal bars, thus coupling, increases with decreasing span to depth ratio. However, for very low span to depth ratios, deterioration occurs more rapidly during cyclic loading due to increased amount of shear stress.

In addition to above mentioned conclusion, a number of problems associated with diagonally reinforced coupling beams were pointed out, such as; difficulty in compaction of concrete within closely spaced reinforcement, difficulty in estimation of elongation and stiffness properties of coupling beams and great importance of accurate estimation of the amount of shear forces transmitted to coupled walls which can induce higher tension or compression stress than predicted at each wall.

The following stage of experimental program in University of Canterbury was tests of two quarter scale full size seven story reinforced concrete coupled shear wall models. Coupled wall systems, one with conventionally reinforced coupling beams and the other one with diagonally reinforced coupling beams, were tested under static reversed cyclic loading by Santhakumar and Paulay [28-29].

Based on early investigations, Santhakumar and Paulay were aware of possible failure types of coupling beams and possible effects of coupling beam characteristics on wall response such as; high axial tension and compression forces on tension and compression wall could lead to early degradation of concrete shear resistance in tension wall, and decrease in ductility of compression wall because of high axial compression force. Yet, these tests not only clarified the reality of those expectations but also put forward the crucial characteristics of coupled wall system which were going to be

investigated in more detail for the following forty years. Conclusions of this study are as following;

- In coupled wall system with conventionally reinforced coupling beams, beam sliding shear failure governed the behavior of coupling beams, causing full depth cracking and severe damage on coupling beams. However, these coupling beams provided considerable ductility, sustaining their strength with little loss during cyclic loading.
- Shear deformations and damage due to opening and closing of cracks in diagonally reinforced coupling beams were significantly less than conventionally reinforced coupling beams. Behavior of diagonally reinforced coupling beams was dominated by diagonal bars only after a few cycles of high intensity loading. Therefore, superior characteristics of diagonally reinforced coupling beams over their conventionally reinforced counterparts such as stable non-degrading hysteresis loops, larger energy absorption capacity, significantly less shear deformation and much less overall damage, were proven once more in these tests.
- In coupled wall system with conventionally reinforced coupling beams, pinching in the hysteresis of load-top floor deflection relationship was more pronounced because of considerable shear deformations, which resulted in decrease in stiffness at latter high intensity cycles. On the other hand, coupled wall system with diagonally reinforced coupling beams had more stable hysteresis loops, indicating larger cumulative ductility without strength loss.
- Length of plastic hinge of a coupled wall pier, hence the magnitude of section curvature depends on amount of axial forces on the wall. The length of plastic hinge increases with axial tension.
- For both models, 80% of the top floor deflection arose from flexural deformation on the walls as observed from strain measurements made on flexural reinforcement.
- In coupled wall system with conventionally reinforced coupling beams, wall failure was initiated in the tension wall. Because of early deterioration of concrete in the narrow compression region of tension wall, major portion of the shear force was resisted by a single layer of flexural reinforcement with dowel action causing severe shear displacement and buckling of the bars. While in coupled wall system with diagonally reinforced coupling beams, buckling of reinforcement in the compression

wall was developed before in the tension wall because of higher axial compression force transferred by coupling beams.

- The most important conclusion was driven for both coupled wall systems as the first time in the literature; shear transfer from tension wall to the compression wall. Shear force carrying capacity of tension wall was reduced significantly because of inclination of diagonal cracks changed with progressive cyclic loading while shear force carrying capacity of compression wall was increased with increasing axial compression stress. Therefore, significant amount of shear force transferred occurred from tension wall to compression wall, resulting 75% of the total shear was resisted by compression wall at ultimate load.

Beside above mentioned valuable outcomes on behavior of coupled wall systems obtained from experiments, Santhakumar also proposed a step by step analysis procedure, using a finite difference method for elastic-plastic analysis of coupled wall systems. In this procedure, the sequence of plastic hinge formation could be detected instead of assuming that all coupling beams yield prior to yielding of walls. Crack section stiffness values were determined for coupling beams and coupled walls, and used in the analysis. Moreover, effect of axial force on effective bending and axial rigidity of the section were taken into account and varied at each incremental load step.

In 1976, Mahin and Bertero [30] performed static and dynamic analyses of coupled wall system of an actual building. The purpose was to evaluate response characteristics of coupled wall systems and identify main parameters that must be considered in design and repair. Coupling beams were idealized as inextensible members connected to the centroid of the cores by rigid beams. Both bending and axial deformations were considered in modeling the core and axial force-moment interaction was taken into account through interaction curves. Although, coupling beams in actual building failed in shear because of large duct openings, three behavior types were considered in the nonlinear analyses; premature shear failure, ductile bilinear flexural yielding with or without stiffness degradation while shear failure was prevented until full flexural capacity.

Observations of this study, being one of the first dynamic analyses of coupled wall systems, are as following;

- The fundamental period of coupled wall system and lateral displacements were significantly increased with loss of coupling action because of premature shear failure of coupling beams. For ductile behavior mode in coupling beams, inelastic flexural deformations must be allowed by providing sufficient shear capacity.
- Second mode response on coupled wall system was evident, increasing the number of shear reversals on coupling beams at upper stories.
- With increasing degree of coupling, story drifts were decreased, and moment demand of coupled walls became smaller than uncoupled walls.
- With increasing flexural capacity of coupling beams, coupling beam shear forces hence axial forces transmitted to walls were increased, resulting larger shear and moment capacity at compression wall due to larger compression forces, and lower shear and moment capacity at tension wall because of axial tension forces which may even cause uplift of tension wall.
- Nonlinear static analysis seemed to be useful for evaluating structural behavior and estimating internal forces. However, a good indication of seismic response could be provided by nonlinear dynamic analysis.
- Further improvements for modeling force-deformation relationships taking into account axial load, shear and bending interactions were found to be necessary.
- Attention must be paid to the effects of near fault ground motions with long acceleration pulses.

In 1976, Aristizabal-Ochoa and Sozen [31] performed dynamic tests of four 1/12-scale, 10 story coupled wall systems, having variables of coupling beam strength and ground motion. Span to depth ratio of coupling beams was 2.67 while the overall aspect ratio of coupled walls was 5. In one of the coupled wall systems, coupling beam reinforcement arbitrarily increased as double of other three coupled wall system. Main conclusions of the tests are as following;

- An important characteristic of the response is rapid reduction of natural frequencies immediately after initial maximum excursions. Reductions in first and second mode natural frequencies are 50% and 40% respectively.
- For all test structures the displacement waveforms were similar to structure base moment wave form, while peaks of different stories tended to occur at the same time.

Displacements were dominated by the first mode. Contribution of higher modes to the maximum top displacement was less than 7%.

- The coupled wall system with double flexural reinforcement in coupling beams, had critical damage at exterior edges of bases of walls in addition to spalling of concrete at the ends of coupling beams. While the other three had more pronounced damage in the coupling beams with form of flexural cracks, then spalling of concrete at exterior edges of the piers was observed during subsequent test runs.
- Coupling beams at intermediate stories had more damage.

Immediately after these tests, in 1977, Takayanagi [32-33-34] developed an analytical model which can trace the failure mechanism of coupled wall systems under dynamic and static loads. The analytical model was based on line elements, representing the coupled walls and coupling beams. For coupling beams, rotational springs were assigned at ends of each coupling beam, while for coupled walls, each wall member were subdivided into sub-elements considering propagation of inelastic deformations. Hysteresis rules, including effects of pinching action and strength decay for coupling beams and axial force-moment interaction for the wall sub-elements, were defined for each constituent element. However, effect of axial force on bending rigidity of wall section was not taken into account; instead a tri-linear primary curve is used in the hysteresis rules for wall sub-elements. Ten-story coupled wall system models tested by Aristizabal-Ochoa and Sozen were analyzed and following conclusions were driven;

- Yielding of coupling beams occurred before coupled walls, initiated in the intermediate stories and then propagated to the upper and lower stories.
- It was found necessary to include axial inelastic rigidity in the wall section.
- Significant amount of shear force was transferred from tension wall to the compression wall. Because of early initiation of inelastic deformations in the tension wall, only 28% of the shear force was resisted by tension wall before yielding of compression wall. After yielding of both walls, the proportion of the shear force in the tension wall started to increase again.
- Base moment of tension wall was continuously decreasing throughout the analysis. At the end of analysis, contribution of tension wall, compression wall and coupling

effect on base overturning moment was 10%, 30% and 60% respectively. Therefore, strength of coupling beams played a major role in controlling the response.

- Degree of coupling continuously changed during the analysis, starting from 71% and decreasing to 55% until both coupled walls yielded, then increased again up to 60%.
- Pinching action and strength decay of which incorporated to hysteresis characteristics of coupling beams caused larger displacement in subsequent cycles and increased the rate of deterioration of structural stiffness. However, no effect of these variables was observed on maximum moments.
- The response waveform of base moment and displacement were governed by first mode, while some influence of the second mode was observed on the response waveform of base shear.
- Although, natural frequencies of vibration modes decreased considerably because of decrease in structural stiffness, mode shapes of the coupled wall systems did not change during the dynamic motion.

In the second series of tests six 6-story coupled wall systems, having 1/12-scale were tested under dynamic and static loading by Lybas and Sozen [36]. Main variables were the strength and stiffness of coupling beams. In addition to above mentioned conclusions, observations from these tests are as following;

- Relative contribution of higher modes to base shear increased with decreasing stiffness and strength of coupling beams. In other words, effectiveness of higher modes increased with decreasing degree of coupling.
- Energy dissipation characteristics of the structure were strongly affected by hysteresis relations of coupling beams.

In 1980, Saatçioğlu *et al.* [37-38-39-40] developed a *degrading stiffness* column element, taking into account the effects of axial force on both moment capacity and stiffness of a wall member. This frame element was implemented in DRAIN-2D [35] to represent wall elements. Afterwards, analyses were performed to investigate dynamic inelastic response of coupled wall system of a reduced 10-story model of a 20-story prototype structure. Investigated parameters are as following;

- Effects of axial force, shear yielding and other features of force-deformation hysteresis relationship such as post-yield stiffness, pinching, strength decay under cyclic loading, reloading and unloading stiffness,
- Wall strength, beam-to-wall stiffness ratio and beam-to-wall strength ratio,
- Significance of earthquake frequency characteristics, intensity and duration.

Based on the analyses results, following conclusions were made;

- Axial force-moment interaction effects should be considered in dynamic analyses, since response envelopes of walls can be increased by 50%, depending on the degree of coupling.
- Maximum forces and displacements did not appear to be significantly affected by shear yielding or pinching in hysteresis loops during dynamic analyses. However, if decrease in shear stiffness under cyclic loading is very high, sizable effects in some response quantities could be observed. Increase in shear component of total deformation can cause a decrease in flexural component, such that at some instances horizontal displacement due to shear yielding reached more than 50% of total displacement at hinging region as observed in static tests of uncoupled walls. However, under dynamic loading conditions shear deformations and maximum flexural deformations do not occur simultaneously, implying that displacement response envelopes did not necessarily reflect the same effect of shear yielding as it was observed from static loading.
- Strength decay in coupling beams can significantly affect the dynamic response of coupling beams, since rotational ductility of coupling beams drastically change with this parameter. Early and rapid strength decay can cause an increase of two to four times in rotational ductility requirement.
- Moderate variations in post-yield loading, unloading and reloading branches of the hysteresis loops did not significantly affect dynamic response.
- Inelastic deformations could increase significantly with decreasing yield level.
- *Beam-to-wall strength ratio* is an important parameter that controls inelastic behavior of members. An optimum degree of coupling should be achieved to prevent undesirable behavior such as; early yielding of walls because of strong coupling or excessive ductility demands on walls and coupling beams because of weak coupling.

- Level of axial load on a wall section controls the capacity and ductility requirements of that section. If transmitted axial forces due to coupling were high, then high initial compression stress due to gravity loading could be an advantage for the wall section, since increased gravity loads in walls can reduce the ductility requirements and improve the behavior.
- Performed analyses showed that variation in earthquake frequency characteristics can affect displacement and ductility response as much as 50%.

While researches were kept going on the overall behavior of coupled wall systems, some researchers started to investigate effectiveness of various reinforcement detailing options for coupling beams other than conventional and diagonal reinforcement. Within this context, in 1980, Barney *et al.* [41] tested eight specimens under cyclic loading, having span to depth ratio of 2.5 and 5.0, with conventional reinforcement, diagonal reinforcement and diagonal bars in the hinging region in addition to conventional reinforcement. Compared to coupling beams tested by Paulay and Binney [27], span to depth ratio of these eight specimens were quite high. Results of the tests are as following;

- Sliding shear failure was observed in conventionally reinforced coupling beams even though transverse reinforcements were provided to carry the entire shear forces without yielding. Sliding shear cracks developed between transverse reinforcement and stirrups eventually became ineffective.
- Improving the performance of conventionally reinforced coupling beams by using diagonal reinforcement within hinging regions at each end of beam was not efficient considering added complexity and cost.
- Coupling beams having full-length diagonal reinforcement showed the best performance in terms of strength, ductility, and energy dissipation characteristics among those tested.

In the beginning of 1980's, a series of coupled wall tests were performed at University of California, Berkeley. In 1982, Aktan *et al.* [42-43] performed an analytical investigation on behavior of coupled wall systems as part of this integrated analytical and experimental research program on the seismic responses of reinforced concrete coupled wall-frame systems. Results of experimental part of the research were evaluated in more

detailed by Ozselcuk, A. in 1989 [44]. 1/3 scale, 4-1/2 story coupled wall sub-assemblages of a 15-story reinforced concrete coupled wall-frame prototype structure were tested under cyclic loading conditions. First test specimen (1C) was tested and repaired. After testing the repaired specimen (1CR), it was repaired once more (1CRR) and re-tested. Also another specimen (2C) having lower degree of coupling with weakest possible coupling beams was built and tested in parallel to 1C, 1CR and 1CRR specimens. Aims of these studies were to figure out the state of the art for inelastic response prediction and design practice of reinforced concrete coupled wall-frame structural systems. Here are the conclusions of this study;

- The main problem on analytical modeling of reinforced concrete members was found to be the uncertainties regarding realistic assessment of the axial, shear, torsional, flexural stiffness and strength values as well as force-deformation hysteresis characteristics.
- Although the structure was designed based on 1973 Uniform Building Code, early shear-compression failure was observed because of high flexural capacity of strong coupling beams, leading to excessive wall axial forces causing flexural overstrength of compression wall, and very large unfavorable redistribution of shear force. Experiment showed that even at low levels of lateral force, compression wall was resisting 90% of the total shear force. However, when yielding initiated at compression wall, shear force in the tension wall began to increase slowly. Significant shear redistribution was caused by not only variations in flexural stiffness and strength, but also variations in shear stiffness [43-44]. Stiffness of walls was greatly affected by loading program and deformation history as well. Even under serviceability level lateral loading, cyclic nature of loading was found to affect shear, flexural and axial stiffness considerably [44]. When flexural yielding occurred in tension wall, shear stiffness of tension and compression walls reduced to 16% and 74% respectively, in specimen 1C. When both walls in specimen 2C yielded in flexure, tension and compression walls had 14% and 18% of initial shear rigidity, respectively.
- Compression wall displacement was greater than tension wall displacement, indicating that the diaphragm grew substantially. Observed difference between displacements of compression and tension walls was attributed to the distortion of

two walls caused by diagonal cracks in the panels and elongation of the coupling beams. Discrepancy in the displacements increased with increasing load level and it was larger at the first two stories since diagonal cracking was more extensive [44].

- With increasing degree of coupling, axial compression force on compression wall increased, thus leading bending capacity of compression wall increased while ductility capacity was reduced. Eventually, shear demand on compression wall increased due to this flexural overstrength. Whereas stiffness and bending capacity of tension wall decreased because of higher axial tension force. Increasing degree of coupling was also a consequence of overstrength in coupling beams [44].

In 1984, Shiu *et al.* [45] performed a series of tests in order to investigate,

- effects of beam strength on behavior of coupled wall systems,
- effects of axial forces induced through coupling beams on the strength and ductility of coupled walls,
- redistribution of shear and moment between coupled walls,
- critical design parameters for coupled wall systems.

Two coupled wall system specimens, one with weak and other one with strong coupling beams, representing 1/3 scale of a 6-story coupled wall system, were tested under cyclic loading. First of all, the specimen with weak coupling beams was exposed three load reversal of which coupling beams remained below yield level. Then, test procedure was followed by three additional load reversals with sufficient intensity to form yielding at all coupling beams and base sections of both walls. Afterwards, coupling beams were repaired and loading protocol was repeated on the repaired specimen (which is attributed as the second coupled wall system with strong coupling beams). Eight more cycles were applied; first four had sufficient intensity to induce yielding of the strengthened beams between the third and sixth floors and the last four cycles caused yielding of remaining coupling beams and walls reached to ultimate capacity at the end of test. Furthermore, analytical models of coupled wall systems were developed and validity of the models was confirmed by comparing analytical and experimental results. Following conclusions were driven;

- During the first test, coupling action contributed only 10-20% of the total overturning moment because of weak coupling beams. When both walls yielded, all coupling beams had already suffered extensive damage.
- For repaired coupled wall system, contribution of coupling action to overturning moment capacity varied between 50-75%.
- In design of coupled wall systems, strength of coupling beams was found to be an important parameter on ductility of beams and walls. Behavior of lightly coupled walls was governed by the behavior of individual walls; therefore inelastic shear behavior of walls became significant. While in a strongly coupled wall system, large axial forces were induced in the walls through coupling beams which increases the importance of the interaction of axial and flexural effects in wall behavior.
- Based on the analyses results, redistribution of shear and moment was significant in strongly coupled wall system; at the end of the analyses, 80% of base shear and 40% of overturning moment was resisted by compression wall, while coupling action and tension wall contributed to overturning moment by 50% and 10%, respectively.

In 1985, Keshavarzian and Schnobrich [46, 47] created another column element model, taking into account the effect of changing axial force not only on the flexure yield surface but also in the element stiffness. After analyzing the models tested by Lybas and Sozen [36] and Aristizabal-Ochoa and Sozen [31], following conclusions were made;

- The *migration* of base shear from tension wall to compression wall would cause the generation of axial force in the coupling beams, altering the stiffness, strength and ductility of those members. This effect could not be seen in the vicinity of a rigid diaphragm.
- Even though shear forces and corresponding bending moments in each pier were significantly affected by fluctuations of axial force, total shear force acting on the structure did not change, indicating that overall structural stiffness was not affected significantly.

From the end of 1990's until the end of 2000's, some researchers have focused on achieving more efficient coupling beam design in terms of strength and ductility capacity, as well as constructability. In some of these studies, either different reinforcement layouts for coupling beams were tested as in the case of Barney *et al.* [41] in 1980 or behavior of

steel coupling beams with or without post-tensioning were investigated as an alternative of reinforced concrete coupling beams.

In 1996, Tassios *et al.* [48] performed cyclic loading tests of 1/2 scale coupling beams with span to depth ratio of 1.00 and 1.66, having different reinforcement layouts including conventional reinforcement, diagonal reinforcement, diagonal bent-up bars at the hinging region in addition to conventional reinforcement and conventional reinforcement with long and short dowels at the ends of coupling beams controlling sliding shear failure. Test results indicated that diagonally reinforced coupling beams showed the highest overall performance among all layouts and performance of conventionally reinforced coupling beams were unsatisfactory, however, could be improved with additional diagonal bent-up bars. Although, sliding shear failure was prevented by using short and long dowels, most brittle behavior was observed in coupling beams with short dowels and slightly better with long dowels.

In 1997, Harries *et al.* [49] tested *shear critical steel coupling beams* and *flexure critical steel coupling beams* as assumed to be alternative of diagonally reinforced coupling beams and conventionally reinforced coupling beams, respectively. Cyclic loading test results showed that; shear critical steel coupling beams could be a practical alternative to diagonally reinforced coupling beams, being capable of absorbing greater amounts of energy and providing higher ductility. Section height of diagonally reinforced coupling beams should be adequate so that diagonal bundles could provide sufficient shear capacity. However, section height of shear critical steel coupling beams could be smaller for providing same amount of shear capacity. Similarly, flexure critical steel coupling beams had same advantages compare to conventionally reinforced concrete counterparts. Moreover, use of steel coupling beams can simplify formwork and reduce on-site labor requirements. As a second stage, Harries *et al.* [50] performed nonlinear dynamic analyses of 18-story coupled wall systems, having flexure and shear critical steel coupling beams as well as conventionally and diagonally reinforced concrete coupling beams. Flexure critical steel coupling beams and conventionally reinforced coupling beams had span to depth ratio of 4.86 and 4.28 respectively, while shear critical steel coupling beams and diagonally reinforced coupling beams had span to depth ratio of 2.00 and 1.71 respectively. Analyses results showed that for same degrees of coupling, ductility demands on beams and walls

were reduced due to improved hysteretic response of the steel beams. Besides, steel coupling beams provided higher ductility capacity.

In 2000, Galano [51] *et al.* investigated the differences in behavior of coupling beams having conventional reinforcement, diagonal reinforcement with or without transverse confinement ties and rhombic type reinforcement, with span to depth ratio of 1.5. Under monotonic and cyclic loading, with rhombic type reinforcement layout, slightly higher rotational ductility and considerably lower ultimate strength were obtained compared to diagonal reinforcement layout. In addition, diagonal cleavage shear fracture was prevented. Diagonally reinforced coupling beams without confinement ties suffered from early buckling failure of compression strut because of lack of confinement ties and low concrete compressive strength.

In 2002, Shen and Kurama [52] created the concept of post-tensioned hybrid coupled walls. As a different alternative, steel coupling beams were not embedded to walls and coupling of coupled walls was achieved by post-tensioned steel coupling beams using unbounded tendons. Another advantage of this system is its applicability for coupling of existing uncoupled walls as part of a strengthening and retrofit scheme. Results of analytical and experimental work are as following;

- Nonlinear deformations occurred primarily as a result of opening of gaps at the contact regions near the beam-to-wall interfaces. Top and seat angles at the beam-to-wall interfaces were used for inelastic energy dissipation, which can be replaced after the earthquake.
- Initial stiffness's of the system with post-tensioned steel coupling beams and the system with embedded steel coupling beams were similar.
- There was a restoring force due to post-tensioning that closed the gaps and pulled walls and beams back toward their un-displaced position.

In 2004, Hindi and Hassan [53] created an analytical model to predict the monotonic load-deformation behavior of diagonally reinforced coupling beams, assuming that moment and corresponding shear capacity of coupling beams is provided by diagonal tension and compression forces, generated on diagonal bundles. Since diagonal

compression force can be larger than diagonal tension force due to contribution of concrete, difference between horizontal components of diagonal tension and compression forces was assumed to be resisted by top and bottom longitudinal reinforcement of coupling beam and an effective portion of slab. The proposed model gave reasonable results in terms of shear strength and deformation response compared with experimental evidence. Furthermore, there are a few studies in the literature on modeling of coupling beams, using more sophisticated modeling techniques such as nonlinear finite element models allowing the reinforcement to be modeled as smeared component of the concrete shell element [54-55-56-57]. However, accuracy of these more sophisticated models is not higher than the model proposed by Hindi and Hassan.

In 2002, El-Tawil *et al.* [58-59] performed nonlinear static analyses of three dimensional nonlinear finite element models representing one half of 6-story and 12-story *two cell cores* with steel coupling beams, created and discretized by using the computer program DIANA-2000 [60]. Results of nonlinear static analyses, including monotonic loading, are as following;

- For 30% degree of coupling, coupled walls behaved similar to uncoupled walls, deformed in single curvature and inelastic behavior was observed at the base of each wall. With increasing degree of coupling, deflection profile changed slightly from single to double curvature, thus negative wall rotations were observed in top six and eight stories, however, they remained small.
- Wall rotation values tended to decrease significantly with increasing degree of coupling compared to uncoupled condition. However, when degree of coupling exceeded 45%, wall rotations slightly increased. Similar behavior was observed for shear distortions.
- No shear redistribution was observed in contrast to previous analytical and experimental research. Since walls in the analysis were flanged, different than previously analyzed rectangular walls, the compression region of compression wall was in the flange and entire web was exposed to tensile stress, hence reducing the shear capacity through extensive cracking of concrete. On the other hand, compression stress in the tension wall was resisted by the web regions of which could resist significant shear forces.

- For decreasing coupling, coupling beam chord rotations were high at upper stories. As degree of coupling increases, coupling beam chord rotations were getting higher at lower stories.
- For decreasing coupling, cracking was concentrated at base of walls while for increasing coupling, cracking spread upwards from base sections. The optimum combination of reduced distribution and intensity of cracking was observed between 30% and 45% degree of coupling.

Afterwards, nonlinear dynamic analyses were performed [61] and following results were obtained in addition to above mentioned observations;

- Amount of base shear magnification decreased with increasing degree of coupling.
- Higher mode effects were somewhat more pronounced with lower degrees of coupling.

In 2009, Naish *et al.* [62] tested eight coupling beam specimens with different reinforcement layouts; conventional reinforcement, post-tensioning in addition to conventional reinforcement, diagonal reinforcement with confinement around diagonal reinforcement bundles, and diagonal reinforcement having full section confinement. Coupling beam specimens, having span to depth ratios varying between 2.40 and 3.33, were tested under cyclic loading. Observations from these tests are as following;

- Coupling beams having diagonal bars and full section confinement had better performance in terms of strength and ductility than coupling beams with confined diagonal reinforcement bundles.
- Shear strength of coupling beams were increased by including reinforced concrete slab or adding post tensioning with amount of 15-20% and 10% respectively.
- Effective elastic stiffness values for test beams were approximately determined as 15%.
- Slip/extension deformations were found to be crucial, since most of the damage experienced by coupling beams with aspect ratios of 2.40 to 3.33 was concentrated at beam-wall interface, even in the case of applying axial load with post-tensioning.

- Nonlinear behavior of coupling beams could be accurately modeled by using either moment hinges or shear hinges. However, load-deformation responses obtained by analyses were strongly influenced by modeling parameters, such as unloading and reloading stiffness values. Therefore, coefficients used for modeling were still question marks as they had always been since from early research.
- Shear flexure interaction studies showed that shear deformations were found to be more important for beams with span to depth ratio less than 2.25. Exceeding this limit, flexure deformations were more prominent.
- Variations in coupling beam stiffness and strength directly affected coupling beam rotation demands.

In 2011, a research was undertaken by Turgeon *et al.* [79-80] to investigate the response of a midrise coupled wall designed to meet current codes. A test specimen was created for lower 3 stories of a 10-story building and demands from the upper stories were imposed on each pier in terms of shear, moment, axial loads and displacements as in the case of coupled wall experiments performed by University of California, Berkeley [42-43-44]. The motivation of the study was to test and analyze a modern planar coupled wall system representing the characteristics of the current practice. Results of the cyclic loading tests could be summarized as following;

- Yielding of second and third story coupling beams was followed by yielding at base sections of walls and finally first story coupling beam. However, it was expected that all coupling beams would yield prior to base sections of walls, as assumed in the design.
- The most extensive damage to diagonally reinforced coupling beams was spalling of concrete and bar fracture did not occur. The maximum end rotation of coupling beam was measured less than 5%.
- Compression wall had extensive damage including damage in core concrete and buckling of reinforcement, led to a sudden failure at 2.27% building drift resulting in loss of both lateral and axial load-carrying capacities.
- The degree of coupling computed from experiment ranged between 50% and 60% which was consistent with the theoretical value of 53%.

In 2012, Barbachyn [63] *et al.* performed nonlinear static analyses of coupled wall systems with DRAIN-2DX [64] by using strut and tie analogy for modeling diagonally reinforced coupling beam and nonlinear fiber beam-column elements for modeling coupled walls. Differences of strut and tie analogy used in this study compared to recommended by Hindi and Hassan [53] were that in addition to two diagonal strut elements taking into account the contribution of concrete, four diagonal strut elements for concrete at mid-span and two longitudinal strut elements for top and bottom concrete were modeled as well as a single axial element between mid-points of the beam to simulate axial restraint conditions because of prevention of axial elongation of coupling beam by stiff coupled walls. Conclusions of this study are as follows;

- Strut-and-tie model was found to be relatively simple yet powerful tool for simulating the behavior of diagonally reinforced coupling beams under cyclic loading.
- Axial elongation of coupling beams could be restrained by stiff coupled walls under lateral loading, which induce axial compression forces into coupling beams, especially at lower floors. Therefore, compression stress on concrete diagonal struts would be underestimated unless axially restraint condition is not taken into account.
- On the other hand, large tension forces can also develop in the coupling beams, which may cause more critical conditions than previously considered low-cycle fatigue fracture of the diagonal reinforcement.

2.3. Preliminary Design Issues

As previously mentioned in the introduction part summarizing the current design practice, preliminary design stage needs to be given a special emphasis for the development of a suitable tall building structural system later to be evaluated / designed on performance basis through nonlinear seismic analysis.

In this respect, LATBSDC [8] considers the preliminary design stage as merely equivalent to the application of *capacity design rules* while SFDBI [12] applies the *prescriptive* code provisions including the *minimum base shear* strength requirement. On the other hand TBI [10] treats the preliminary design issue in a more detailed fashion, additionally including recommendations on system configuration, wind effects, limiting building deformations, setbacks and offsets, diaphragm demands, outrigger elements, etc.

Capacity design rules are intended to insure that "structural system for the building has well defined inelastic behavior where nonlinear actions and members are clearly defined and all other members are stronger than the elements designed to experience nonlinear behavior." Detailed lists are provided in both TBI [10] and LATBSDC [8] to identify the "zones and actions commonly designated for nonlinear behavior".

When applying capacity design principles, it is stated in LATBSDC [8] that "linear analysis may be used to determine the required strength of the yielding actions". This recommendation is problematic in the sense that linear analysis cannot correctly estimate the internal force redistribution due to nonlinear behavior in real response. On the other hand "capacity protected actions" such as shears in beams and columns may be estimated by capacity design principles to an acceptable accuracy, but shears in walls would be grossly underestimated. In this respect, a frequently encountered example is the preliminary design of coupled core wall systems.

Core walls with peripheral columns represent the most common structural system of tall buildings. Frames with down stand beams are rarely used and in many cases, even completely eliminated leading to flat plate systems. Thus, the so-called dual systems with moment-resisting frames (back-up systems) are practically discarded. A number of

engineers who faithfully provided the back-up systems in all their past prescriptive code applications appear to be hesitant in accepting this new situation. However it can be argued that properly designed coupled walls with sufficiently stiff and strong coupling beams effectively provide a similar back-up action expected from the moment resisting frames of dual systems with cantilever walls [15].

Both coupled walls and coupling beams generally undergo significant nonlinear response and coupling beams experience excessive plastic deformations throughout the height of the building. The nonlinear behavior of wall pieces is significantly influenced by the stiffness and strength of coupling beams.

Engineers often experience difficulty in preliminary sizing of coupled core wall systems. Reliable practical analysis tools that would help consider the nonlinear seismic behavior of wall piers and coupling beams as well as their combined effect in seismic response of coupled wall systems are not available. In the current practice, linear analysis is being employed inevitably in the preliminary design stage to identify the stiffness and strength of coupled wall components and their distribution. Such a procedure would most likely lead to an overdesign of coupling beams with inappropriate and probably heavily congested reinforcement requirements. On the contrary, a preliminary design based on a linear analysis with reduced seismic loads may result in under-designed wall elements especially in terms of their shear strength [15].

Based on Incremental Response Spectrum Analysis – IRSA Method by Aydınoğlu [16, 17], multi-mode pushover analysis has proven to be a useful tool in preliminary proportioning of coupled core wall systems [15]. In the following, even simpler but very powerful capacity and demand estimation tools are presented.

2.4. Objectives and Scope of Dissertation

As emphasized in literature and design practice review, interaction between coupling beams and coupled walls identifies the behavior of coupled wall system. Since behavior of coupled walls is governed by transmitted axial force through coupling beams and initial axial load due to gravity, strength of coupling beams hence sum of shear forces acting on coupled walls should be determined as accurate as possible. Thus, sizing and reinforcing of coupling beams and coupled walls are of primary concern.

In this study, *capacity and ductility estimation procedures* for preliminary seismic design of coupled core wall systems are developed, which could be utilized for sizing and reinforcing of coupling beams and coupled walls. Then inelastic deformation demands could be checked by means of nonlinear dynamic analysis for maximum considered earthquake level in performance evaluation or design improvement stage.

For a set of coupled core wall systems, proposed capacity and ductility estimation procedures are applied and validated by means of pushover and nonlinear response history analysis. Moreover, inelastic strains of coupled walls and coupling beams, as well as shear effects on coupled walls in terms of shear migration and dynamic shear amplification are evaluated by nonlinear response history analysis.

3. A CAPACITY ESTIMATION PROCEDURE FOR PRELIMINARY DESIGN OF COUPLED CORE WALL SYSTEMS

A simple, *strength-of-materials approach* is developed to estimate the base overturning moment capacity of a typical coupled core wall system starting from the *first principles*, which will be explained in this section. Based on the estimated overturning moment capacity, the simple approach is further extended to estimate the ductility demand of the coupled core wall system utilizing a novel modification of the pushover concept, which will be explained in the next section.

It is assumed that the coupled core wall system shown in Figure 3.1 responds to earthquake action on its own as the main structural system without stiffness and strength contribution of any other structural element. Actually this is the case in most of tall buildings with core wall at the center and gravity frames along the periphery, e.g. see Figure 2.1.

Using simple equilibrium equations, individual wall axial reaction forces at the base can be expressed as

$$N_1 = -N_{01} + T \qquad ; \qquad N_2 = N_{02} + T \tag{3.1}$$

where N_1 is considered positive in tension and N_2 positive in compression as indicated in Figure 3.1, representing the axial force reactions of the so-called *tension wall* and *compression wall*, respectively. N_{01} and N_{02} represent gravity axial loads of walls and T refers to the so-called *total coupling shear* representing the sum of shear forces developed in coupling beams throughout the building. The sense of earthquake direction is assumed from left to right. If opposite, then subscripts 1 and 2 should be interchanged.

The base section of the coupled core wall system is the most critical section controlling the nonlinear behavior of the entire structure. Total base overturning moment reaction of the coupled wall system can be expressed by the following equilibrium equation:

$$M_{\text{tot}} = M_1 + M_2 + Tc \tag{3.2}$$

where M_1 and M_2 represent the bending moments of the tension and compression walls, respectively, and c refers to lever arm between the centroids of walls.

The contribution of the force couple, Tc, in total base overturning moment is traditionally represented by *degree of coupling parameter*, A, as follows:

$$A = \frac{Tc}{M_{\text{tot}}} = \frac{Tc}{M_1 + M_2 + Tc} \tag{3.3}$$

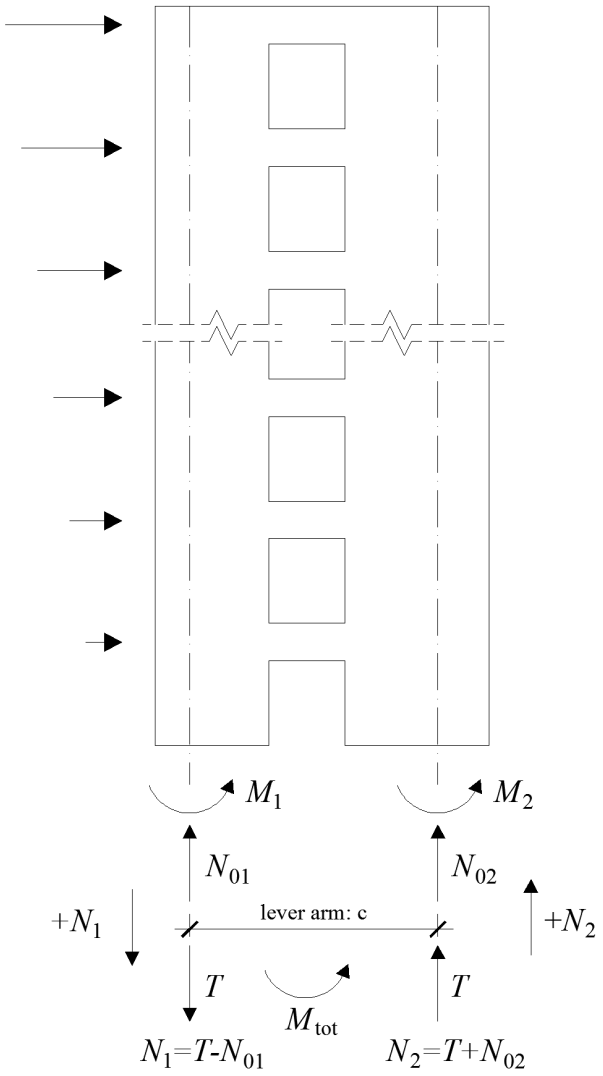

Figure 3.1. Base reactions and coupling shear forces acting on coupled wall system.

The reaction forces and the degree of coupling parameter given above are traditionally evaluated as *demand quantities* obtained from the linear analysis of a given

system under a given earthquake action [21]. However, here they are considered to represent the corresponding *strength capacities*. The ultimate capacity term that would control the coupled wall design is the *total base overturning moment capacity* defined by Eq.(3.2).

It is clear that maximizing the force couple, i.e. the *coupling shear*, would correspond to maximizing the overturning moment capacity. However, inspection of Eq.(3.1) suggests that coupling shear T should not be increased arbitrarily, as it would lead to increasing tension strains in the tension wall, i.e., spreading of the yielding from the base to the upper parts and hence larger concrete cracking along the wall. At the same time it would lead to increasing compression strains in the compression wall, even it could cause non-ductile compression failure if compressive axial force N_2 exceeds the balance point of axial force-moment interaction. Moreover increased coupling shear would result in reinforcement congestion and construction difficulties in coupling beams.

Thus, it is imperative that a reasonable compromise should be achieved between the strength capacities of individual walls and the coupling beams and such a *balanced solution* has to be worked out during the preliminary design stage. This observation has motivated the development of the following *capacity estimation procedure* for the initial sizing of the individual walls and the coupling beams in the preliminary design stage.

In order to proceed with a non-dimensional formulation, the quantities given the first of Eq.(3.1) are normalized as

$$n_{\mathrm{i}} = \frac{N_{\mathrm{i}}}{A_{\mathrm{ci}} f_{\mathrm{ce}}} \qquad ; \qquad n_{0\mathrm{i}} = \frac{N_{0\mathrm{i}}}{A_{\mathrm{ci}} f_{\mathrm{ce}}} \qquad ; \qquad n_{\mathrm{Ti}} = \frac{T}{A_{\mathrm{ci}} f_{\mathrm{ce}}} \tag{3.4}$$

where A_{ci} (i = 1, 2) represents the gross section area of the tension and compression walls, respectively, and f_{ce} denotes the *expected compressive strength* of concrete.

Total coupling shear and consequently base overturning moment capacity of a coupled core wall system is essentially controlled by the following three independent parameters:

a) Normalized gravity load of tension wall, n_{01}, which is defined by Eq.(3.4),

b) Mechanical reinforcement ratio of the tension wall, ρ_{m1}, which is defined as

$$\rho_{m1} = \frac{f_{ye}}{f_{ce}}\rho_1 \qquad ; \qquad \rho_1 = \frac{A_{s1}}{A_{c1}} \tag{3.5}$$

where A_{s1} represents the reinforcement area of the tension wall and f_{ye} denotes the *expected yield strength* of reinforcing steel.

c) *Relative yield parameter* of the tension wall, β_1, by which axial force of the tension wall is defined as a fraction of its full yield strength in tension (strain hardening of reinforcing steel is omitted for simplicity):

$$\beta_1 = \frac{N_1}{A_{s1} f_{ye}} = \frac{n_1}{\rho_{m1}} \tag{3.6}$$

Thus normalized axial force of the tension wall is defined as

$$n_1 = \beta_1 \rho_{m1} \tag{3.7}$$

Utilizing the first of Eq.(3.1) with Eq.(3.4) and Eq.(3.7), normalized total coupling shear can be expressed in terms of the above-defined three independent parameters as

$$n_{T1} = n_{01} + \beta_1 \rho_{m1} \tag{3.8}$$

from which application range of the relative yield parameter β_1 can be defined as

$$-\frac{n_{01}}{\rho_{m1}} \le \beta_1 \le 1 \tag{3.9}$$

This relationship suggests that the limiting condition $\beta_1 = 1$ corresponds to the largest attainable axial tension force in the tension wall and hence greatest coupling shear according to Eq.(3.1). On the other hand $\beta_1 = -n_{01} / \rho_{m1}$ corresponds to the other limiting condition leading to zero coupling shear, i.e., $n_{T1} = 0$ in Eq.(3.8), which corresponds to the degeneration of the coupled wall system into two individual cantilever walls with axial force reactions equal to their gravity loads only, i.e., $-n_{0i}$.

It should be emphasized that the key relationship between the reinforcement requirements of the tension wall and of the coupling beams throughout the building is the

one given above by Eq.(3.8). By an appropriate selection of the tension wall reinforcement ratio, ρ_{ml}, and the relative yield parameter, β_l, design engineer can readily estimate the total coupling shear from Eq.(3.8), which would lead to the selection of coupling beam reinforcements. Implementation of the procedure is explained after the next section.

Following the estimation of total coupling shear from Eq.(3.8), normalized axial force of the compression wall can be obtained from the second of Eq.(3.1) and Eq.(3.4) as

$$n_2 = n_{02} + n_{T2} \tag{3.10}$$

Once total coupling shear is found from Eq.(3.8) based on three independent parameters, *total base overturning moment capacity* can be readily obtained from Eq.(3.2) by calculating individual wall bending moment capacities from the corresponding *N-M* yield surfaces (interaction diagrams at yield) under wall axial forces calculated from Eqs.(3.7, 3.10). Figure 3.2 typically depicts such yield surfaces of individual walls of a coupled core wall system where yield points associated with various values of relative yield parameter β_l are indicated. In order to avoid concrete crushing failure, it should be ensured that the compressive axial wall reaction N_2 does not exceed the axial force corresponding to balance point on the yield surface.

In addition, *degree of coupling parameter* can also be calculated using Eq.(3.3), although it is no longer a decisive parameter in the proposed capacity estimation procedure, as opposed to traditional practice [21].

Note that calculated total base overturning moment capacity corresponds to an upper limit. While full yielding would most likely develop at the base section of the tension wall and in almost all coupling beams, the base section of the compression wall may not fully yield. Therefore the calculated total base overturning moment capacity should be considered as a conservatively estimated quantity. However, implementation studies based on nonlinear analyses have shown that the effect of such conservatism is not of concern. This is mainly due to the fact that the term *Tc* always dominates the total base overturning moment capacity as given by Eq.(3.2), especially in the case of $\subset\supset$ shaped individual walls with relatively longer lever arm *c* as compared to rectangular walls.

As a final note in this section, it is reminded that in the case of non-symmetrical core wall systems the above analysis should be repeated by interchanging the subscripts 1 and 2.

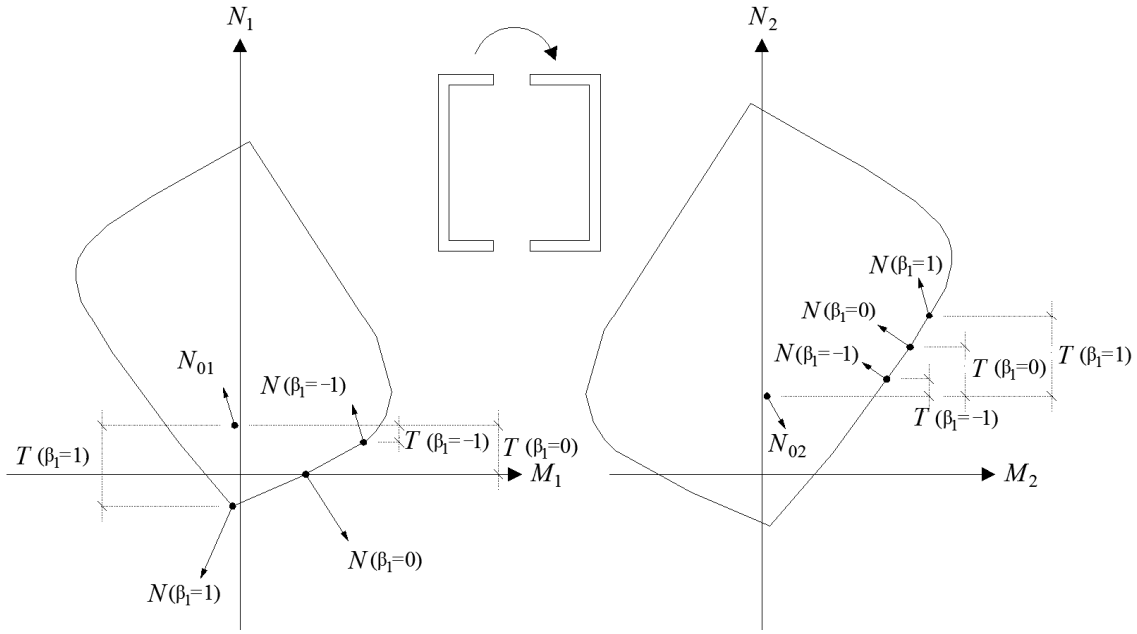

Figure 3.2. N-M yield surfaces (interaction diagrams at yield) of individual walls of a coupled core wall system where yield points associated with various values of relative yield parameter are indicated.

4. A DUCTILITY DEMAND ESTIMATION PROCEDURE FOR PRELIMINARY DESIGN OF COUPLED CORE WALL SYSTEMS

In order to evaluate the sufficiency of the total base overturning moment capacity, an approximate estimation of the *overall ductility demand* of the coupled core wall system can be achieved through a novel application of an alternate pushover concept as explained below.

Static-equivalent seismic load vector $\mathbf{f}$ and the displacement vector $\mathbf{u}$ are expressed in terms of first (dominant in a given earthquake direction) mode parameters as follows [18]:

$$\mathbf{f} = \mathbf{M}\,\boldsymbol{\Phi}_1\,\Gamma^*_{x1}\,a_1 \qquad ; \qquad \mathbf{u} = \boldsymbol{\Phi}_1\,\Gamma^*_{x1}\,d_1 \tag{4.1}$$

where $\mathbf{M}$ represents the lumped mass matrix and $\boldsymbol{\Phi}_1$ is the first (dominant) mode shape vector. a_1 and d_1 denote modal pseudo-acceleration and modal displacement, respectively. Γ^*_{x1} refers to the participation factor of the first mode for an x-direction earthquake action, which is defined as

$$\Gamma^*_{x1} = \frac{L^*_{x1}}{M^*_1} \qquad ; \qquad L^*_{x1} = \boldsymbol{\imath}_x^{\mathrm{T}}\,\mathbf{M}\,\boldsymbol{\Phi}_1 \qquad ; \qquad M^*_1 = \boldsymbol{\Phi}_1^{\mathrm{T}}\,\mathbf{M}\,\boldsymbol{\Phi}_1 \tag{4.2}$$

where $\boldsymbol{\imath}_x$ refers to a vector whose elements are unity for degrees of freedom in x earthquake direction while others are zero.

In the conventional pushover analysis, pushover curve is typically plotted as a base shear versus top (roof) displacement relationship and subsequently converted to a modal capacity diagram in terms of an equivalent single-degree-of-freedom system parameters a_1 and d_1. The base shear, V_b, can be obtained from Eq.(4.1) as

$$V_b = \boldsymbol{\imath}_x^{\mathrm{T}}\,\mathbf{f} = \boldsymbol{\imath}_x^{\mathrm{T}}\,\mathbf{M}\,\boldsymbol{\Phi}_1\,\Gamma^*_{x1}\,a_1 \qquad ; \qquad V_b = L^*_{x1}\,\Gamma^*_{x1}\,a_1 \tag{4.3}$$

From Eq.(4.3) modal pseudo-acceleration a_1 is obtained as follows:

$$a_1 = \frac{V_b}{m^*_{x1}} \qquad ; \qquad m^*_{x1} = L^*_{x1}\,\Gamma^*_{x1} \tag{4.4}$$

where m^*_{x1} represents the *participating modal mass for the base shear* of the first (dominant) mode. On the other hand, modal displacement d_1 is directly obtained from Eq.(4.1) in terms of top (roof) displacement, u_{N1}, and the corresponding mode shape amplitude, Φ_{N1}, as follows:

$$d_1 = \frac{u_{N1}}{\Gamma^*_{x1}\,\Phi_{N1}} \tag{4.5}$$

On the other hand, since total base overturning moment capacity governs the coupled core wall system design, an alternate pushover curve can be developed and plotted in terms of *base overturning moment versus top displacement* and the same modal capacity diagram can be obtained by converting such an alternate pushover curve. Actually such an alternative is more meaningful, because overturning moment capacity can be estimated more correctly by a single-mode pushover analysis compared to the base shear capacity. To this end, the first-mode expression for the base overturning moment, M_o, can be written from Eq.(4.1) as

$$M_o = \mathbf{h}_o^T\,\mathbf{f} = \mathbf{h}_o^T\,\mathbf{M}\,\boldsymbol{\Phi}_1\,\Gamma^*_{x1}\,a_1 \qquad ; \qquad M_o = L^*_{o1}\,\Gamma^*_{x1}\,a_1 \tag{4.6}$$

where $\mathbf{h}_o$ refers to a vector whose elements are the story elevations each measured from the base level for the degrees of freedom in x earthquake direction while others are zero. Thus modal pseudo-acceleration a_1 is alternatively obtained from Eq.(4.6) as follows:

$$a_1 = \frac{M_o}{m^*_{o1}} \qquad ; \qquad m^*_{o1} = L^*_{o1}\,\Gamma^*_{x1} \qquad ; \qquad L^*_{o1} = \mathbf{h}_o^T\,\mathbf{M}\,\boldsymbol{\Phi}_1 \tag{4.7}$$

where m^*_{o1} represents the *participating modal mass for the base overturning moment* of the first (dominant) mode. Modal displacement is the same as given by Eq.(4.5).

It is worth to remind that base overturning moment, M_o, can be written in terms of base shear, V_b, as

$$M_o = V_b H_o \qquad ; \qquad H_o = \frac{L^*_{o1}}{L^*_{x1}} \tag{4.8}$$

where H_o represents level of the resultant (total) equivalent seismic loads as measured from the base level. Inspecting Eq.(4.4) through Eq.(4.8) reveals that both pushover alternatives actually yield the same modal pseudo-acceleration a_1.

Note that base overturning moment capacity M_{tot} is obtained in the previous section without actually running a pushover analysis, but with a capacity estimation procedure based on a simple *strength of materials approach*. Thus this moment capacity can be directly used to calculate the *modal yield pseudo-acceleration*, a_{Y1}, of the modal capacity diagram using Eq.(4.7) by replacing M_o with M_{tot} as follows:

$$a_{Y1} = \frac{M_{tot}}{m^*_{o1}} \tag{4.9}$$

Both pushover and modal capacity diagrams, which are idealized as elastic-plastic bilinear diagrams, are shown in Figure 4.1. $M_o = M_{tot}$ and $a_1 = a_{Y1}$ are indicated on the figure as capacity (or yield) parameters of the coupled wall system where the former is actually calculated with the proposed simple approach.

The slope of the linear portion of the modal capacity diagram shown in Figure 4.1(b) is equal to ω_1^2, i.e., the first (dominant) natural frequency squared, which is obtained as the first eigenvalue from the free vibration analysis of the coupled wall system considering the effective (cracked) section stiffness. Acceleration-Displacement Response Spectrum (ADRS) corresponding to a standard MCE code spectrum is also superimposed on Figure 4.1(b). Thus, *yield strength reduction factor*, R_Y, can be readily calculated as

$$R_Y = \frac{S_{ae}(T_1)}{a_{Y1}} \tag{4.10}$$

where $S_{ae}(T_1)$ refers to first-mode spectral pseudo-acceleration.

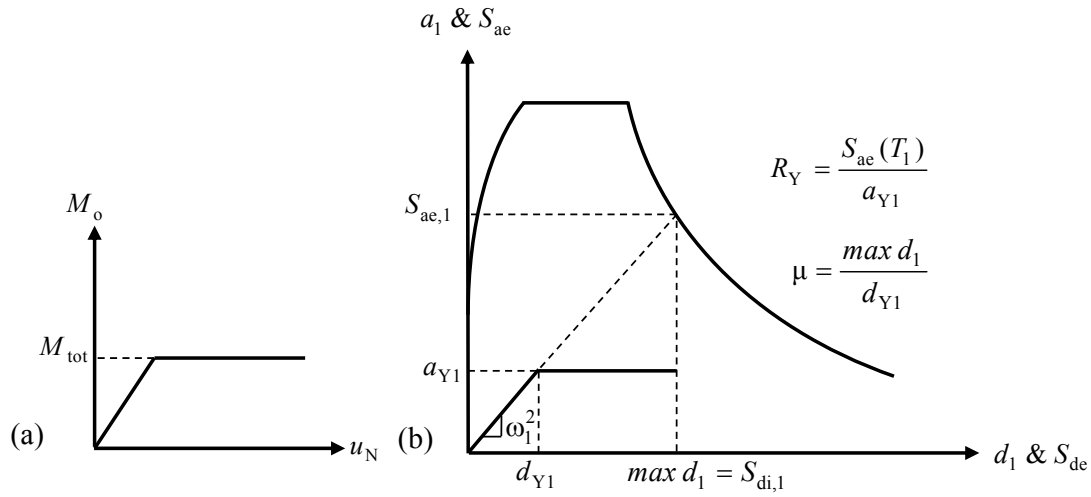

Figure 4.1. (a) Idealized pushover curve in terms of overturning moment vs. top displacement, (b) Corresponding modal capacity diagram in terms of modal acceleration vs. modal displacement with superimposed acceleration-displacement response spectrum.

Finally overall *ductility demand* of the coupled wall system under specified MCE earthquake can be readily estimated utilizing the well-known *equal displacement rule* as follows:

$$\mu = R_Y = \frac{S_{ae}(T_1)}{a_{Y1}} \qquad \rightarrow \qquad \mu = S_{ae}(T_1)\frac{m_{o1}^*}{M_{tot}} \tag{4.11}$$

If calculated ductility demand falls below the acceptable value, the preliminary design may be deemed to be successfully completed. For a satisfactory seismic performance under MCE level earthquake, results of the nonlinear response history analyses have suggested that overall ductility demand of a typical coupled core wall system should be bounded within the limits of $2.5 \le \mu \le 3.5$.

If the ductility demand is found acceptable, nonlinear performance evaluation stage can be initiated based on reinforcements calculated for the individual walls and the coupling beams, the latter of which is selected on the basis of estimated total coupling shear capacity. Detailed implementation of the procedure is described in the next section.

In conclusion, *total base overturning moment capacity* as well as the *ductility demand* of a coupled wall system can be estimated with a simple *strength of materials*

approach based on *first principles* followed by a novel alternate application of the pushover concept. There is no doubt that results obtained from those simple analyses provide very valuable information to the structural design engineer in the preliminary seismic design stage of a tall building project containing a coupled core wall system.

It is worth to remind that the same ductility demand estimation procedure is equally applicable to the base sections of the cantilever core wall systems following the straightforward estimation of the cantilever wall base overturning moment capacities.

5. IMPLEMENTATION AND EVALUATION OF CAPACITY AND DUCTILITY DEMAND ESTIMATION PROCEDURES FOR PRELIMINARY DESIGN OF COUPLED CORE WALL SYSTEMS

The implementation steps of the above-described capacity and ductility estimation procedures for preliminary design of a coupled core wall system are given in detail in the following. Also presented is the evaluation of the effects of the independent parameters on the capacity of the coupled core wall system.

5.1. Implementation Steps for Capacity and Ductility Demand Estimation Procedures

Step-by-step implementation of the capacity and ductility estimation procedures can be described as follows:

1) Establish the tall building structural system. Set the geometry of the coupled core wall system;
2) Run a static gravity load analysis (e.g., dead loads plus 30% of live loads) and calculate gravity loads, N_{0i}, and their normalized values, n_{0i}, acting on tension and compression walls (i = 1, 2);
3) Select concrete and reinforcing steel classes. Determine expected strengths, f_{ce} and f_{ye} from corresponding characteristic strengths, f_{ck} and f_{yk} according to $f_{ce} = 1.3 f_{ck}$ and $f_{ye} = 1.17 f_{yk}$, respectively;
4) Preliminarily reinforce the base sections of the tension and compression walls based on judgment or according to minimum code requirements. Determine A_{si}, ρ_i and ρ_{mi} using Eq.(3.5);
5) Plot $N_i - M_i$ yield surfaces (interaction diagrams at yield) of individual walls by neglecting strain-hardening. For practical purposes, equivalent yield strains of concrete and reinforcing steel can be taken as 0.003 and 0.01, respectively;
6) Select a relative yield parameter for the tension wall, β_1, considering the application range given by Eq.(3.9);

7) Calculate total coupling shear, n_{T1}, from Eq.(3.8) and calculate n_1 and n_2 from Eq.(3.7) and Eq.(3.10), respectively. Convert to corresponding forces T, N_1 and N_2, respectively, using Eq.(3.4). To avoid concrete crushing failure, ensure that N_2 has not exceeded the axial force corresponding to balance point on the yield surface.

   Comment: The last point may be critical for rectangular wall sections. Unless wall gravity loads are very high, concrete crushing due to bending is highly unlikely in ⊃ shaped walls, because the neutral axis lies almost always within the thickness of the flange, leading to very small compressive concrete strains.

8) Calculate bending moment capacities of individual walls M_1 and M_2 associated with the above-calculated axial forces N_1 and N_2, respectively, using *N-M* yield surfaces (Figure 3.2);

9) Calculate the *total base overturning moment capacity*, M_{tot}, using Eq.(3.2);

10) Calculate *participating modal mass for the base overturning moment*, m_{o1}^*, given by Eq.(4.7) and the natural period, T_1, of the first (dominant) mode of the tall building structural system, using appropriately estimated cracked section stiffness parameters;

    Comment: Recommended stiffness modifiers are 0.50 for walls, 0.15 – 0.20 for diagonally reinforced coupling beams and 0.30 for regularly reinforced coupling beams.

11) Calculate *modal yield pseudo-acceleration*, a_{Y1}, from Eq.(4.9); calculate y*ield strength reduction factor*, R_Y, under specified MCE earthquake from Eq.(4.10) and finally overall *ductility demand*, μ, of the coupled wall system under the same earthquake from Eq.(4.11);

12) If calculated ductility demand exceeds the acceptable ductility limit given in the previous section ($2.5 \le \mu \le 3.5$), preliminary design has to be repeated by increasing one or more of the three independent parameters specified in Section 3, namely, n_{0i}, ρ_{mi} and β_1. Since implementation of the above-described procedure is very easy and not time consuming, several trials can be made to search for an acceptable solution. Some guidance will be provided in Section 5.3 as to the effect of each independent parameter based on nonlinear evaluation studies performed.

Caution: Increasing the independent parameters would lead to a higher base overturning moment and hence a lower R_Y *and* μ. *However, increasing the independent parameters would also increase the coupling shear leading to overly strong coupling beams, which could create serious construction problems and at the same time could amplify the tensile strains in the tension wall to unacceptable levels. Therefore the lower limit of ductility factor* (*e.g.,* $\mu = 2.5$) *has to be observed as well.*

13) If calculated ductility demand is found satisfactory according to the ductility acceptance criterion given in the previous section ($2.5 \le \mu \le 3.5$), the *preliminary bending design of the wall base sections* may be deemed to be successfully completed for a symmetrical core wall system. If unsymmetrical, the above described steps are to be repeated by interchanging the tension and compression walls.

14) A preliminary estimation may also be made for the base shear demands of tension and compression walls by amplifying the first-mode base shear, which can be approximately calculated in terms of M_{tot}. Based on nonlinear response history analysis performed for the symmetrical coupled core wall systems presented in the following sections, base shear demand for each individual wall may be estimated for preliminary design purpose as

$$V_{base} \cong \frac{M_{tot}}{0.7H} \alpha_{VH} \alpha_{VM} \tag{5.1}$$

where H represents the total building height, α_{VH} is the dynamic shear amplification factor accounting for higher mode effects and α_{VM} denotes the dynamic shear amplification factor representing shear migration from the yielding tension wall to the compression wall at sections near the base. Recommended dynamic shear amplification factors for preliminary design are:

$$\alpha_{VH} \cong 1.5 \quad ; \quad \alpha_{VM} \cong 2 \tag{5.2}$$

15) The last step is the selection of the coupling beam reinforcements based on total coupling shear, T, calculated above in Step 7. It is assumed that this total shear force is distributed to coupling beams throughout the building and that all have yielded.

Comment: Preferred reinforcement scheme for the coupling beams is diagonal reinforcement. In the evaluation studies given below, all coupling beams have been dimensioned with a depth/span ratio of 1/2 with diagonal reinforcement.

5.2. Example Coupled Core Wall Systems

In order to evaluate the effects of the three independent parameters controlling the capacity of the coupled core wall system, a parametric study is performed and several tall buildings with a central core wall system and peripheral gravity columns are designed, ranging from 25 to 50 stories. Properties of designed coupled core wall systems are as following;

- All cores are of square hollow sections in plan with openings only in one direction spanned by coupling beams with a constant depth/span ratio of ½, thus forming a symmetrical coupled core wall system.
- Thickness of wall sections is reduced gradually at two levels through the height of buildings. Thickness of coupling beams is equal to thickness of wall sections at each storey level.
- Outer plan dimensions of square cores are selected as 10 m, 12 m, 14 m and 16 m, called CW10, CW12, CW14 and CW16, respectively.
- Heights of the coupled core wall systems are arranged so that aspect ratio (height over length) of the core would be equal to 10 and 14.
- For each building type, two sets of wall gravity loading were considered by changing the tributary floor areas for walls while keeping the total floor masses unchanged. This has been deliberately arranged such that normalized wall gravity loads are specified as 0.075 and 0.125 at the base level of buildings with aspect ratio of 10, 0.175 and 0.225 for the buildings with aspect ratio of 14. Thus for each building type, only one linear model is defined based on the linear stiffness characteristics, while two different nonlinear are defined based on different strength characteristics due to different gravity loading applied to the core walls. Masses are the same in both linear and nonlinear models.
- Walls are reinforced according to the requirements of the Turkish Seismic Design Code [5]. Minimum wall total reinforcement ratio is designated as $\rho_I = \rho_{mI}$. However, for CW12 coupled core wall systems, additional models were created for two higher levels of wall reinforcement ratio. In these models, mechanical wall

reinforcement ratio is increased by only increasing the reinforcement ratio of wall boundary zones ($\rho_m = 2\rho_{mI}$ and $\rho_m = 3\rho_{mI}$).

Properties of designed coupled core wall systems are summarized in Table 5.1 through Table 5.8 and typical plans of coupled core wall systems are shown in Figure 5.1.

Table 5.1. CW10 models with 25 stories.

CW10	Number of stories	Height of each storey *(m)*	Aspect Ratio	n_0	ρ_m	Length of wall web *(m)*	Length of wall flanges *(m)*	Thickness of wall at 1^{st}-9^{th} stories *(m)*	Thickness of wall at 10^{th}-17^{th} stories *(m)*	Thickness of wall at 18^{th}-25^{th} stories *(m)*	Height of coupling beams *(m)*	Critical wall height - H_{cr} *(m)*
CW10-0.075	25	4	10	0.075	ρ_{mI}	10	4	0.6	0.5	0.4	1	16
CW10-0.125	25	4	10	0.125	ρ_{mI}	10	4	0.6	0.5	0.4	1	16

Table 5.2. CW10 models with 35 stories.

CW10	Number of stories	Height of each storey *(m)*	Aspect Ratio	n_0	ρ_m	Length of wall web *(m)*	Length of wall flanges *(m)*	Thickness of wall at 1^{st}-15^{th} stories *(m)*	Thickness of wall at 16^{th}-25^{th} stories *(m)*	Thickness of wall at 26^{th}-35^{th} stories *(m)*	Height of coupling beams *(m)*	Critical wall height - H_{cr} *(m)*
CW10-0.175	35	4	14	0.175	ρ_{mI}	10	4	0.6	0.5	0.4	1	24
CW10-0.225	35	4	14	0.225	ρ_{mI}	10	4	0.6	0.5	0.4	1	24

Table 5.3. CW12 models with 30 stories.

CW12	Number of stories	Height of each storey *(m)*	Aspect Ratio	n_0	ρ_m	Length of wall flanges *(m)*	Length of wall webs *(m)*	Thickness of wall at 1^{st}-10^{th} stories *(m)*	Thickness of wall at 11^{th}-20^{th} stories *(m)*	Thickness of wall at 21^{th}-30^{th} stories *(m)*	Height of coupling beams *(m)*	Critical wall height - H_{cr} *(m)*
CW12-0.075	30	4	10	0.075	ρ_{mI}	12	4.75	0.75	0.6	0.45	1.25	20
CW12-0.075	30	4	10	0.075	$2\rho_{mI}$	12	4.75	0.75	0.6	0.45	1.25	20
CW12-0.075	30	4	10	0.075	$3\rho_{mI}$	12	4.75	0.75	0.6	0.45	1.25	20
CW12-0.125	30	4	10	0.125	ρ_{mI}	12	4.75	0.75	0.6	0.45	1.25	20
CW12-0.125	30	4	10	0.125	$2\rho_{mI}$	12	4.75	0.75	0.6	0.45	1.25	20
CW12-0.125	30	4	10	0.125	$3\rho_{mI}$	12	4.75	0.75	0.6	0.45	1.25	20

Table 5.4. CW12 models with 40 stories.

CW12	Number of stories	Height of each storey *(m)*	Aspect Ratio	n_0	ρ_m	Length of wall web *(m)*	Length of wall flanges *(m)*	Thickness of wall at 1^{st}-15^{th} stories *(m)*	Thickness of wall at 16^{th}-28^{th} stories *(m)*	Thickness of wall at 29^{th}-40^{th} stories *(m)*	Height of coupling beams *(m)*	Critical wall height - H_{cr} *(m)*
CW12-0.175	40	4	14	0.175	ρ_{mI}	12	4.75	0.75	0.6	0.45	1.25	28
CW12-0.175	40	4	14	0.175	$2\rho_{mI}$	12	4.75	0.75	0.6	0.45	1.25	28
CW12-0.175	40	4	14	0.175	$3\rho_{mI}$	12	4.75	0.75	0.6	0.45	1.25	28
CW12-0.225	40	4	14	0.225	ρ_{mI}	12	4.75	0.75	0.6	0.45	1.25	28
CW12-0.225	40	4	14	0.225	$2\rho_{mI}$	12	4.75	0.75	0.6	0.45	1.25	28
CW12-0.225	40	4	14	0.225	$3\rho_{mI}$	12	4.75	0.75	0.6	0.45	1.25	28

Table 5.5. CW14 models with 35 stories.

CW14	Number of stories	Height of each storey *(m)*	Aspect Ratio	n_0	ρ_m	Length of wall web *(m)*	Length of wall flanges *(m)*	Thickness of wall at 1^{st}-11^{th} stories *(m)*	Thickness of wall at 12^{th}-23^{th} stories *(m)*	Thickness of wall at 24^{th}-35^{th} stories *(m)*	Height of coupling beams *(m)*	Critical wall height - H_{cr} *(m)*
CW14-0.075	35	4	10	0.075	ρ_{mI}	14	5.75	0.85	0.7	0.55	1.25	24
CW14-0.125	35	4	10	0.125	ρ_{mI}	14	5.75	0.85	0.7	0.55	1.25	24

Table 5.6. CW14 models with 50 stories.

CW14	Number of stories	Height of each storey *(m)*	Aspect Ratio	n_0	ρ_m	Length of wall web *(m)*	Length of wall flanges *(m)*	Thickness of wall at 1^{st}-20^{th} stories *(m)*	Thickness of wall at 21^{th}-35^{th} stories *(m)*	Thickness of wall at 36^{th}-50^{th} stories *(m)*	Height of coupling beams *(m)*	Critical wall height - H_{cr} *(m)*
CW14-0.175	50	4	14	0.175	ρ_{mI}	14	5.75	0.85	0.7	0.55	1.25	40
CW14-0.225	50	4	14	0.225	ρ_{mI}	14	5.75	0.85	0.7	0.55	1.25	40

Table 5.7. CW16 models with 35 stories.

CW16	Number of stories	Height of each storey *(m)*	Aspect Ratio	n_0	ρ_m	Length of wall web *(m)*	Length of wall flanges *(m)*	Thickness of wall at 1^{st}-11^{th} stories *(m)*	Thickness of wall at 12^{th}-23^{th} stories *(m)*	Thickness of wall at 24^{th}-35^{th} stories *(m)*	Height of coupling beams *(m)*	Critical wall height - H_{cr} *(m)*
CW16-0.075	35	4.5	10	0.075	ρ_{ml}	16	6.5	1	0.8	0.6	1.5	27
CW16-0.125	35	4.5	10	0.125	ρ_{ml}	16	6.5	1	0.8	0.6	1.5	27

Table 5.8. CW16 models with 50 stories.

CW16	Number of stories	Height of each storey *(m)*	Aspect Ratio	n_0	ρ_m	Length of wall web *(m)*	Length of wall flanges *(m)*	Thickness of wall at 1^{st}-20^{th} stories *(m)*	Thickness of wall at 21^{th}-35^{th} stories *(m)*	Thickness of wall at 36^{th}-50^{th} stories *(m)*	Height of coupling beams *(m)*	Critical wall height - H_{cr} *(m)*
CW16-0.175	50	4.5	14	0.175	ρ_{ml}	16	6.5	1	0.8	0.6	1.5	45
CW16-0.225	50	4.5	14	0.225	ρ_{ml}	16	6.5	1	0.8	0.6	1.5	45

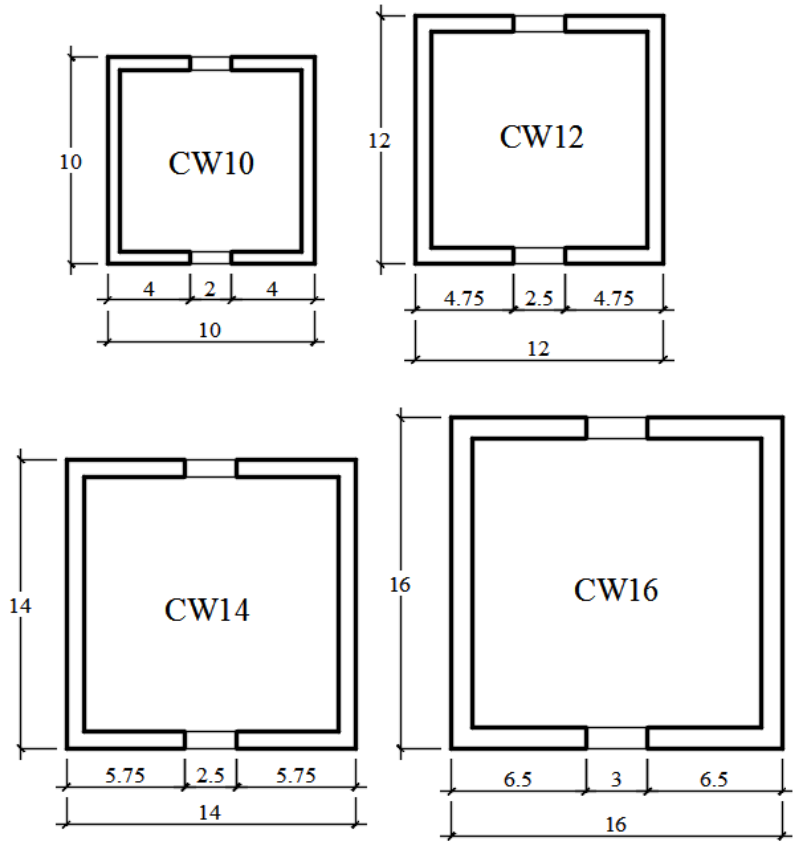

Figure 5.1. Four types of coupled core wall systems (all dimensions are in meters).

5.3. Evaluation of Effects of Independent Parameters on Coupled Core Wall Capacity and Ductility Demand

Since analyses of the above-defined core wall systems exhibit rather similar results, only 12 m square symmetrical core wall system, called CW12 is evaluated here, as shown in Figure 5.2. Evaluations are performed under a MCE level earthquake with a typical code pseudo-acceleration spectrum as given in Figure 5.3.

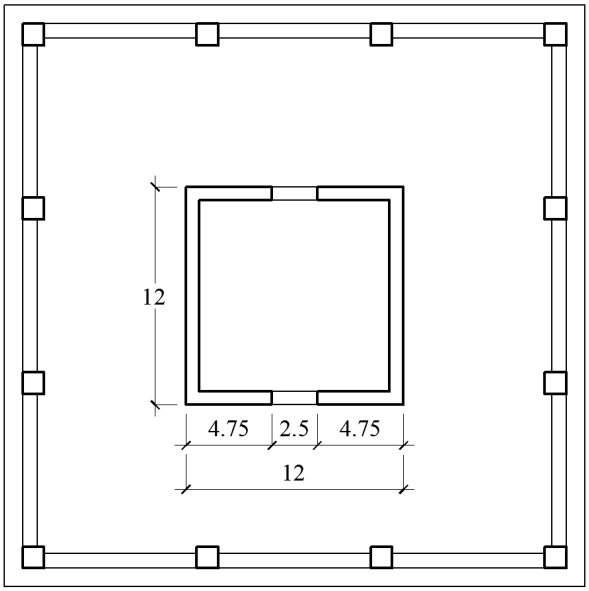

Figure 5.2. Coupled core wall system CW12 where effects of independent parameters are evaluated.

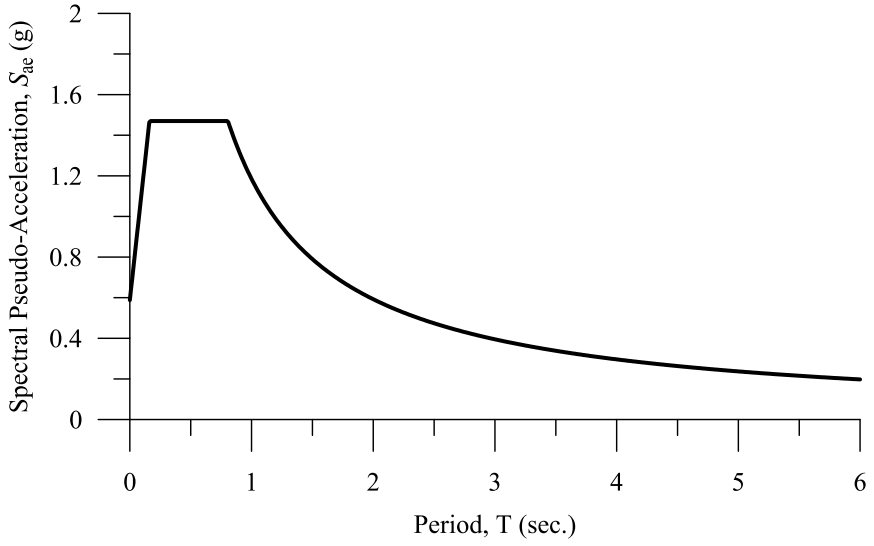

Figure 5.3. Pseudo-acceleration spectrum of MCE level earthquake used for evaluations.

Table 5.9 summarizes the evaluation results in terms of total coupling shear and ductility demand for four levels of normalized wall gravity load, three levels of wall reinforcement ratio and five levels of relative yield parameter of the tension wall. Results are also presented in graphical form in Figure 5.4 through Figure 5.7. Wall numbers in subscripts are dropped due to symmetrical arrangement of the coupled core wall system. *Expected material strengths* are used as indicated at the footer of Table 5.9.

Figure 5.8 successfully confirms the total base overturning moment capacities obtained by the proposed procedure by comparing them with those obtained by nonlinear response history analysis with respect to several values of ductility factors. Details of nonlinear modeling and nonlinear response history analysis of coupled core wall system will be presented in Chapter 6 and Chapter 7, respectively.

Some important conclusions may be drawn from Table 5.9 and Figure 5.4 through Figure 5.7.

a) As long as concrete crushing is avoided in the compression wall, higher values of wall gravity loads n_0 are beneficial in $\supset$ shaped walls, as indicated in implementation step 7 of the capacity estimation procedure given in Section 5.1. The outcome would be a direct increase in base overturning moment capacity and decrease in overall ductility demand. However cautious application reminded in Step 12 of the capacity and demand estimation procedures is to be observed.

b) Contribution of $\beta\rho_m$ is more pronounced for lower n_0 levels. For higher values of n_0, contribution of $\beta\rho_m$ remains limited.

c) For $\beta < 0$, increase in ρ_m causes further decrease in n_T, leading to a lower overturning moment capacity. In other words, it would correspond to a design state with higher amount of reinforcement in walls, but lower amount of reinforcement in coupling beams. Hence behavior of coupled core wall system approaches to behavior of two uncoupled walls. Therefore, it is not a convenient design option, since axial force and bending capacities of both walls could not be used effectively.

d) For $\beta > 0$, increase in ρ_m causes further increase in n_T, leading to a larger overturning moment capacity. In other words, it would correspond to a design state with increasing amount of reinforcement in walls and coupling beams

simultaneously. Hence, behavior of coupled core wall system approaches to the behavior of single tube section. Therefore, considerable degree of coupling shear capacity is obtained, thus leading to a larger overturning moment capacity and lower system ductility demand.

e) Considering two coupled core wall systems having same dimensions and wall reinforcement (same ρ_m) but different axial gravity loads, in order to reach the same coupling shear capacity and similar values of ductility demand, the coupled core wall system having lower axial gravity load would need higher β value than the one with higher axial gravity load (see Eq.(3.8)). Since β is the *relative yield parameter*, when higher β is used in capacity estimation procedure, higher inelastic tension strains would take place at base section of tension wall.

Considering two coupled core wall systems having same dimensions, coupling beam reinforcement and β value but different axial gravity loads, the coupled core wall system having lower axial gravity load would need higher amount of reinforcement in walls than those with the higher axial gravity load.

Thus, axial gravity load could be advantageous for coupled core wall systems for either reducing inelastic tensile strains in tension wall or reducing amount of reinforcement in walls.

Table 5.9. Variation of n_T and $\mu = R_Y$ with respect to n_0, ρ_m and β for CW12.

ρ_m	β	30 story building				40 story building			
		$T_1 = 3.3\ s$				$T_1 = 5.7\ s$			
		$n_0 = 0.075$		$n_0 = 0.125$		$n_0 = 0.175$		$n_0 = 0.225$	
		n_T	μ	n_T	μ	n_T	μ	n_T	μ
ρ_{mI}	– 1.0	0.041	7.1	0.091	4.3	0.141	4.2	0.191	3.3
	– 0.5	0.058	6.0	0.108	3.9	0.158	3.9	0.208	3.1
	0	0.075	5.3	0.125	3.6	0.175	3.7	0.225	3.0
	0.5	0.092	4.7	0.142	3.3	0.192	3.5	0.242	2.8
	1.0	0.110	4.2	0.160	3.1	0.210	3.3	0.260	2.7
$2\rho_{mI}$	– 1.0	0.006	8.9	0.056	4.8	0.106	4.6	0.156	3.5
	– 0.5	0.041	6.1	0.091	3.9	0.141	3.9	0.191	3.1
	0	0.075	4.6	0.125	3.3	0.175	3.5	0.225	2.8
	0.5	0.110	3.8	0.160	2.9	0.210	3.1	0.260	2.6
	1.0	0.144	3.2	0.194	2.5	0.244	2.8	0.294	2.4
$3\rho_{mI}$	– 1.0	-	-	0.022	5.6	0.072	5.1	0.122	3.7
	– 0.5	0.023	6.2	0.073	3.9	0.123	4.0	0.173	3.1
	0	0.075	4.2	0.125	3.0	0.175	3.3	0.225	2.7
	0.5	0.127	3.2	0.177	2.5	0.227	2.9	0.277	2.4
	1.0	0.179	2.6	0.229	2.2	0.279	2.5	0.329	2.2
$f_{ce} = 65\ Mpa$; $f_{ye} = 491.4\ Mpa$; $\rho_I = 0.00457$; $\rho_{mI} = (f_{ye} / f_{ce})\rho_I = 0.0345$									

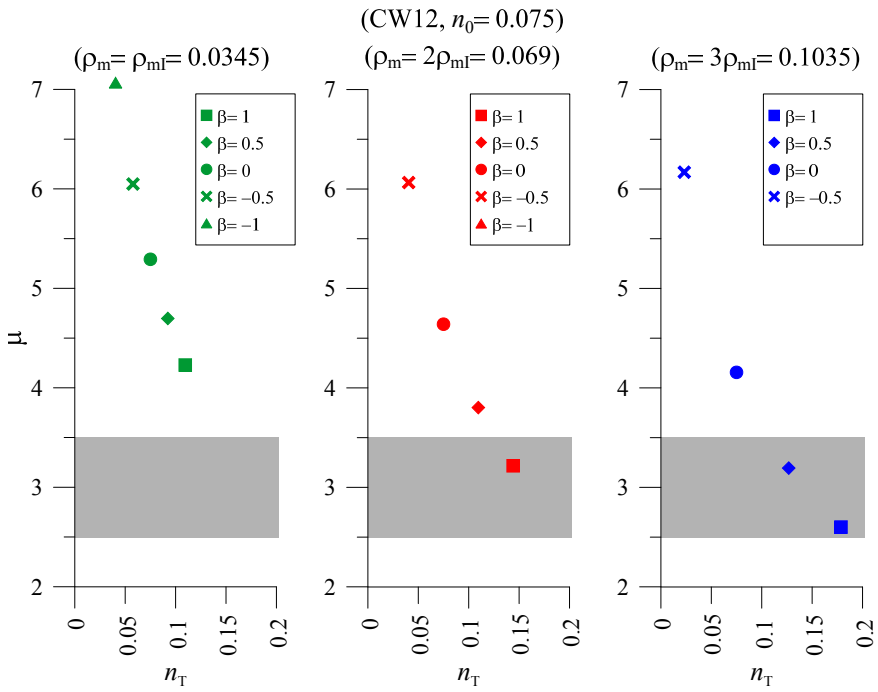

Figure 5.4. Ductility demand vs total coupling shear for various combinations of wall mechanical reinforcement ratio and relative yield parameter (CW12, n_0 = 0.075).

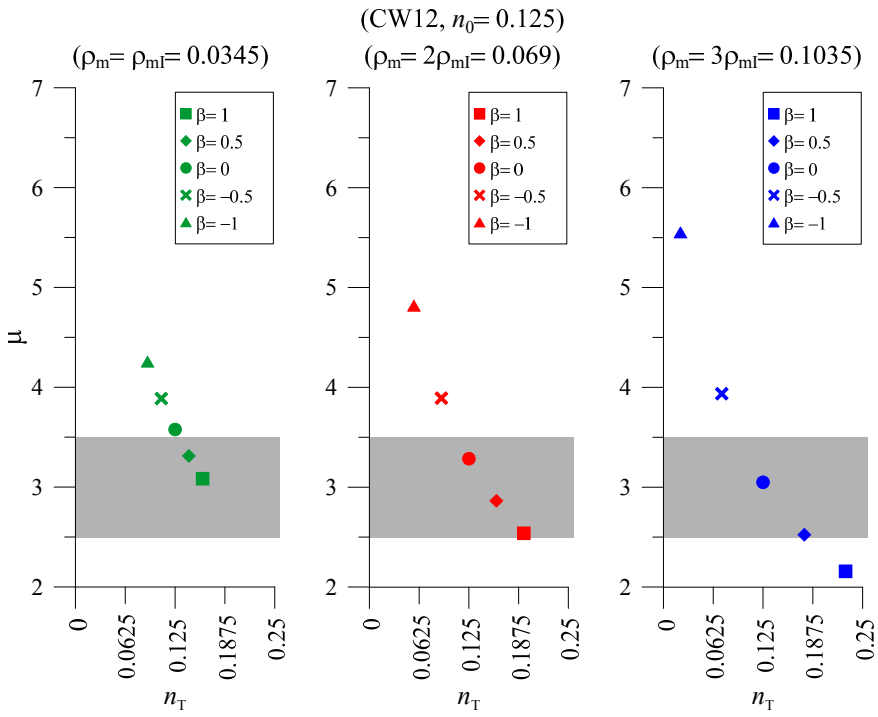

Figure 5.5. Ductility demand vs total coupling shear for various combinations of wall mechanical reinforcement ratio and relative yield parameter (CW12, n_0 = 0.125).

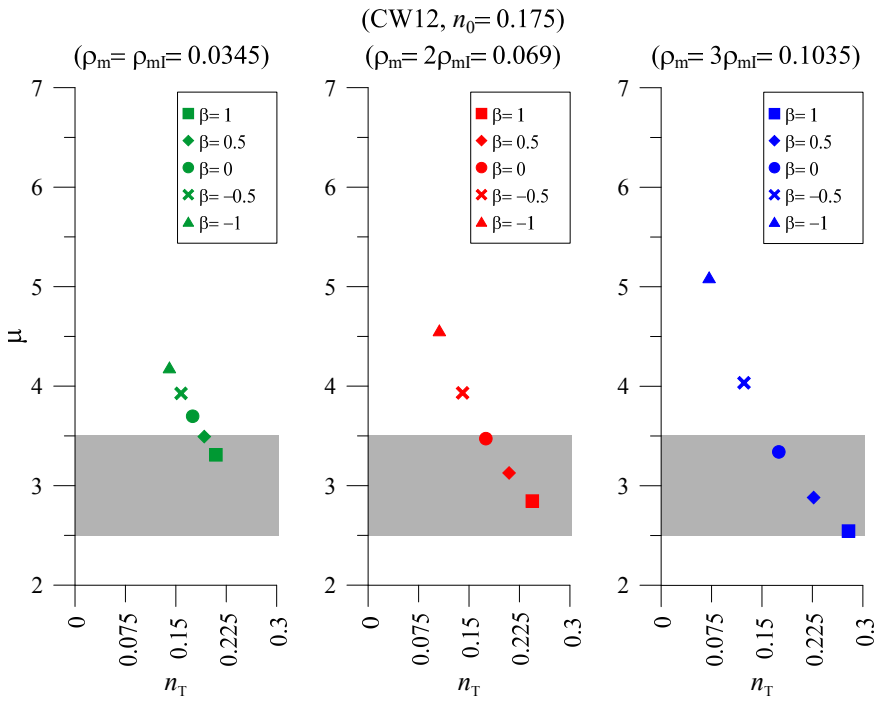

Figure 5.6. Ductility demand vs total coupling shear for various combinations of wall mechanical reinforcement ratio and relative yield parameter (CW12, n_0 = 0.175).

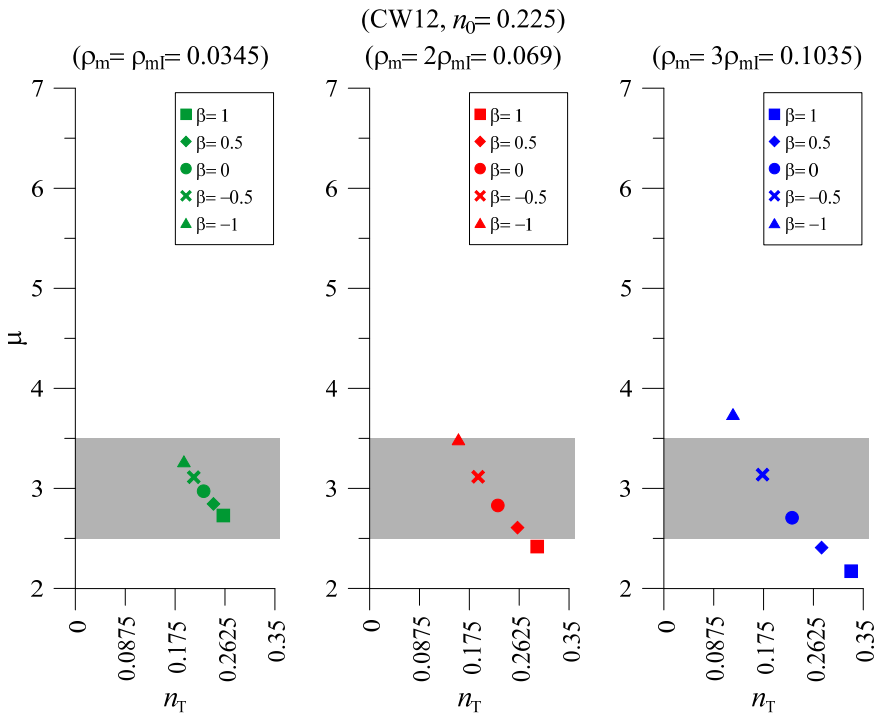

Figure 5.7. Ductility demand vs total coupling shear for various combinations of wall mechanical reinforcement ratio and relative yield parameter (CW12, n_0 = 0.225).

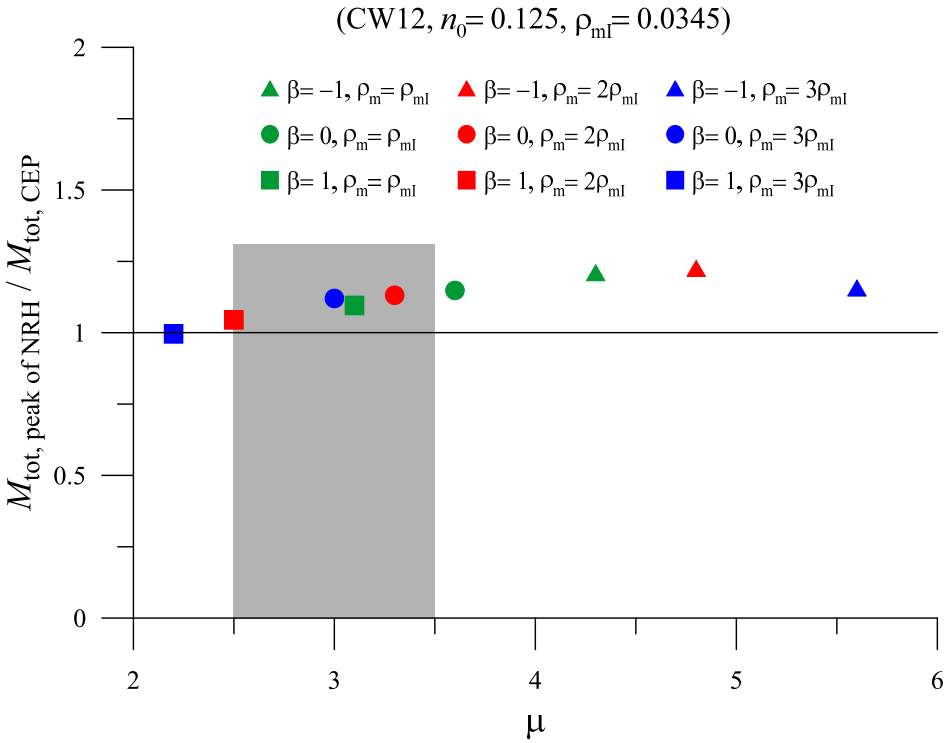

Figure 5.8. Total base overturning moment capacity obtained from NRHA divided by the same from proposed procedure versus ductility demand (CW12, n_0 = 0.125, Chi-Chi earthquake).

6. NONLINEAR MODELING OF COUPLED CORE WALL SYSTEMS

6.1. General

Nonlinear modeling of structural components has always been a challenge for researchers. Basic criteria that should be taken into account in nonlinear modeling could be summarized as follows;

- Nonlinear model of a structural component should adequately reflect actual behavior of that component under all possible loading types.
- Computational effort, thereby elapsed time for performing nonlinear analysis should be reasonably low.
- Nonlinear model should be general rather than being case sensitive.

Nonlinear analysis of a structure is a combination of nonlinear model of structural members, nonlinear models of structural materials and definition of loading and solution procedures. Even assumptions are inevitable within this combination, they should always be consistent and reasonable in order to reach an acceptable degree of accuracy.

In state of the art, structural component model types for simulating nonlinear response of reinforced concrete members can be grouped into two categories, based on the way of modeling the spread of plasticity [65-11-66], namely, concentrated (lumped) plasticity and distributed plasticity models (Figure 6.1).

Concentrated plasticity models involve elements with plastic hinges or nonlinear spring hinges at each end of the member, while distributed plasticity models include elements with either finite length plasticity zones or spread of plasticity along the whole length of element.

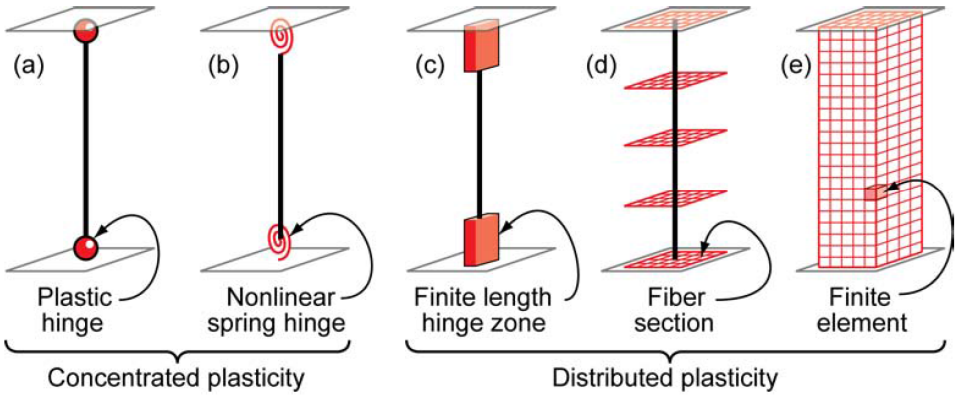

Figure 6.1. Idealized models of beam-column elements [65].

In concentrated plasticity models, overall force-deformation response of the member, associated with observed behavior and hysteretic test data, is defined through plastic hinges or nonlinear spring hinges. As mentioned in the literature review, lumped plasticity approach has long been used for both beam and column elements in terms of moment-rotation relationships with or without including axial force-flexure and shear force-flexure interaction effects. The key point is the definition of hysteretic rules in calibration with member test data. Therefore, nonlinear response parameters, such as strength degradation, unloading and reloading stiffness values, pinching effects, nonlinear interaction of axial force-shear-flexure, are obtained by experiments and then imposed as hysteretic rules. Advantages of concentrated plasticity models are having relatively condensed, numerically efficient formulations and providing plastic rotation values which are easy to interpret with convenient acceptance criteria.

In distributed plasticity models with fiber sections, the element is subdivided into a number of longitudinal uniaxial fibers, which represent a particular material of the section governed by a stress-strain relation defined for that material. Therefore, constitutive force-deformation relationship of the element is not prescribed; instead, it is derived by integration of each fiber's uniaxial stress-strain relation through the cross section and along the member with enforcing the "plane section remains plane" assumption. State of stress and strain values of each fiber are provided as an output of inelastic deformation, which can be quite sensitive to the moment gradient, element length, integration method and strain hardening parameters [65].

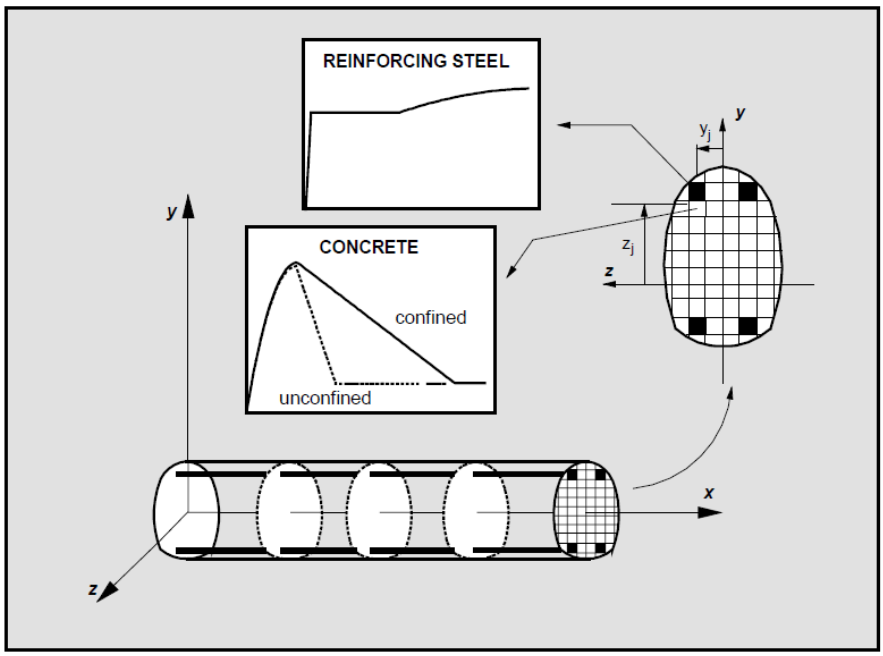

Figure 6.2. Fiber Element: Distribution of Control Sections and Section Subdivision into Fibers [66].

In finite length hinge zone models, cross sections in the inelastic hinge zones could be characterized by explicit fiber-section integrations. Integration of deformations along the hinge length captures the spread of plasticity as superiority over concentrated hinge models as the finite length of plasticity zone could also be calculated.

Continuum finite element models are the most complex distributed plasticity models of which nonlinear behavior of structural members are modeled explicitly. Two or three dimensional finite elements are used representing the concrete, longitudinal reinforcement and shear reinforcement, of which associated constitutive models would represent concrete crushing-cracking-dilatation, steel yielding-buckling-fracture, and bond transfer between steel and concrete [11]. In that sense, continuum finite element models are more capable of capturing the physics of nonlinear behavior of reinforced concrete members without using prescribed rules of force-deformation relationships, stiffness values, strength and deformation capacities, as these effects are inherently taken into account by nonlinear material models. The disadvantage of continuum finite element model is the requirements of excessive amount of time spent for modeling of a structure and analyzing it with higher computational effort.

6.2. Modeling of Structural Walls

Considering nonlinear behavior of reinforced concrete columns and walls, significant effort has been spent for modeling these structural components.

In plastic hinge models, effects of axial force-flexure interaction could be taken into account by defining an axial force-moment interaction surface which assumes either constant stiffness values within the yield surface [30-32-33-34] or changing stiffness depending on axial force level [37-38-46]. However, behavior under coupled shear-flexure interaction could never been modeled with lumped plasticity models, although shear yielding and degrading shear rigidity were employed with inelastic shear springs independent of flexure actions [32-33-34-37-38-39-40].

As an alternative modeling technique, multiple-vertical-line-element-model (MVLEM) has been formulated for modeling of reinforced concrete wall members in order to capture experimentally observed behavior that cannot be obtained by using one dimensional frame elements. This wall element model is based on idealization of a wall member with multiple vertical line elements connected to infinitely rigid beams at top and bottom of element (Figure 6.3). More detailed information about development of multiple vertical line element analogy could be found in Vulcano [68] and Orakcal *et al.* [67]. As described in Figure 6.3, while axial and flexural behavior is represented by vertical springs with axial stiffness K_1 to K_n, a horizontal spring with stiffness K_h with an appropriate hysteretic behavior characterizes the nonlinear shear response of the wall element. A relative rotation is assumed to occur around a point that was defined at a distance from the bottom of the element on centroid axis. In MVLEM, each vertical line element represents a force-deformation relationship obtained by an axial-stiffness hysteresis model [68] (Figure 6.4).

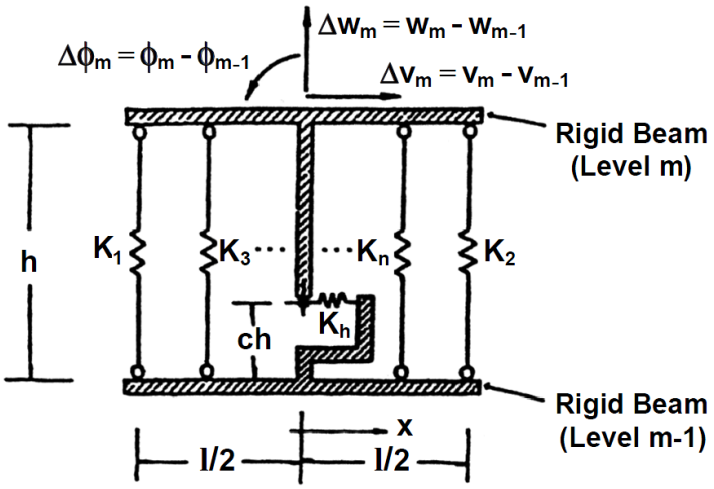

Figure 6.3. Multiple-vertical-line-element model [68].

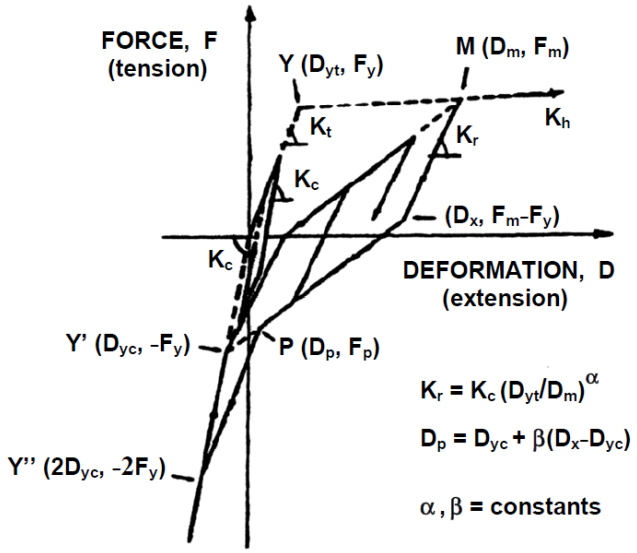

Figure 6.4. Axial-stiffness hysteresis model [68].

The so-called fiber modeling may be considered as an improved version of MVLEM where each fiber's force-deformation response is obtained by constitutive cyclic nonlinear material models created for confined concrete and reinforcing steel (Figure 6.5, Figure 6.6 and Figure 6.7).

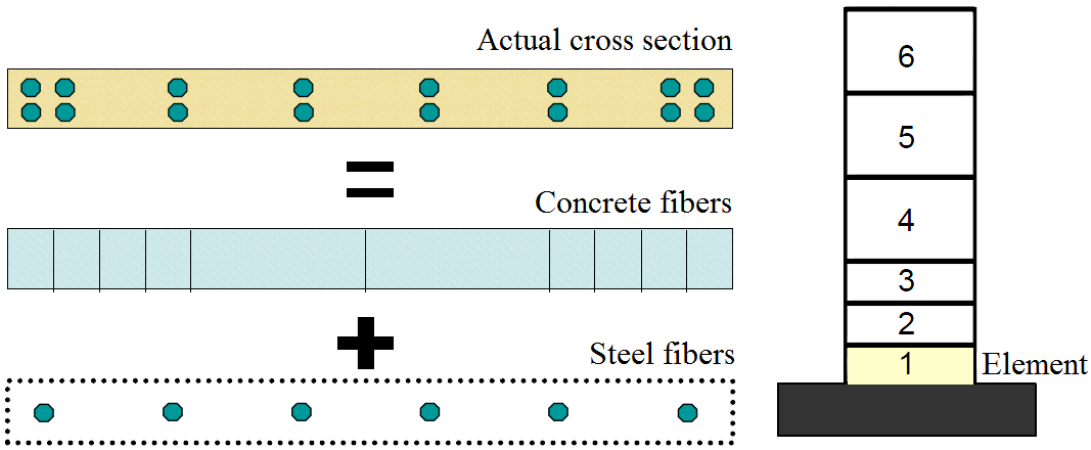

a) Fiber model of cross-section b) Elevation of wall

Figure 6.5. Fiber element representation of a reinforced concrete wall segment [11].

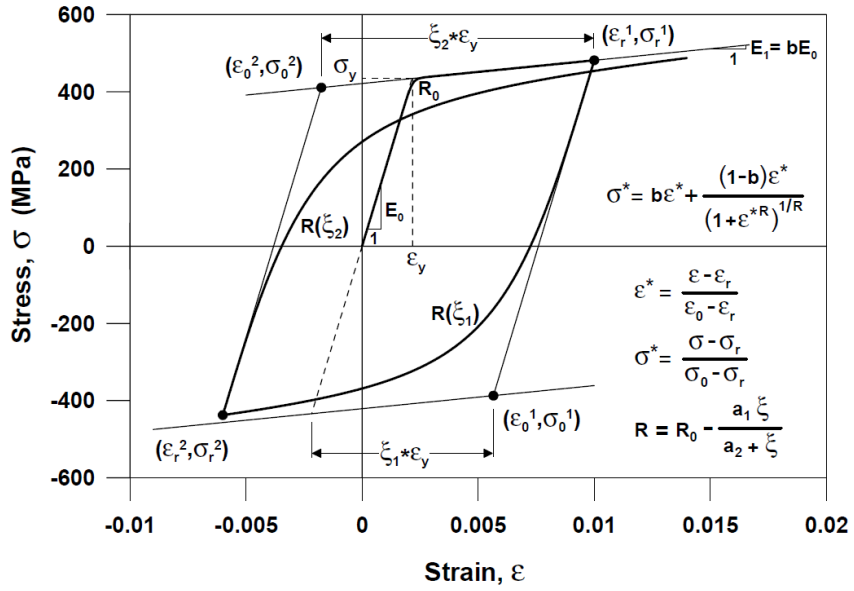

Figure 6.6. Constitutive model parameters for reinforcing steel [70-67].

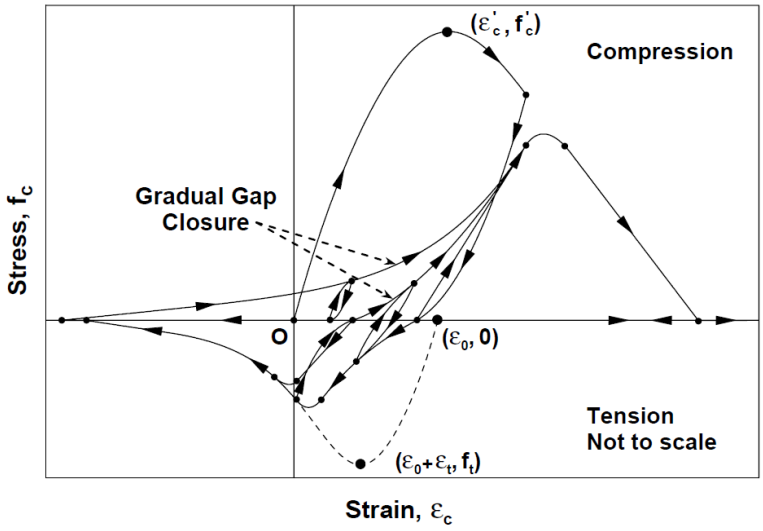

Figure 6.7. Constitutive model parameters for concrete [71-67].

Fiber model has several superiorities over one dimensional equivalent beam-column element models. As such, instead of assigning constant effective flexural stiffness or assuming a degrading stiffness model depending on axial load, axial and flexural stiffness are calculated based on the specified material relations, varying depending on the magnitude of axial load. Also, spread of plasticity could be represented by stacking of elements one over another (Figure 6.5) and migration of neutral axis through the section under cyclic loading could be accurately captured. Although shear and flexure behaviors are uncoupled in fiber model, various attempts were made for modeling coupled shear-flexure interaction effects [67-72-73-74-75].

As third modeling option, reinforced concrete structural walls could be modeled by using two-dimensional nonlinear finite-elements [58-60]. As an example of continuum finite element model [58], wall members were represented with three and four node shell elements of which main flexural reinforcing bars are modeled by discrete truss elements with perfect bond between steel. Although continuum finite element models are most convenient for the physical behavior of structural walls, these models cannot be widely used by practicing structural engineers for the time being, since they require very complicated modeling and excessive amount of analysis time.

In this study, PERFORM-3D [76] structural analysis software is used for modeling and analyzing coupled core wall systems, which utilizes fiber elements for modeling of structural walls. Some details for wall sections of coupled core wall systems designed in this study are presented in the following figures.

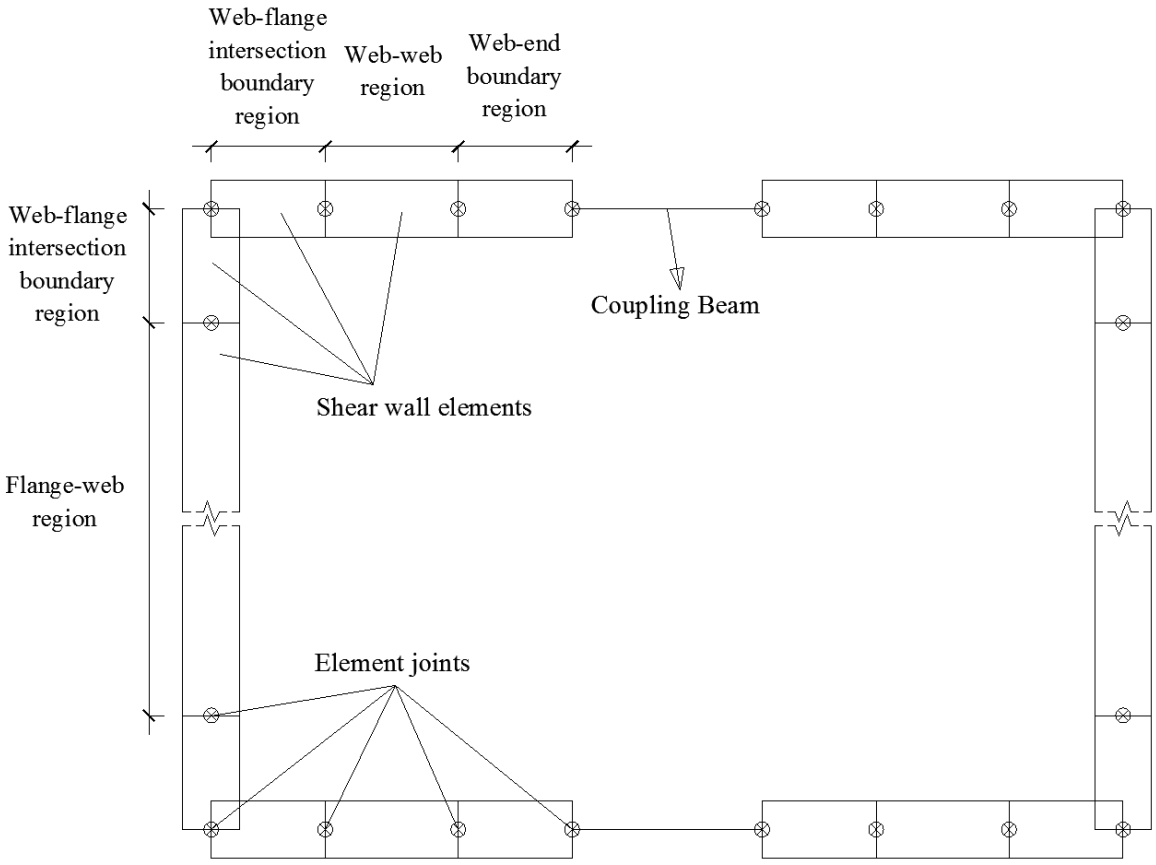

Figure 6.8. Typical coupled core wall system modeled in PERFORM-3D.

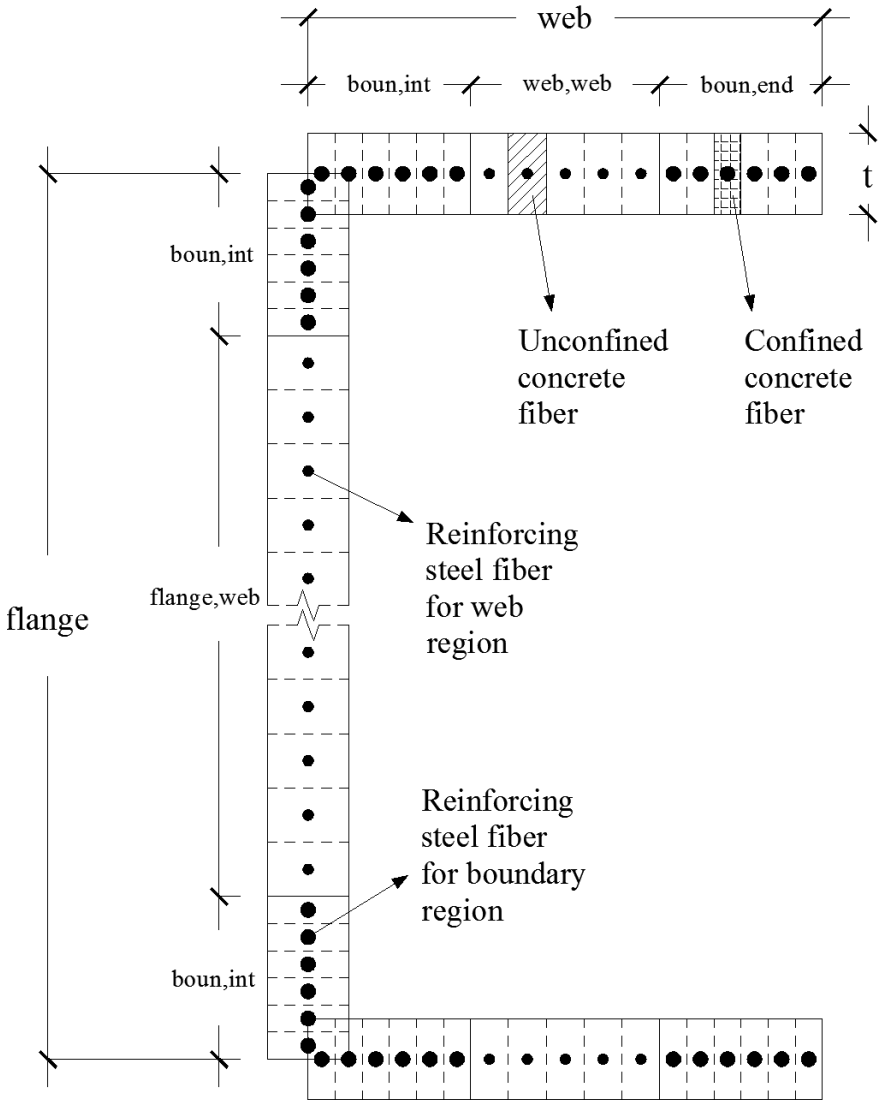

Figure 6.9. Details of shear wall elements.

Each pier is modeled by 9 shear wall elements, 3 for flange of pier and 3 for each web of pier (Figure 6.8). Lengths of boundary and web regions are defined as per provisions of Turkish Seismic Design Code. Each element is divided by a number of fibers representing reinforcement and concrete as shown in Figure 6.9. For three types of fibers representing unconfined concrete, confined concrete and reinforcement, *expected material stress-strain* relationships are defined with cyclic degradation characteristics (Figure 6.10, Figure 6.11, Figure 6.12). Elastic shear material is defined for shear wall elements superimposed as an additional layer onto concrete fiber elements with an effective shear modulus, equal to 10% of modulus of elasticity of concrete material ($G=0.1E_c$) [78].

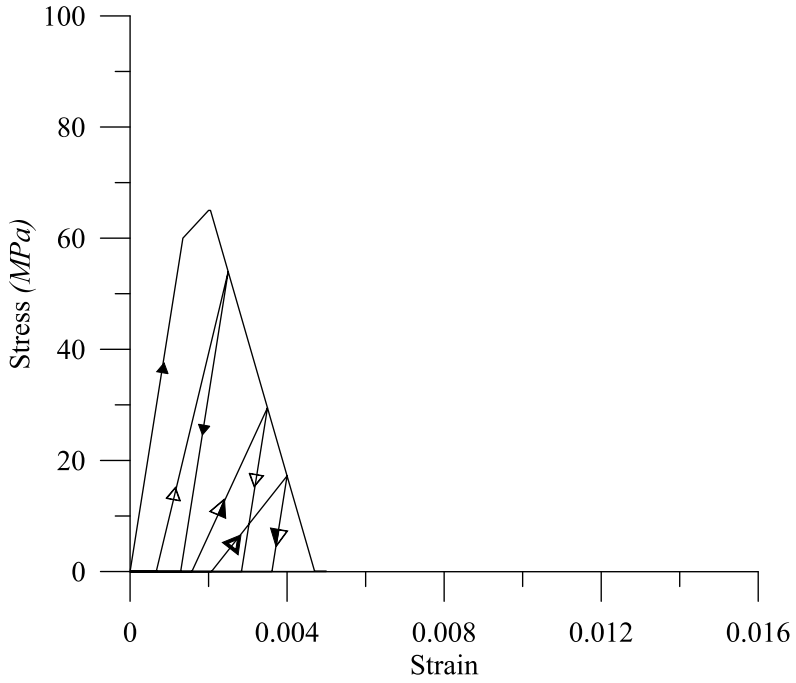

Figure 6.10. Unconfined concrete stress – strain relationships used in this study.

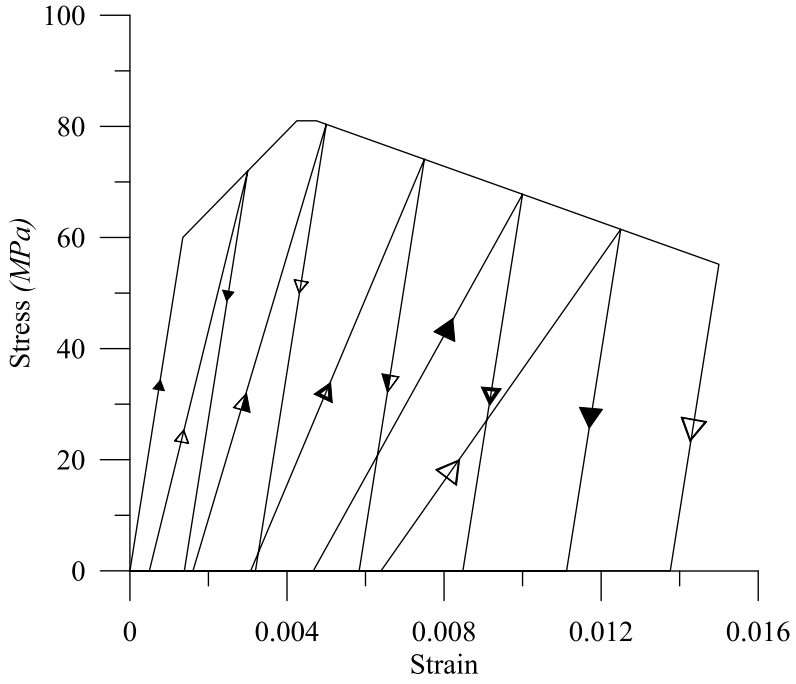

Figure 6.11. Confined concrete stress – strain relationships used in this study.

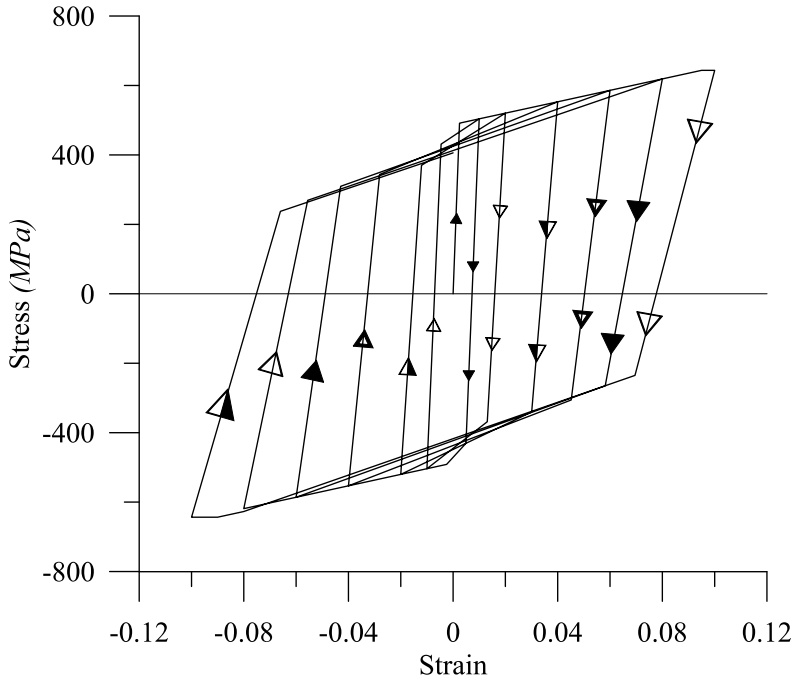

Figure 6.12. Reinforcing steel stress – strain relationships used in this study.

6.3. Modeling of Coupling Beams

In order to have benefit of coupling action between wall piers and coupling beams, the latter must be *sufficiently strong*. In the literature, it has been observed that slender beams with conventional reinforcement could not exhibit adequate strength and deformation capacity necessary for providing required level of coupling. Therefore, alternative forms have been searched for coupling beams with low span to depth ratio that are capable of resisting high shear stress. Diagonally reinforced coupling beams have been found to be a convenient option of which shear capacity is provided by confined diagonal bundles including reinforcement and concrete. Difficulties in placing reinforcement and casting concrete inside these congested bundles have led to searching better alternatives such as diagonal reinforcement with full section confinement instead of bundle confinement, rhombic reinforcement layout, and steel coupling beams with or without post-tensioning. However, designing diagonally reinforced coupling beams with confined bundles is the most common option in the current state of the art for coupling beams with depth to span ratio around ½ or even less.

No matter how the coupling beams are designed, designer ends up with two questions, of which answers directly affect the behavior of coupled core wall system; what should be the strength capacity of coupling beams, in other words how much shear force should be transmitted to walls for axial force coupling, and secondly what could be the ductility capacity of those coupling beams?

In this study, diagonally reinforced coupling beams with confined bundles are selected and modeled with strut and tie analogy, as similar to Hindi and Hassan [53]. Diagonal reinforcement and core concrete inside the bundles are modeled with *steel ties* and *concrete struts*, respectively, as described in Figure 6.13. Reinforcement and confined concrete stress-strain relationships with hysteresis characteristics were assigned to steel ties and concrete struts. Moreover, top and bottom reinforcement of coupling beam, used for constructive purposes, are modeled as steel ties. Since there will be a difference between tension and compression strengths of diagonal bundles due to contribution of confined concrete, an unbalanced tension force would create tensile stress on top and bottom reinforcements of coupling beam. Confined concrete stress-strain relationship determined

for boundary regions of walls is used for concrete struts. Similarly, same reinforcement characteristics are used for steel ties representing diagonal reinforcement inside the bundles, as well as top and bottom reinforcement of coupling beam. Constructive rules are taken into account while defining area of concrete strut (bundle area) and top and bottom reinforcement of coupling beam. Area of diagonal steel ties is calculated through the capacity estimation procedure as described in Section 3 and Section 5.1.

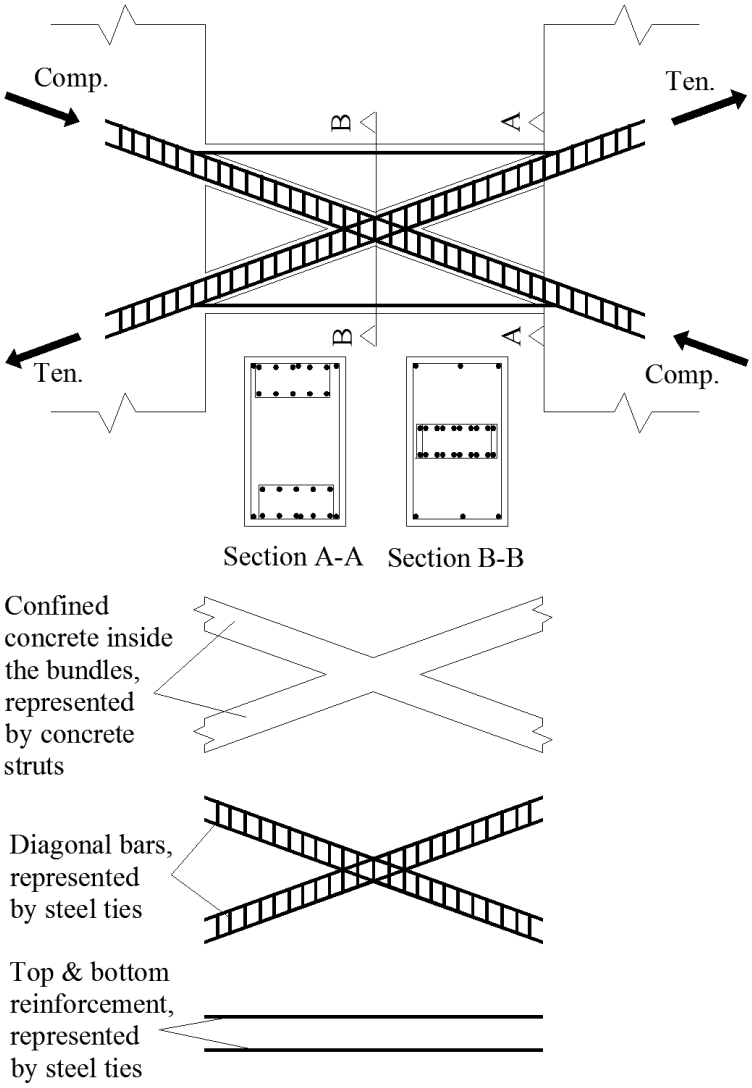

Figure 6.13. Diagonally reinforced coupling beams.

7. VALIDATION OF CAPACITY AND DUCTILITY DEMAND ESTIMATION PROCEDURES BY NONLINEAR ANALYSES

The capacity and ductility demand estimation procedures end up with determination of base overturning moment capacity and ductility demand, and leads structural engineer to decide on an optimum design of coupled core wall system in terms of sizing and reinforcing of walls and coupling beams. Single mode invariant pushover analysis could be useful for verification of overturning moment capacity and modal capacity curve obtained by capacity and ductility demand estimation procedures, respectively. Yet, both capacity and ductility estimation procedures and single mode pushover analysis fall short for determination of inelastic deformation demands and capacities under dynamic loading conditions. Therefore, nonlinear dynamic analysis is an obligation not only for obtaining accurate results for inelastic deformations but also capturing the contribution of higher modes, as well as dynamic shear amplification and shear migration, which are the characteristic consequences of dynamic loading conditions.

Nonlinear static and dynamic analyses have been carried out to validate the above-presented capacity and ductility demand estimation procedures. The coupled core wall systems designed in Section 5.2 used in preliminary estimation studies are analyzed by ignoring for simplicity the stiffness and strength contributions of perimeter frames.

For each coupled core wall system single mode pushover analyses were performed through a displacement pattern compatible with the first fundamental translational mode in coupling direction. Note that sufficiently accurate representation of the base overturning moment can be achieved by the single-mode response. Taking advantage of this fact, an alternate pushover curve has been developed by Eqs.(4.6) and (4.7) as presented in Section 4. Therefore, the base overturning moment obtained by single mode pushover analysis and capacity estimation procedure should be compatible.

Coupled core wall system CW12 is analyzed under two typical MCE level earthquakes. The intention of nonlinear response history analyses is not only confirmation of nonlinear deformation trends that are obtained by simple capacity and ductility demand

estimation procedures, but also comparing the base overturning moment obtained by the capacity estimation procedure. It is expected that the effect of higher mode response on base overturning moment will be limited.

Validation of base overturning moment capacity of the coupled core wall systems by pushover analysis is presented in Section 7.1. Validation of capacity and ductility demand estimation procedures by nonlinear response history analyses, as well as evaluation of nonlinear deformation trends, is presented in Section 7.2.

7.1. Validation of Capacity Estimation Procedure by Pushover Analysis

In Sections 3 and 4, construction of modal capacity curve through proposed capacity and ductility demand estimation procedures is presented. Modal capacity curve could also be obtained by performing single mode pushover analysis. Differences between pushover analysis and the simplified capacity estimation procedure can be summarized as follows:

- Since walls are modeled with fiber elements, there is no need to use interaction diagrams (yield surfaces).
- Assumption of simultaneous yielding of both walls is not necessary.
- Since diagonal bundles of coupling beams are represented as concrete struts and steel ties, contribution of concrete inside the bundles as well as strain hardening of diagonal reinforcement can be taken into account.

As long as core aspect ratio, axial gravity load level, wall reinforcement ratio and β value are kept the same, modal capacity diagrams obtained from pushover analysis and capacity estimation procedure are very similar (Figure 7.1). The results are independent of dimensions of coupling beams and walls.

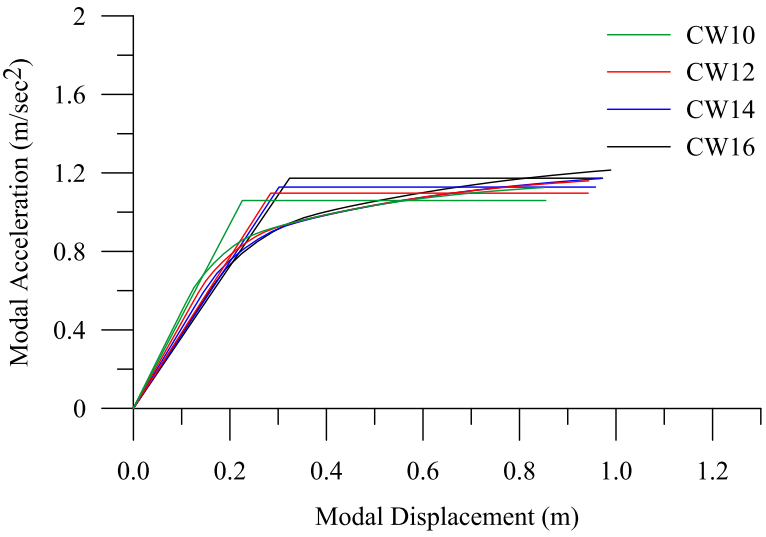

Figure 7.1. Modal capacity diagram for CW10, CW12, CW14, CW16 (β_1=0.5, $\rho_m = \rho_{m1}$, $n_0 = 0.125$).

Comparison of modal capacity diagrams indicates the same trend for all four coupled core wall systems for every axial gravity load levels. In the following graphs, only the modal capacity diagrams obtained for CW12 coupled core wall system with $n_0 = 0.125$ axial load ratio will be presented with respect to each β value. Observations could be summarized as following;

a) Pushover curves obtained by pushover analysis and capacity estimation procedure are compatible. The latter may be considered as an elastic-plastic approximation of the former.

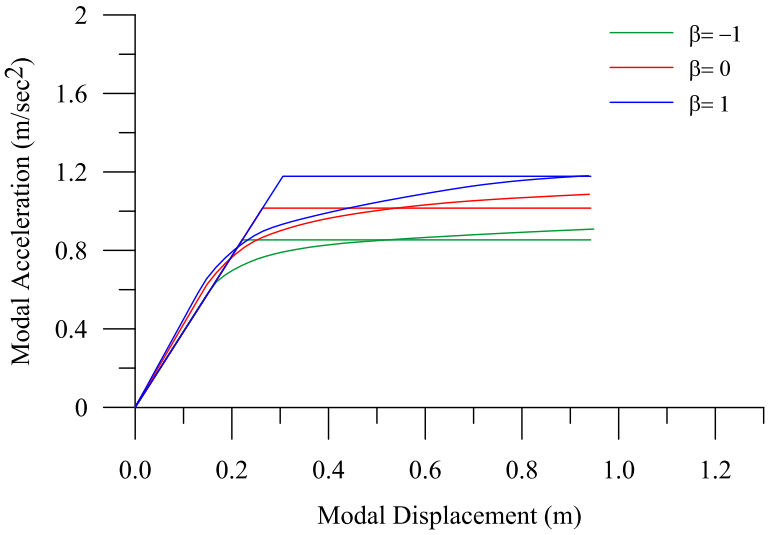

Figure 7.2. Modal capacity diagram (CW12, $\rho_m = \rho_{m1}$, $n_0 = 0.125$).

b) For higher values of ρ_m, overturning moment capacity is slightly overestimated by capacity estimation procedure for β= -1 and β=1.

For $\beta > 0$, both coupling beams and walls are getting stronger with increasing wall reinforcement ratio. If all of the coupling beams do not yield and strain hardening of reinforcement do not take place at yielding coupling beams, coupling shear force would be less than predetermined level. Moreover, walls with higher amount of reinforcement may not yield under realized coupling shear force.

For $\beta < 0$, while walls are getting stronger with increasing wall reinforcement ratio, coupling beams are getting weaker. Thus, generated coupling shear force may not be high enough for causing walls to reach corresponding moment capacity even if all coupling beams would eventually yield. Therefore, overturning moment realized by coupling shear force may be equal to estimated level; however, moment contribution of walls would be less than assumed.

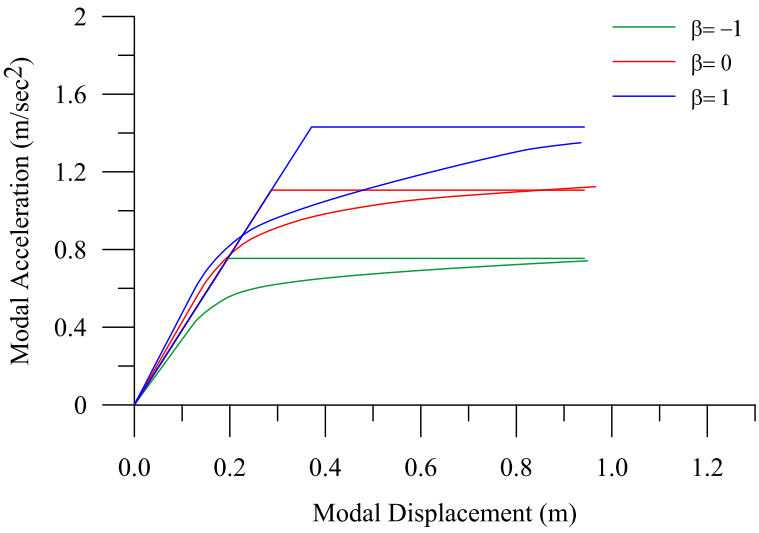

Figure 7.3. Modal capacity diagram (CW12, $\rho_m = 2\rho_{m1}$, $n_0 = 0.125$).

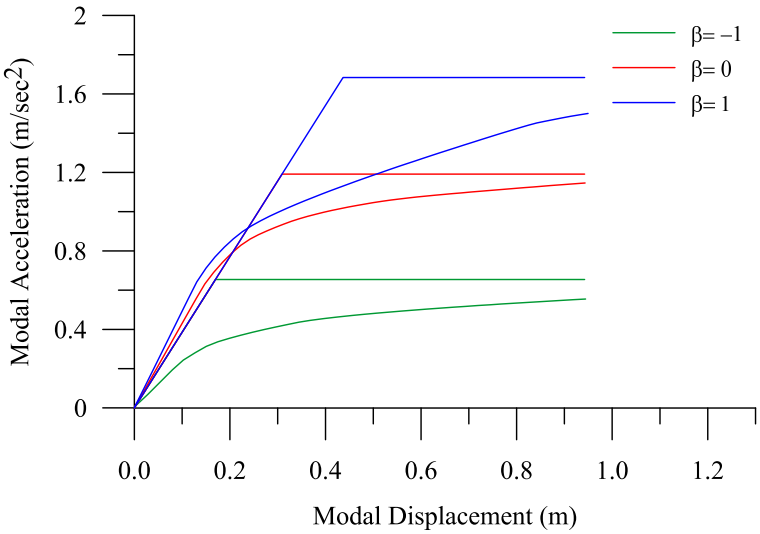

Figure 7.4. Modal capacity diagram (CW12, $\rho_m = 3\rho_{m1}$, $n_0 = 0.125$).

7.2. Validation of Capacity and Ductility Demand Estimation Procedures by Nonlinear Response History Analysis

The coupled core wall system CW12 is analyzed only in coupling direction under single component of two typical MCE level earthquakes; Chi-Chi earthquake (1999) record No.TCU065 and Landers earthquake (1992) record called Yermo Fire Station.

These two earthquake records were chosen from near-field and far-field earthquake record sets presented in Ref. [6] and taken from PEER Strong Ground Motion Database.

A single component of far-field Landers earthquake record is scaled by a factor of 2.4 in order to *bring closer* to the target spectrum used in the ductility demand estimation procedure, while the component of near-field Chi-Chi earthquake record remained as original (unscaled). Elastic response spectrum of each record reasonably matches with the typical code spectrum shown in Figure 5.3, which was used earlier in demand estimation studies. Related information for these records is presented in Table 7.1 through Table 7.3. Acceleration time histories and pseudo-acceleration response spectrum of each record are presented in Figure 7.5 through Figure 7.8.

Table 7.1. Summary of earthquake event and recording station data [6].

	Earthquake			Recording Station	
ID No	M_w	Year	Name	Name	Owner
11	7.3	1992	Landers	Yermo Fire Station	CDMG
12	7.6	1999	Chi-Chi, Taiwan	TCU065	CWB

Table 7.2. Summary of site and source data [6].

	Site Data		Source fault type	Site-Source Distance (km)			
ID No	NEHRP class	V_s30 (m/sec)		Epicentral	Closest to plane	Campbell	Joyner-Boore
11	D	354	Strike-Slip	86	23.6	23.8	23.6
12	D	306	Thrust	26.7	0.6	6.7	0.6

Table 7.3. Summary of PEER NGA Database information and parameters of recorded ground motion [6].

	PEER-NGA Record Information				Recorded Motions	
ID No	Record Sequance No:	Lowest Freq. (Hz)	File Names-Horizontal Records		PGA max (g)	PGV max (cm/sec)
			Component 1	Component 2		
11	900	0.07	LANDERS/YER270	LANDERS/YER360	0.24	52
12	1503	0.08	CHICHI/TCU065_272	CHICHI/TCU065_002	0.82	127.7

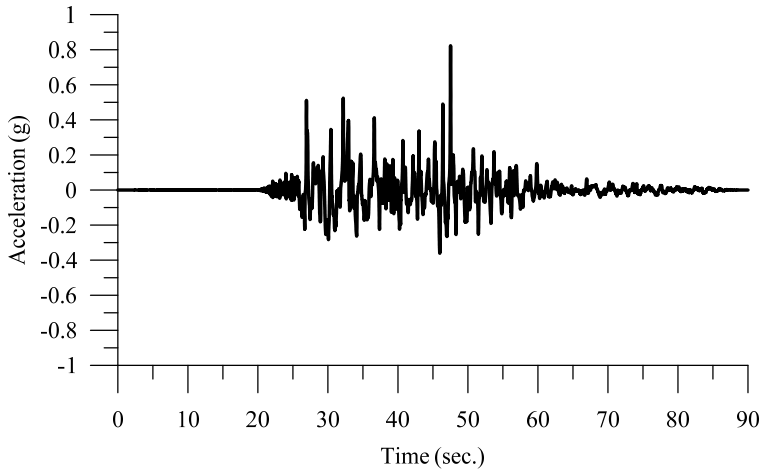

Figure 7.5. Chi-Chi earthquake (1999) record (Record No.TCU065) .

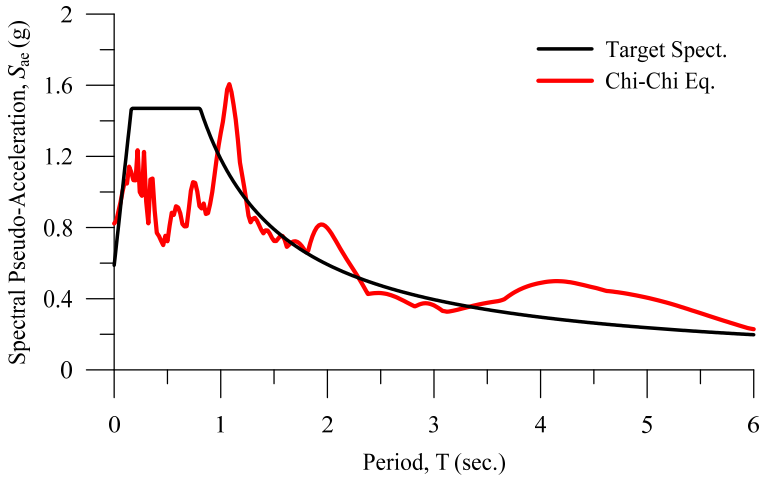

Figure 7.6. Elastic response spectrum of Chi-Chi earthquake (1999) record (Record No.TCU065) superimposed on MCE code spectrum.

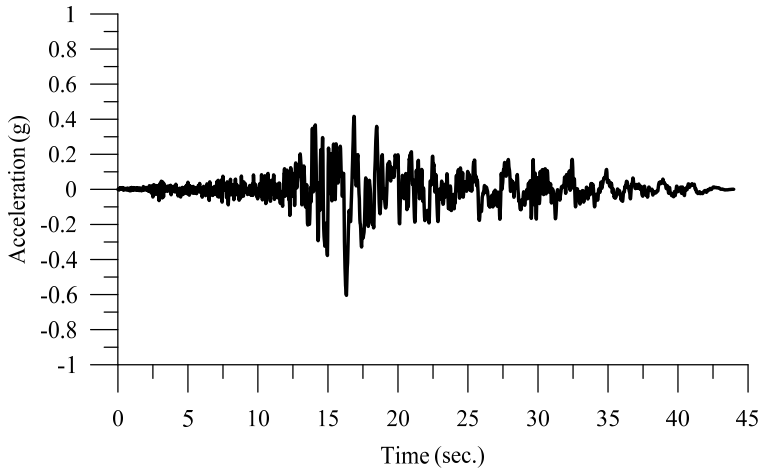

Figure 7.7. Landers earthquake (1992) Yermo Fire Station record.

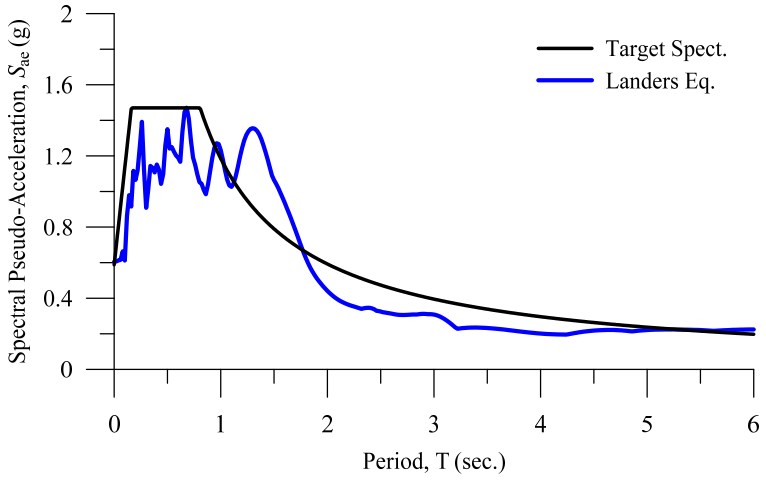

Figure 7.8. Elastic response spectrum of Chi-Chi earthquake (1999) record (Record No.TCU065) superimposed on MCE code spectrum.

In Section 5.3, overturning moment results of nonlinear response history analysis are compared with those calculated by capacity estimation procedure (Figure 5.8.). Vertical axis of diagram represents the ratio of peak value of total overturning moment obtained by nonlinear response history analysis and total overturning moment capacity calculated by capacity estimation procedure. Horizontal axis represents ductility demand of each coupled core wall system calculated by ductility demand estimation procedure. Results showed that deviation in ratio of total overturning moment values is lower than 15% for $2.5<\mu<3.5$.

Figure 7.9 and Figure 7.10 show the envelopes of axial tension strains at the critical points of wall sections (left column) and those at the coupling beam diagonal reinforcements (right column) plotted for three levels of relative yield parameter, $\beta_l = -1$, $\beta_l = 0$, $\beta_l = 1$ with two levels of wall reinforcement represented by mechanical reinforcement ratios of $\rho_m = \rho_{mI} = 0.0345$ (minimum reinforcement) and $\rho_m = 2\rho_{mI} = 0.069$ (double minimum reinforcement), respectively.

An alternate representation of strain profiles of walls is provided in Figure 7.12 through Figure 7.19. In each figure, graph (a) at left shows tension and compression strain envelopes of each pier obtained through nonlinear response history analysis, while graph (b) at right shows tension and compression strains at tension and compression walls, respectively, at the time instant of maximum overturning moment is reached. In each graph two columns at left represent first half of tension and compression walls in height (0 to 60 m), and two columns at right represents second half of tension and compression walls in height (60 m to 120 m).

The cases with $\beta_l = -1$ (represented by top plots in Figure 7.9, Figure 7.10) correspond to very weak coupling between the walls where axial tension strains on diagonal reinforcements of weak coupling beams reach excessive values, in particular for the case of doubled minimum wall reinforcement. Note that ductility demands estimated for those cases in the preliminary design stage (see Table 5.9) were $\mu = 4.3$ and $\mu = 4.8$ for given levels of wall reinforcements, respectively, which actually lie outside the acceptable ductility limits ($2.5 \le \mu \le 3.5$). On the other hand wall axial tension strains slightly exceed steel yield strain at tips of webs in lightly reinforced wall (Figure 7.9) and

significantly exceed in upper stories in doubly reinforced wall (Figure 7.10), reflecting the direct consequences of weak coupling. This conclusion can also be drawn from Figure 7.12 and Figure 7.13.

The cases with $\beta_1 = 0$ (represented by middle plots in Figure 7.9, Figure 7.10) correspond to moderate coupling between the walls where axial tension strains on diagonal reinforcements of moderately strong coupling beams slightly exceeds the acceptable values, the limit of which can be specified as 5% for MCE level of excitation. Ductility demands estimated for those cases in the preliminary design stage (see Table 5.9) were $\mu = 3.6$ and $\mu = 3.3$ for given levels of wall reinforcements, respectively, which nearly lie within the acceptable ductility limits ($2.5 \le \mu \le 3.5$). Note that due to relatively increased coupling, wall axial strains near the base (along the critical wall height of approximately two to three story heights) have increased with respect to the previous case with weak coupling, however strains tend to decrease in the upper parts (see Figure 7.14 and Figure 7.15).

Finally the cases with $\beta_1 = 1$ (represented by bottom plots in Figure 7.9, Figure 7.10) correspond to the strongest possible (maximum) coupling between the walls for given wall reinforcements where axial tension strains on diagonal reinforcements of strong coupling beams remain well below the acceptable values. Ductility demands estimated for those cases in the preliminary design stage (see Table 5.9) were $\mu = 3.1$ and $\mu = 2.5$ for given levels of wall reinforcements, respectively, which comfortably lie within the acceptable ductility limits ($2.5 \le \mu \le 3.5$). Note that in spite of the maximum coupling, wall axial strains near the base (along the critical wall height of approximately two to three story heights) remain within the acceptable limits. On the other hand, wall axial strains at flange-web intersections tend to be closer to those at the web tips, and even exceed them in the case of double minimum reinforcement, reflecting the direct consequences of the strong coupling (see Figure 7.16 and Figure 7.17).

It appears that a near-optimum arrangement could be obtained with the case where relative yield parameter is selected as $\beta_1 = 0.5$ with double minimum wall reinforcement. Relevant plots are given in the upper part of Figure 7.11. Ductility demand estimated for

this case in the preliminary design stage (see Table 5.9) was $\mu = 2.9$. Note that in this case total coupling shear (see Eq.(3.8)) is identical to the case of $\beta_1 = 1$ with minimum wall reinforcement, as evidenced by a similar trend in axial tensile strains on diagonal reinforcements of coupling beams. However wall axial tensile strains are considerably reduced. A further increase of the wall reinforcement to triple the minimum reinforcement with the same $\beta_1 = 0.5$ does not lead to any major improvement with respect to double the minimum reinforcement, as shown in the bottom part of Figure 7.11 (also see Figure 7.18 and Figure 7.19).

Thus it can be concluded that capacity and ductility demand estimation procedures developed for coupled core walls of tall buildings have been successfully validated through nonlinear response history analysis.

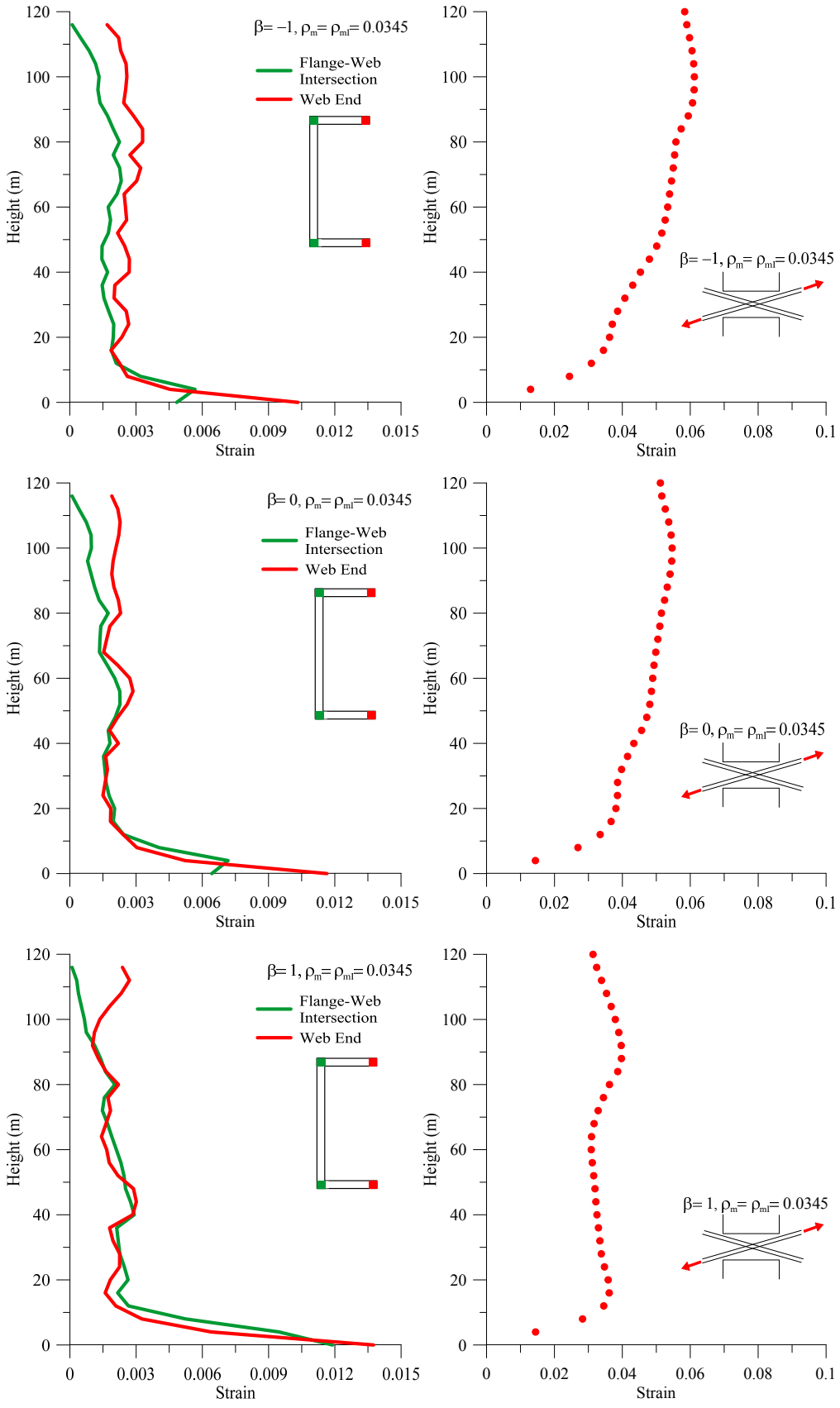

Figure 7.9. Tension strain envelopes of walls and coupling beams for three levels of relative yield parameter β_l and $\rho_m = \rho_{ml} = 0.0345$ (CW12, $n_0 = 0.125$, Chi-Chi earthquake).

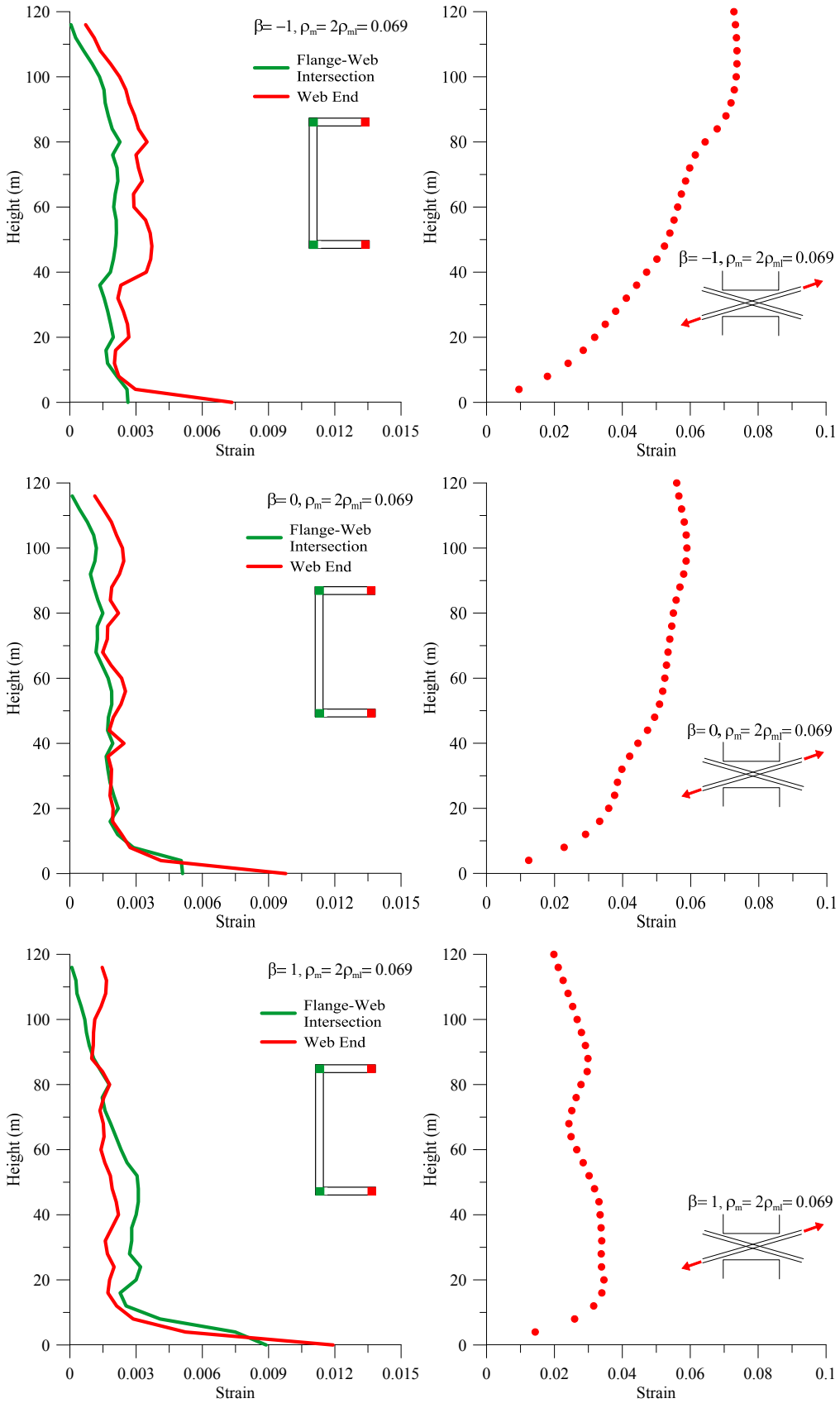

Figure 7.10. Tension strain envelopes of walls and coupling beams for three levels of relative yield parameter, β_1 and $\rho_m = 2\rho_{ml} = 0.069$. (CW12, $n_0 = 0.125$, Chi-Chi earthquake).

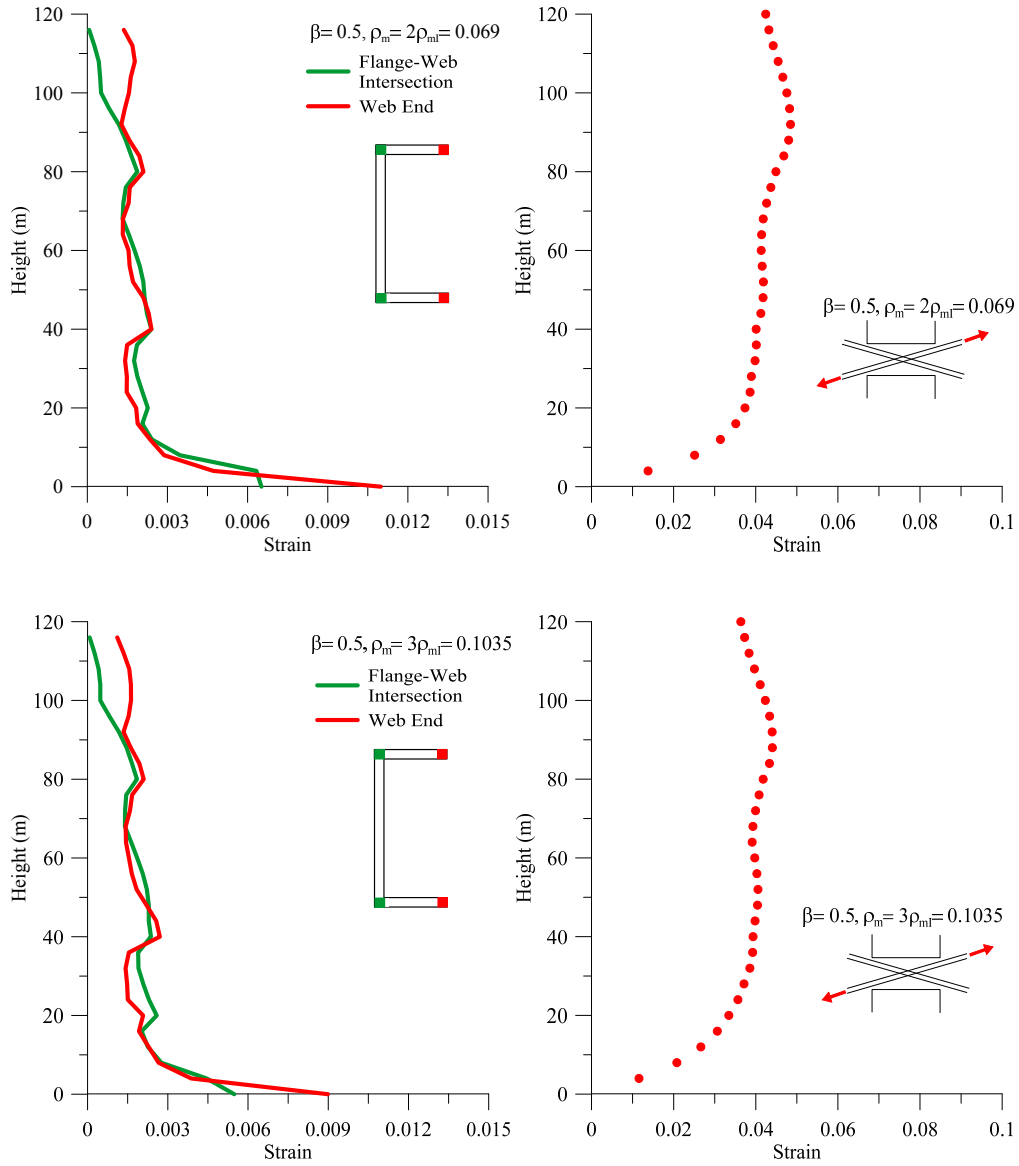

Figure 7.11. Tension strain envelopes of walls and coupling beams for β_l=0.5 with $\rho_m = 2\rho_{ml}$=0.069 and $\rho_m = 3\rho_{ml}$=0.1035 (CW12, n_0 = 0.125, Chi-Chi earthquake).

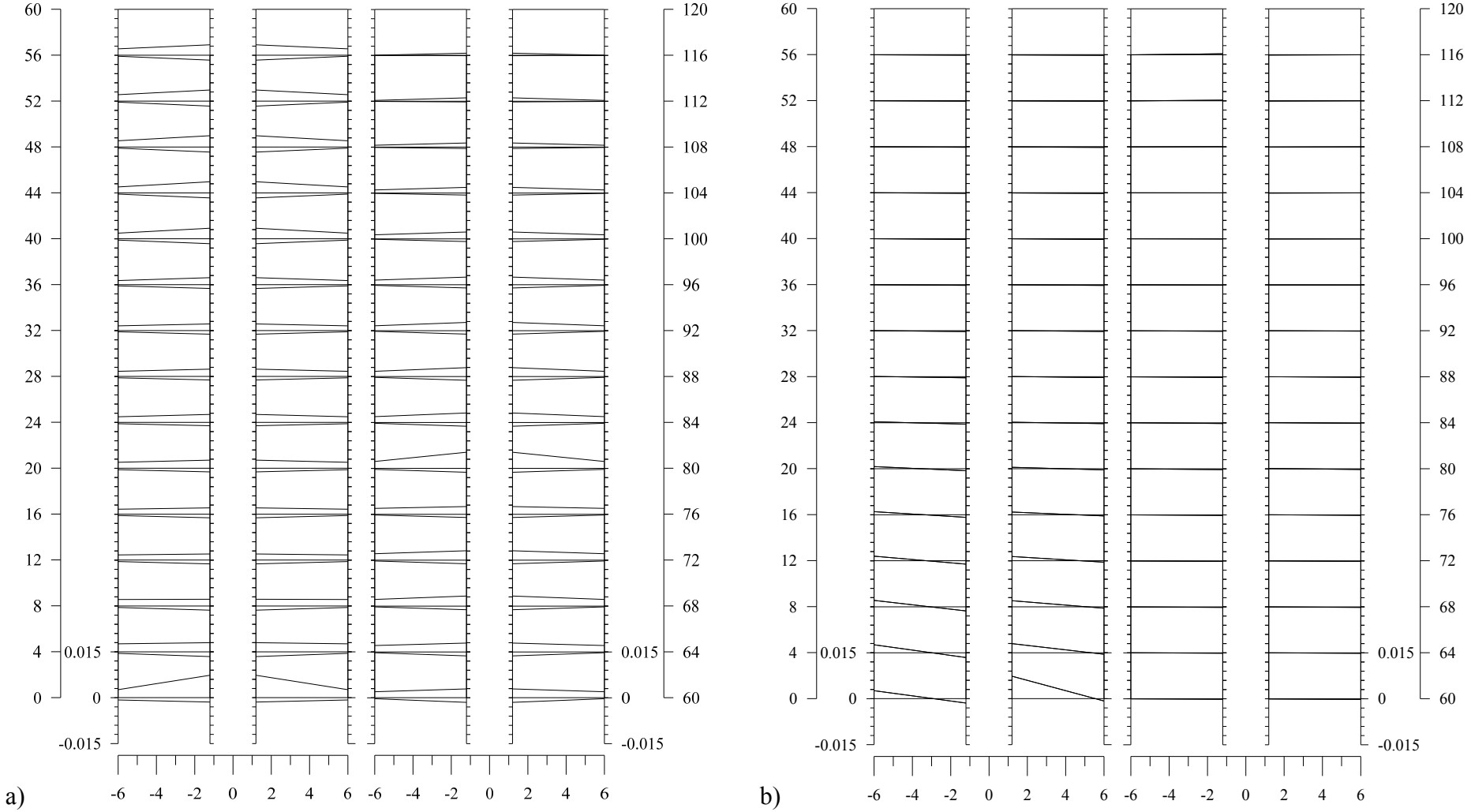

Figure 7.12. Wall Strains vs. Building Height for CW12 coupled core wall system, $n_0 = 0.125$, $\beta = -1$, $\rho_m = 2\rho_{mI}$, a) Envelope, b) at $M_o = M_{o,max}$.

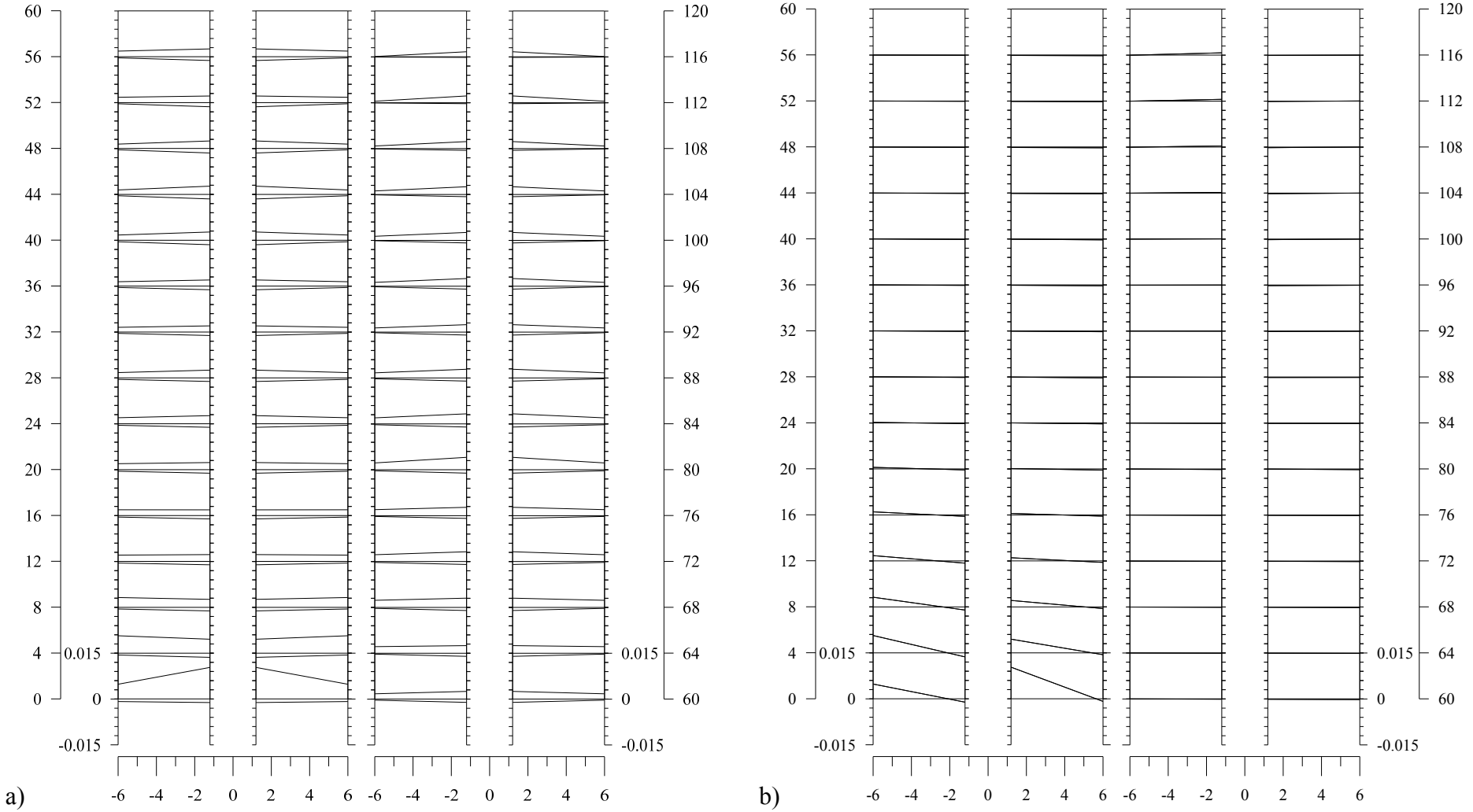

Figure 7.13. Wall Strains vs. Building Height for CW12 coupled core wall system, $n_0 = 0.125$, $\beta = -1$, $\rho_m = \rho_{ml}$, a) Envelope, b) at $M_o = M_{o,max}$.

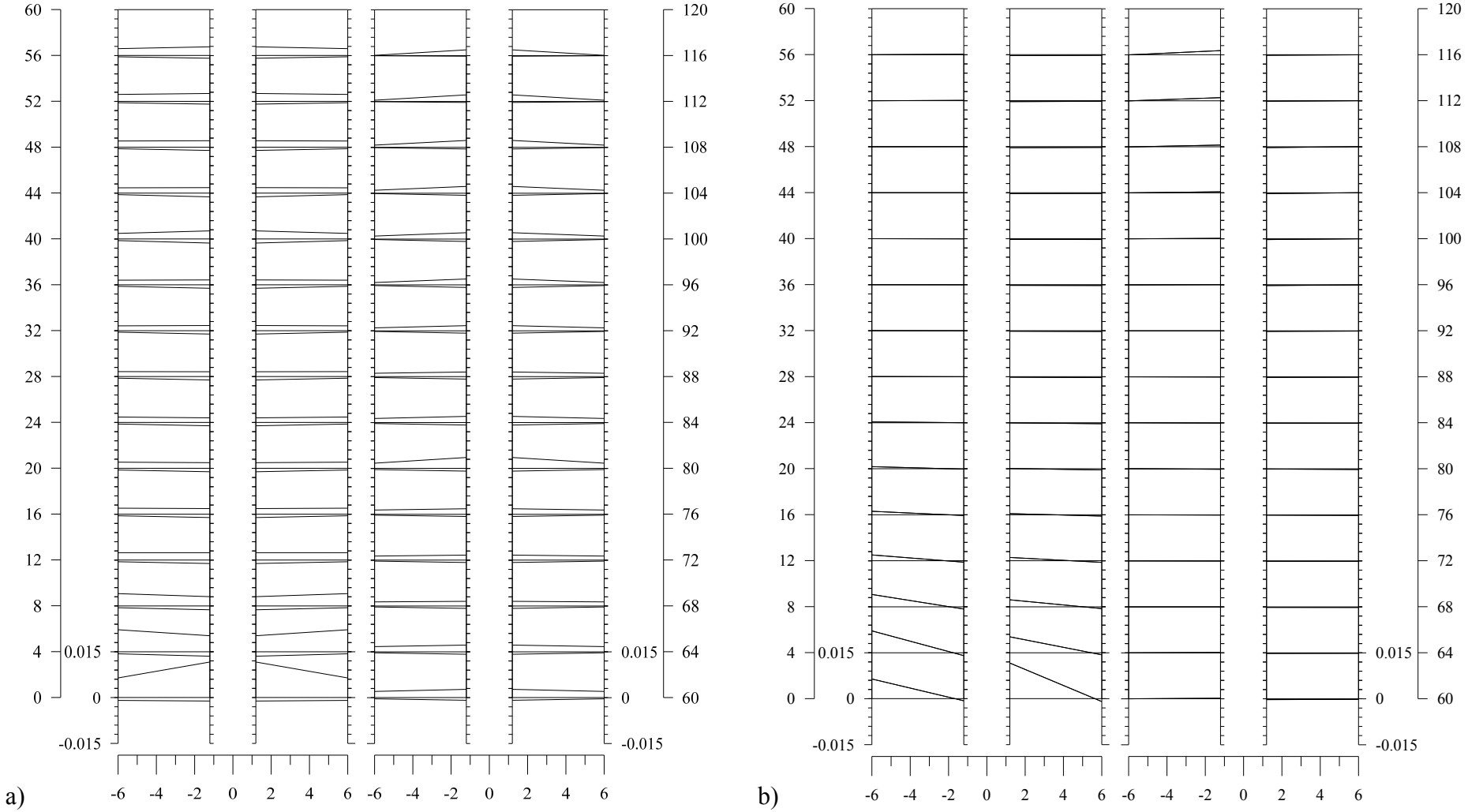

Figure 7.14. Wall Strains vs. Building Height for CW12 coupled core wall system, $n_0 = 0.125, \beta = 0$, $\rho_m = \rho_{mI}$, a) Envelope, b) at $M_o = M_{o,max}$.

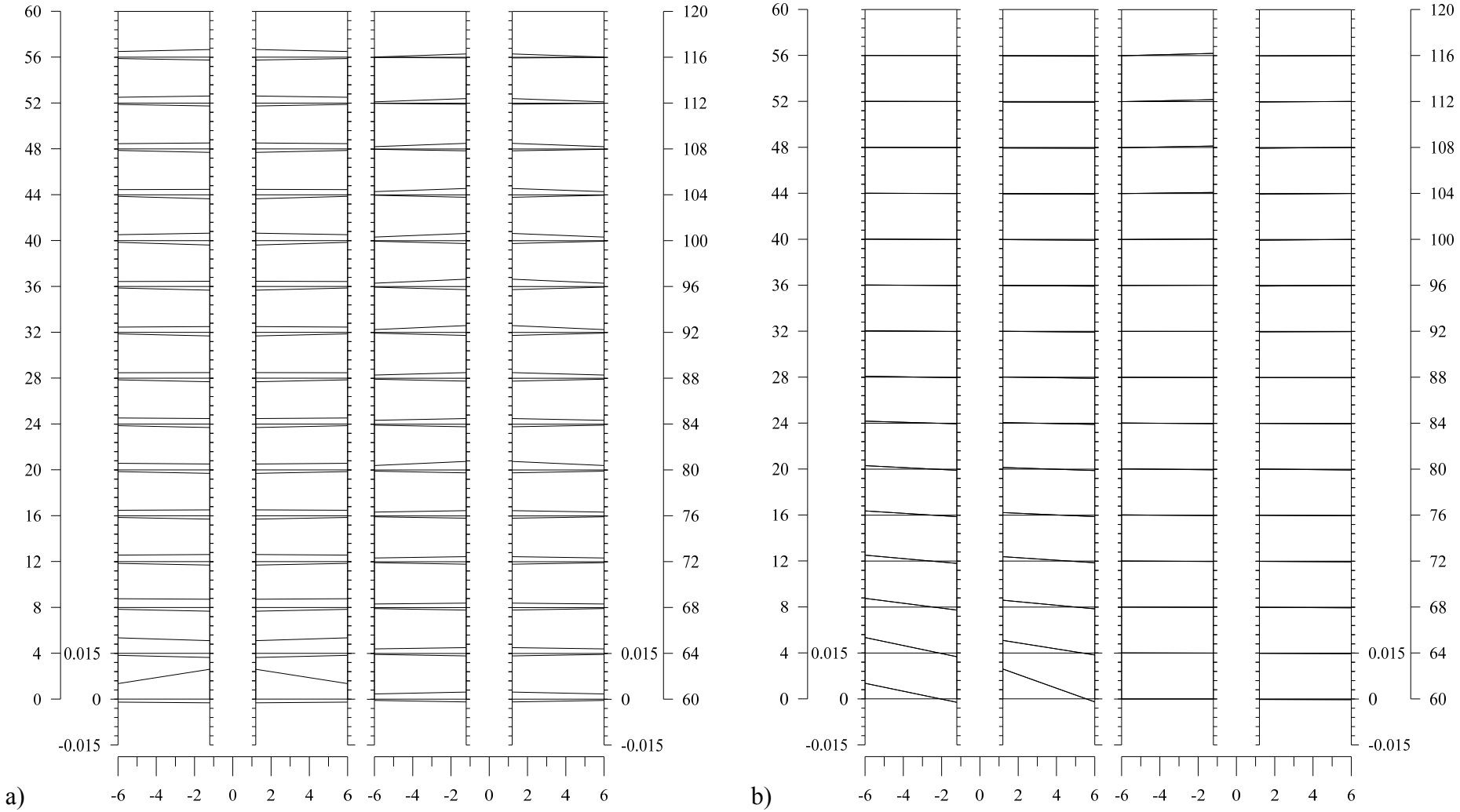

Figure 7.15. Wall Strains vs. Building Height for CW12 coupled core wall system, $n_0 = 0.125$, $\beta = 0$, $\rho_m = 2\rho_{mI}$, a) Envelope, b) at $M_o = M_{o,max}$.

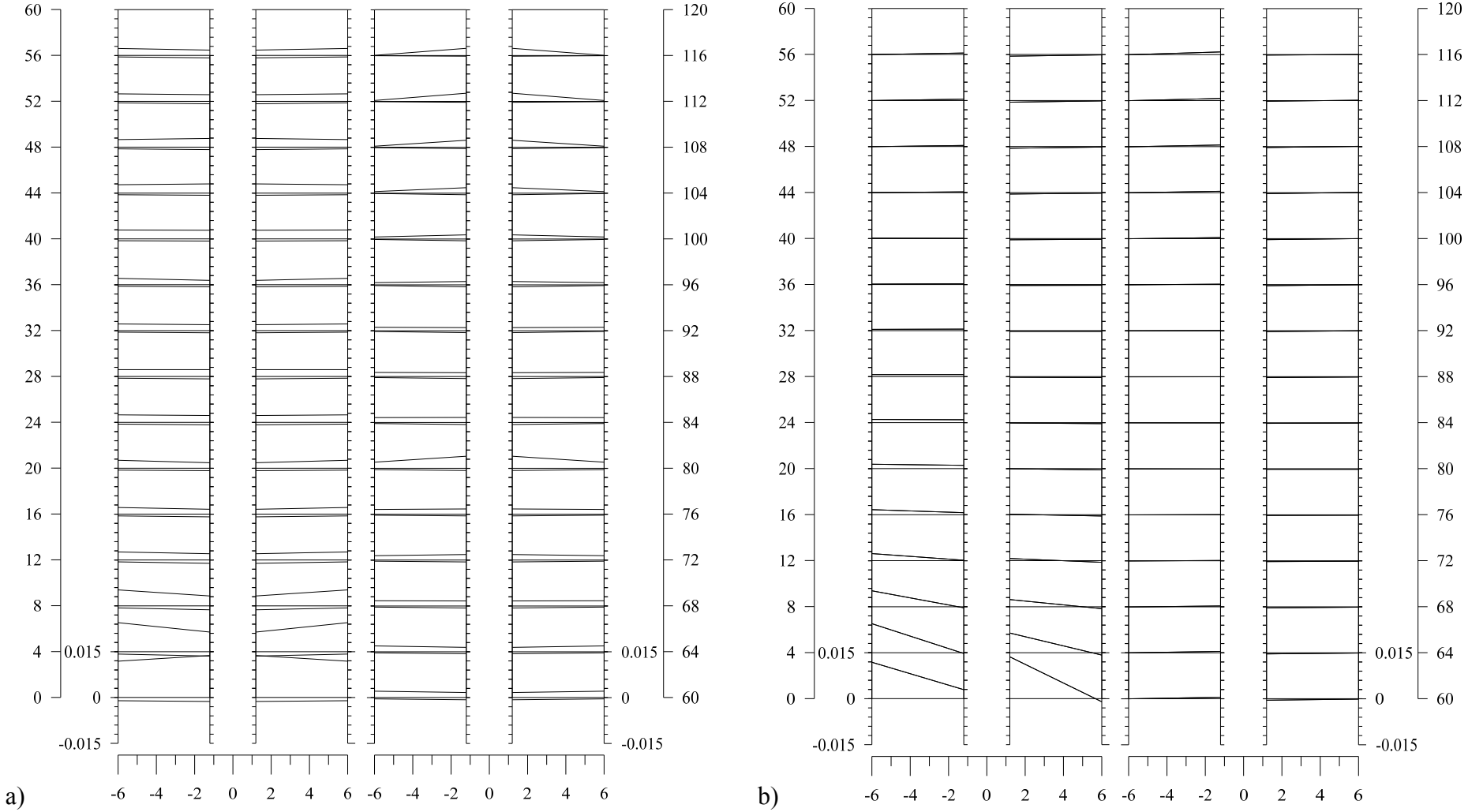

Figure 7.16. Wall Strains vs. Building Height for CW12 coupled core wall system, $n_0 = 0.125, \beta = 1, \rho_m = \rho_{mI}$, a) Envelope, b) at $M_o = M_{o,max}$.

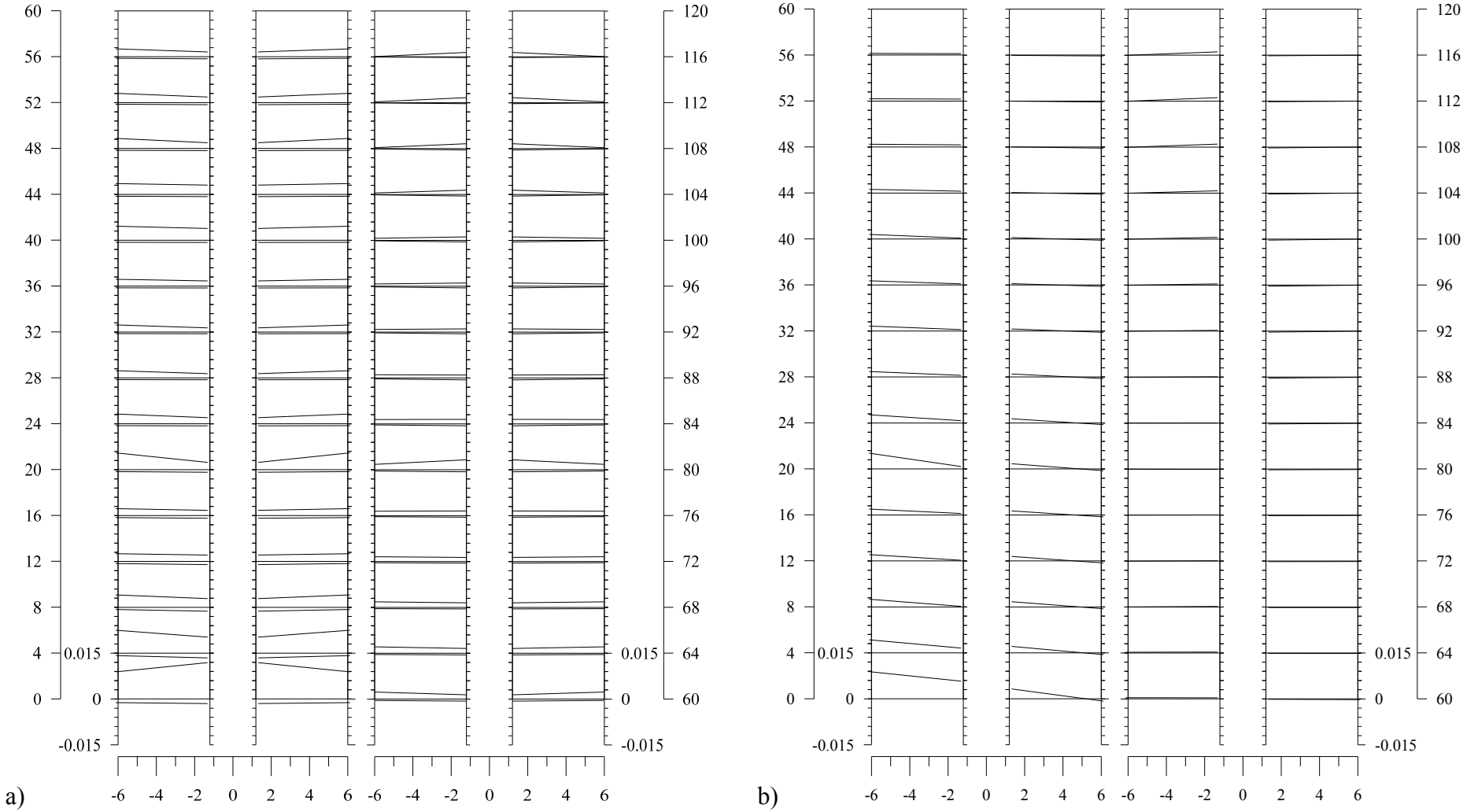

Figure 7.17. Wall Strains vs. Building Height for CW12 coupled core wall system, $n_0 = 0.125, \beta = 1,\ \rho_m = 2\rho_{ml}$, a) Envelope, b) at $M_o = M_{o,max}$.

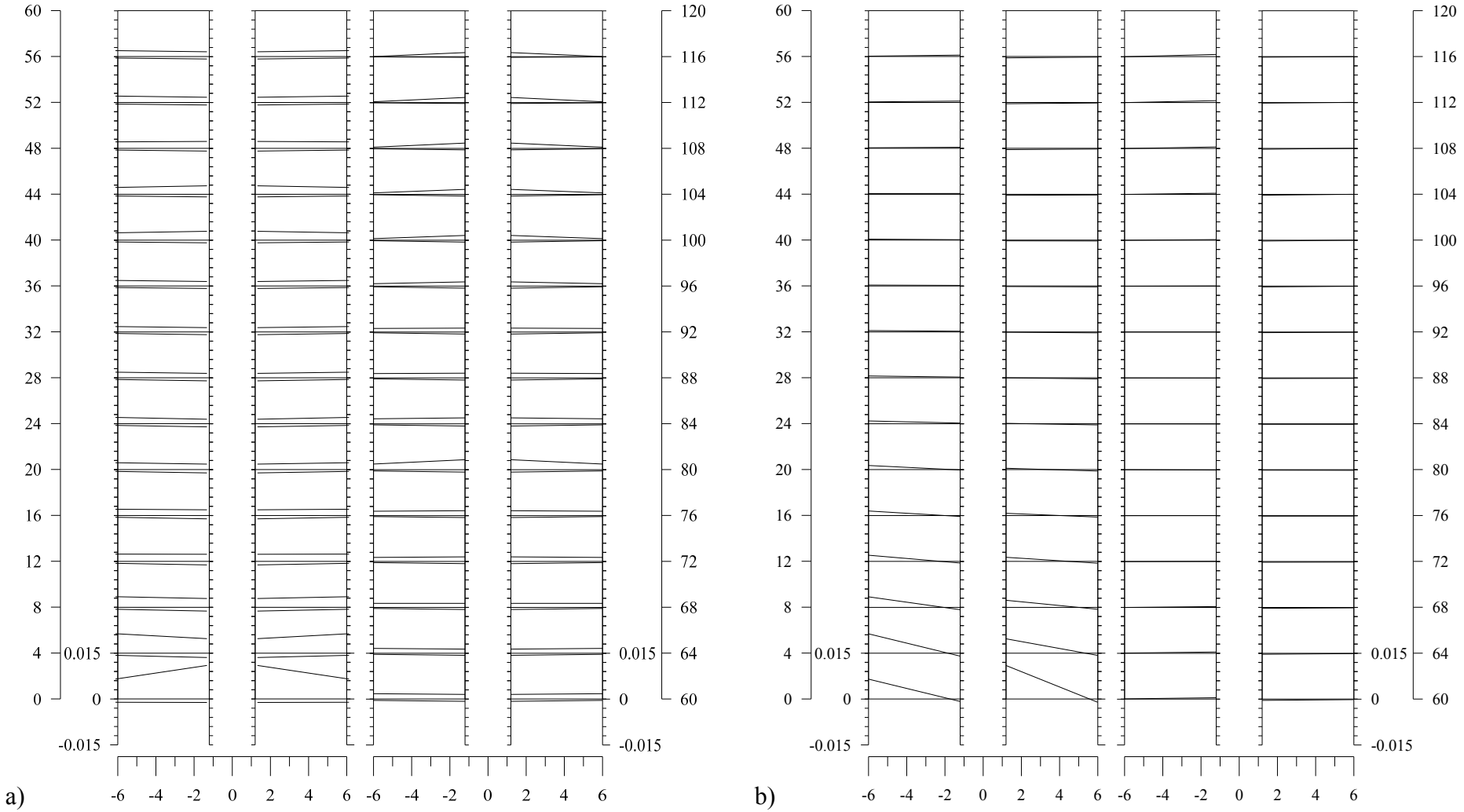

Figure 7.18. Wall Strains vs. Building Height for CW12 coupled core wall system, $n_0 = 0.125$, $\beta = 0.5$, $\rho_m = 2\rho_{ml}$, a) Envelope, b) at $M_o = M_{o,max}$.

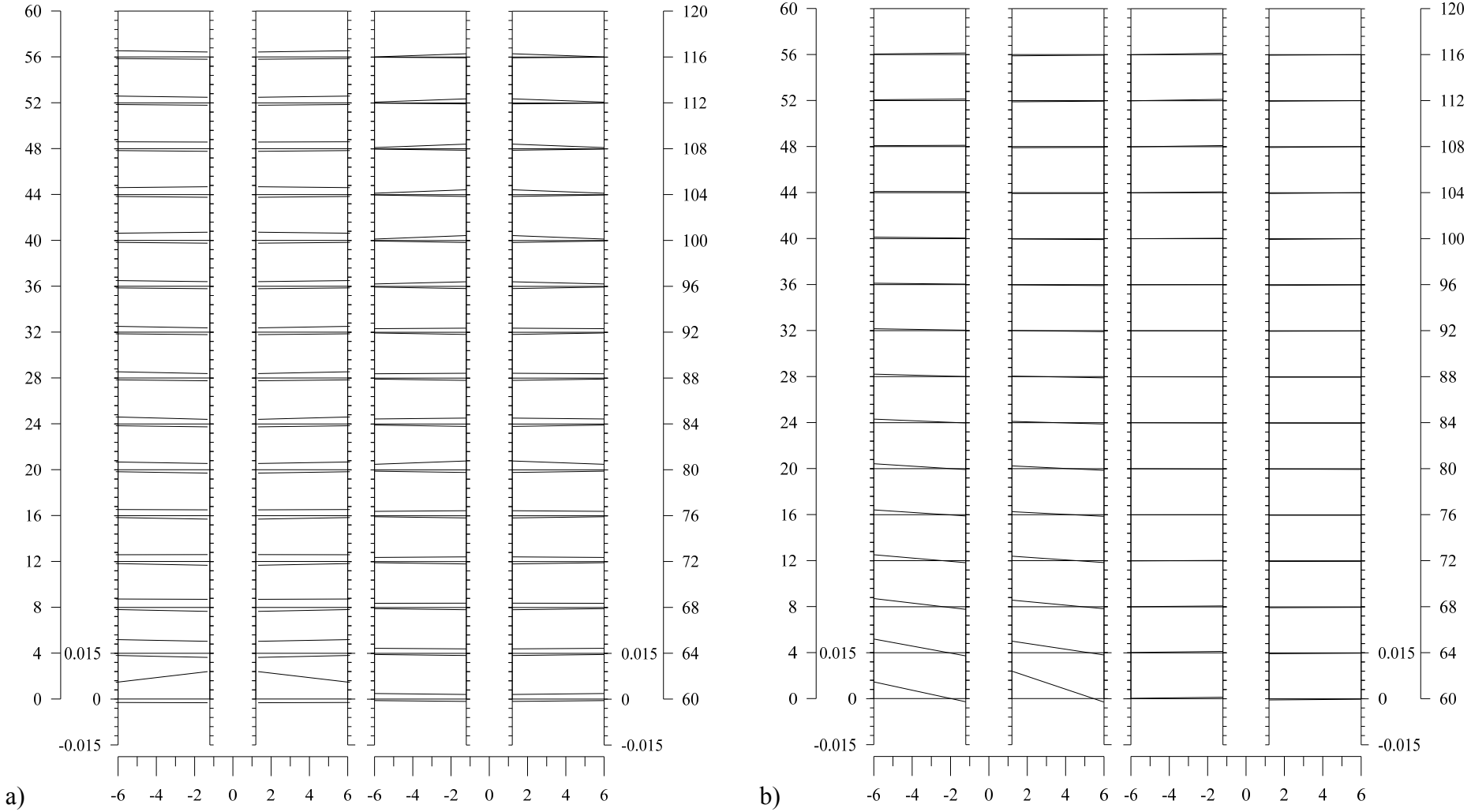

Figure 7.19. Wall Strains vs. Building Height for CW12 coupled core wall system, $n_0 = 0.125$, $\beta = 0.5$, $\rho_m = 3\rho_{ml}$, a) Envelope, b) at $M_o = M_{o,max}$.

8. SHEAR BEHAVIOR of COUPLED CORE WALL SYSTEMS

In Section 2.1, two important aspects of shear behavior of structural walls are introduced; dynamic shear migration and dynamic shear amplification.

Shear migration is a shear behavior phenomenon, of which effects on coupled walls are known since the research by Santhakumar and Paulay [28-29]. Although, its significance is shown both experimentally and analytically in later studies, recent developments in seismic design of buildings do not take into account the effect of shear migration for shear design of structural walls.

In the case of coupled core wall systems, moment capacity of tension wall decreases because of decreasing axial force. Meanwhile, moment capacity of compression wall increases due to increasing axial load, thus compression wall could still behave in elastic manner and moment on compression wall keeps increasing. As a result, shear force that cannot be resisted by tension wall migrates to compression wall, which means that major part of the total shear force is carried by compression wall. Shear migration reaches the peak value at the time instant of maximum overturning moment capacity is reached. At this time instant, coupling shear force and moment of compression wall reach maximum and moment of tension wall reaches to minimum values. Thus, shear migration should be investigated at the time instant of maximum overturning moment.

Dynamic shear amplification is another shear behavior phenomenon mostly developed in cantilever walls. In the case of coupled core wall systems, in coupling direction each pier may behave as two uncoupled cantilevers because of very weak coupling or the whole coupled core wall system can behave as a fully coupled single cantilever as a result of extremely strong coupling. Moreover, shear amplification may also develop in core wall systems similar to those considered in this study, as the coupled core wall system in the perpendicular direction to the coupling direction is nothing but a cantilever wall.

Dynamic shear amplification is a measure of increase in shear force with respect to shear force corresponding to moment hinge formed in the first mode. Dynamic shear amplification should be investigated separately for the whole coupled core wall system and individual piers, at the time instants total core shear and shear of each pier reach to their peaks, respectively. Note that increase in shear in an individual pier may be caused by either dynamic shear migration or dynamic shear amplification. However, when total core shear reaches to its peak value, both piers could be affected, hence, difference in shear in piers, namely migration may not be significant at this instant of time.

As explained in previous paragraphs, three time instants in nonlinear dynamic analysis can be detected at which dynamic shear migration and dynamic shear amplification are expected to occur. These instants are those when peak values of overturning moment, total core shear and shear in one of the piers are reached. In Table 8.1, these instants are shown for each variation of CW12 parameters. Note that, times of peak overturning moment and peak total core shear are different. However, instants that which shear in one of the piers and the base overturning moment reach their peaks are very close.

Eventually, shear forces at these time instants obtained by nonlinear dynamic analysis should be compared with a reference value. In this context, *linear dynamic analysis* is performed for *elastic model* of the CW12 coupled core wall system. In Table 8.1, column (1) and (2) refer to absolute peak values of overturning moment obtained by linear and nonlinear dynamic analysis, respectively. A strength reduction factor, R_{M}, is defined as the ratio between the maximum absolute peak values of overturning moments obtained by linear dynamic analysis and nonlinear dynamic analysis for each variation of CW12, as shown in Table 8.1, column (4). Reference total core shear (Table 8.1, column (6)) is obtained by dividing the corresponding shear obtained from linear dynamic analysis (Table 8.1, column (5)) to the above-defined strength reduction factor determined for overturning moment. Moreover, the first-mode base shear, which is calculated in terms of M_{tot} (Eq. 5.1) in approximate capacity estimation procedure, is shown in the same table Table 8.1, column (7) for comparison.

Nonlinear response history analyses results of CW12 under Chi-Chi earthquake are shown in Table 8.2 through Table 8.4 for critical time instants mentioned above. In these tables columns (8), (9) and (10) show total core shear, shear of the tension wall and shear of the compression wall, respectively.

In Table 8.2 through Table 8.4, Column (11) shows the ratio of shear of compression wall to total core shear, referred to as *amount of shear migration*. At $t = t_{M_{o,max}}$ and $t = t_{V_{pier,max}}$ (Table 8.2 and Table 8.4) this ratio is around 90%. That is to say, 90% of total core shear is resisted by compression wall and 10% is resisted by tension wall. At $t = t_{V_{core,max}}$ (Table 8.3) this ratio becomes 60% and 40%, respectively. Therefore, shear migration is limited when total core shear reaches the peak value.

A comparison is also made in column (12) as the ratio of max total core shear obtained by nonlinear response history analysis to max total core shear obtained by linear response history analysis reduced by yield reduction factor determined according to base overturning moment. On the other hand, similar comparison can be made for individual walls as shown in column (13).

At $t = t_{M_{o,max}}$ and $t = t_{V_{pier,max}}$, values at column (12) is generally around unity, meaning that total core shear calculated by nonlinear and linear dynamic analyses are very close. However, for these instants, column (13) shows that shear forces of compression wall obtained by nonlinear dynamic analysis are approximately 1.9 to 2.0 times the ones obtained from linear dynamic analysis. This means that, shear of compression wall may be amplified by around 2.0 during nonlinear response, although total core shear remains close to that calculated from linear dynamic analysis.

On the other hand, at $t = t_{V_{core,max}}$, values at both column (12) and column (13) vary around 1.3 to 1.5, meaning that either total core shear as well as shear of individual pier obtained from nonlinear analysis is 1.3 to 1.5 times higher than those obtained from linear analysis.

As a result it can be concluded that shear design of individual piers of a coupled core wall system is governed by shear migration phenomenon and it is suggested based on the analysis results that shear design forces obtained through linear analysis should be amplified by around 2.0. These conclusions may also be drawn from Figure 8.1 through Figure 8.4, showing moment and shear demands of individual piers at instants of $t = t_{M_{o,max}}$ and $t = t_{V_{core,max}}$.

Moreover, as previously mentioned, approximate first mode base shear can be determined through capacity and ductility demand estimation procedures (column (7)). Column (14) shows the ratio of max total core shear obtained by nonlinear dynamic analysis over the first mode base shear obtained through capacity estimation procedure. Similar comparison can be made for shear forces of individual piers, as shown in column (15). It can be concluded that shear of individual piers calculated through capacity estimation procedure should be amplified by a factor of 2.5 to 3.0 in order to capture the contribution of higher modes on shear demand and effects of dynamic shear migration.

Table 8.1. Peak values of overturning moment, determined ductility demand and reference shear forces (CW12, $n_0 = 0.125$, Chi-Chi earthquake).

Coupled Core Wall System	β	ρ_m	$t = t_{Mo,max}$ (sec.)	$t = t_{Vcore,max}$ (sec.)	$t = t_{Vpier,max}$ (sec.)	$M_{over,\ linear}$ (1)	$M_{over,\ nonlinear}$ (2)	$M_{over,\ CEP}$ (3)	R_M based on $M_{over,max}$ $\left\{\frac{(1)}{(2)}\right\}$ (4)	$V_{core,\ max,\ linear}$ (5)	$V_{core,\ max,\ linear,\ reduced}$ $\left\{\frac{(5)}{(4)}\right\}$ (6)	$V_{core,\ CEP}$ $\left\{\frac{(3)}{(0.7H)}\right\}$ (7)
CW12	-1	$3\rho_{mI}$	31.9	47.56	31.88	7576795	1298691	1122896	5.83	124038	21261	13368
CW12	-1	$2\rho_{mI}$	31.84	47.56	31.88	7576795	1585913	1294239	4.78	124038	25963	15408
CW12	-1	ρ_{mI}	33	30.18	31.94	7576795	1772753	1464769	4.27	124038	29021	17438
CW12	0	ρ_{mI}	31.94	30.1	31.88	7576795	2001237	1743057	3.79	124038	32762	20751
CW12	0	$2\rho_{mI}$	31.9	30.08	31.82	7576795	2146991	1897880	3.53	124038	35148	22594
CW12	0	$3\rho_{mI}$	31.88	30.12	31.8	7576795	2290086	2044687	3.31	124038	37490	24342
CW12	1	ρ_{mI}	31.78	30.08	31.8	7576795	2214645	2021346	3.42	124038	36255	24064
CW12	1	$2\rho_{mI}$	31.7	30.1	31.74	7576795	2566287	2455885	2.95	124038	42012	29237
CW12	1	$3\rho_{mI}$	31.18	29.96	31.62	7576795	2878068	2889710	2.63	124038	47116	34401

Table 8.2. Shear demands at $t = t_{M_{o,max}}$ (CW12, $n_0 = 0.125$, Chi-Chi earthquake).

	$V_{core,\,nonlinear}$ at $t = t_{Mo,max}$ (8)	$V_{ten.,\,nonlinear}$ at $t = t_{Mo,max}$ (9)	$V_{comp.,\,nonlinear}$ at $t = t_{Mo,max}$ (10)	$\frac{V_{comp,nonlinear}}{V_{core,nonlinear}}$ $\left\{\frac{(10)}{(8)}\right\}$ (11)	$\frac{V_{core,nonlinear}}{V_{core,max,linear,reduced}}$ $\left\{\frac{(8)}{(6)}\right\}$ (12)	$\frac{V_{comp,nonlinear}}{V_{left/right,linear}}$ $\left\{\frac{(10)}{(6)/2}\right\}$ (13)	$\frac{V_{core,nonlinear}}{V_{core,CEP}}$ $\left\{\frac{(8)}{(7)}\right\}$ (14)	$\frac{V_{comp,nonlinear}}{V_{left/right,CEP}}$ $\left\{\frac{(10)}{(7)/2}\right\}$ (15)
$t = t_{Mo,max}$	29427	1464	27963	0.95	1.38	2.63	2.20	4.18
	27389	1334	26055	0.95	1.05	2.01	1.78	3.38
	28559	1740	26819	0.94	0.98	1.85	1.64	3.08
	32289	706	31583	0.98	0.99	1.93	1.56	3.04
	34829	2332	32497	0.93	0.99	1.85	1.54	2.88
	38189	4849	33340	0.87	1.02	1.78	1.57	2.74
	41526	6235	35291	0.85	1.15	1.95	1.73	2.93
	48779	6599	42180	0.86	1.16	2.01	1.67	2.89
	48257	15444	32813	0.68	1.02	1.39	1.40	1.91

Table 8.3. Shear demands of CW12 coupled core wall systems at $t = t_{V_{core,max}}$ (CW12, $n_0 = 0.125$, Chi-Chi earthquake).

$t = t_{Vcore,max}$	$V_{core,\,nonlinear}$ at $t = t_{Vcore,max}$ (8)	$V_{ten.,\,nonlinear}$ at $t = t_{Vcore,max}$ (9)	$V_{comp.,\,nonlinear}$ at $t = t_{Vcore,max}$ (10)	$\frac{V_{comp,nonlinear}}{V_{core,nonlinear}}$ $\left\{\frac{(10)}{(8)}\right\}$ (11)	$\frac{V_{core,nonlinear}}{V_{core,max,linear,reduced}}$ $\left\{\frac{(8)}{(6)}\right\}$ (12)	$\frac{V_{comp,nonlinear}}{V_{left/right,linear}}$ $\left\{\frac{(10)}{(6)/2}\right\}$ (13)	$\frac{V_{core,nonlinear}}{V_{core,CEP}}$ $\left\{\frac{(8)}{(7)}\right\}$ (14)	$\frac{V_{comp,nonlinear}}{V_{left/right,CEP}}$ $\left\{\frac{(10)}{(7)/2}\right\}$ (15)
	47554	19251	28303	0.60	2.24	2.66	3.56	4.23
	33745	12371	21374	0.63	1.30	1.65	2.19	2.77
	38048	16094	21954	0.58	1.31	1.51	2.18	2.52
	46168	19836	26332	0.57	1.41	1.61	2.22	2.54
	46759	20229	26530	0.57	1.33	1.51	2.07	2.35
	47977	19240	28737	0.60	1.28	1.53	1.97	2.36
	51234	21622	29612	0.58	1.41	1.63	2.13	2.46
	55082	22625	32457	0.59	1.31	1.55	1.88	2.22
	57759	26030	31729	0.55	1.23	1.35	1.68	1.84

Table 8.4. Shear demands of CW12 coupled core wall systems at $t = t_{V_{pier,max}}$ (CW12, n_0 = 0.125, Chi-Chi earthquake).

	$V_{core,\,nonlinear}$ at $t = t_{Vpier,max}$ (8)	$V_{ten.,\,nonlinear}$ at $t = t_{Vpier,max}$ (9)	$V_{comp.,\,nonlinear}$ at $t = t_{Vpier,max}$ (10)	$\frac{V_{comp,nonlinear}}{V_{core,nonlinear}}\left\{\frac{(10)}{(8)}\right\}$ (11)	$\frac{V_{core,nonlinear}}{V_{core,max,linear,reduced}}\left\{\frac{(8)}{(6)}\right\}$ (12)	$\frac{V_{comp,nonlinear}}{V_{left/right,linear}}\left\{\frac{(10)}{(6)/2}\right\}$ (13)	$\frac{V_{core,nonlinear}}{V_{core,CEP}}\left\{\frac{(8)}{(7)}\right\}$ (14)	$\frac{V_{comp,nonlinear}}{V_{left/right,CEP}}\left\{\frac{(10)}{(7)/2}\right\}$ (15)
$t = t_{V\,pier,max}$	29676	1368	28308	0.95	1.40	2.66	2.22	4.24
	27962	1385	26577	0.95	1.08	2.05	1.81	3.45
	29186	321	28865	0.99	1.01	1.99	1.67	3.31
	33784	1184	32600	0.96	1.03	1.99	1.63	3.14
	36569	3552	33017	0.90	1.04	1.88	1.62	2.92
	40634	6334	34300	0.84	1.08	1.83	1.67	2.82
	41361	5816	35545	0.86	1.14	1.96	1.72	2.95
	49039	6183	42856	0.87	1.17	2.04	1.68	2.93
	55156	9654	45502	0.82	1.17	1.93	1.60	2.65

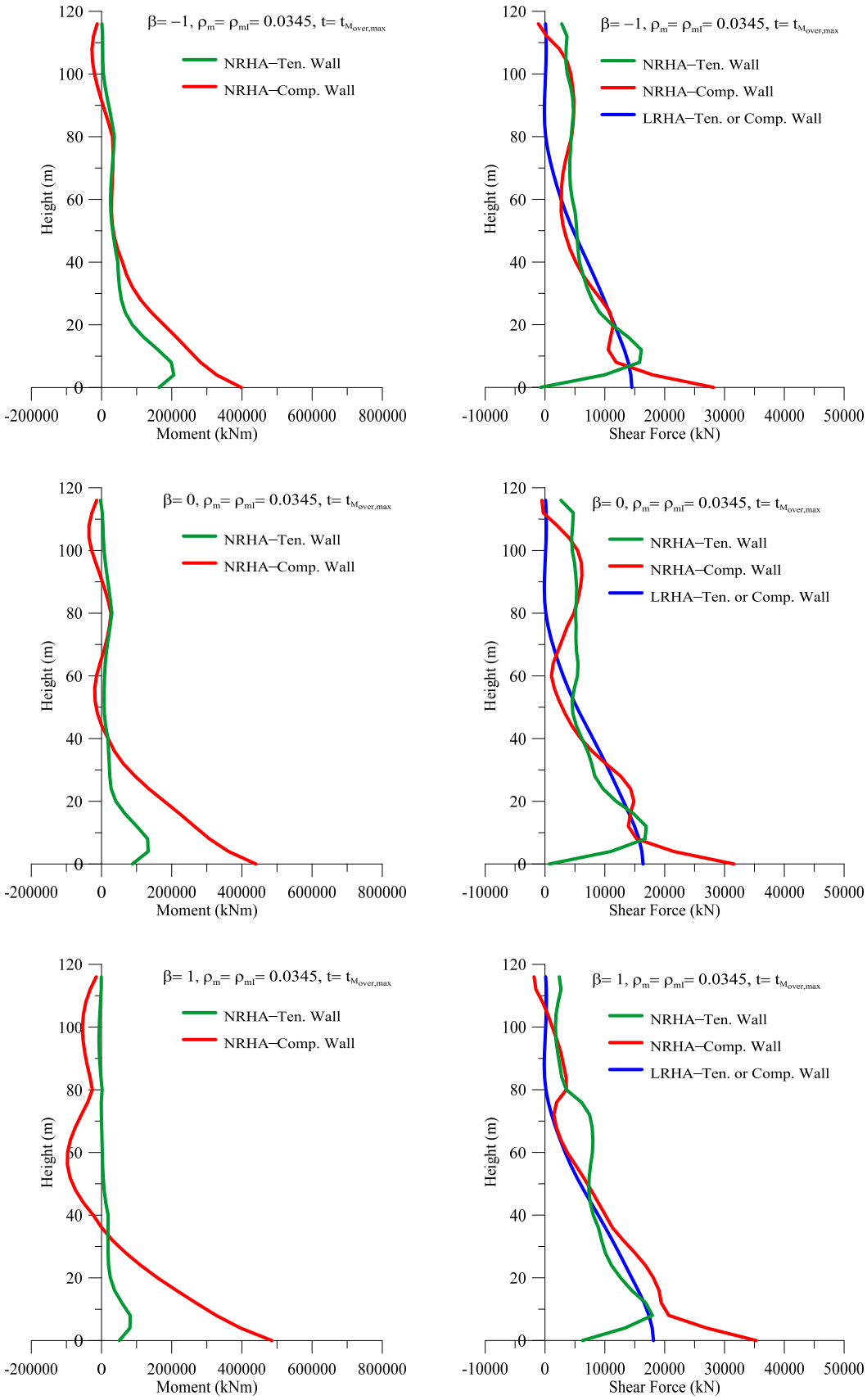

Figure 8.1. Moment and shear demands of walls for three levels of relative yield parameter β_1 and $\rho_m = \rho_{ml} = 0.0345$ at $t = t_{M_{o,max}}$ (CW12, $n_0 = 0.125$, Chi-Chi earthquake).

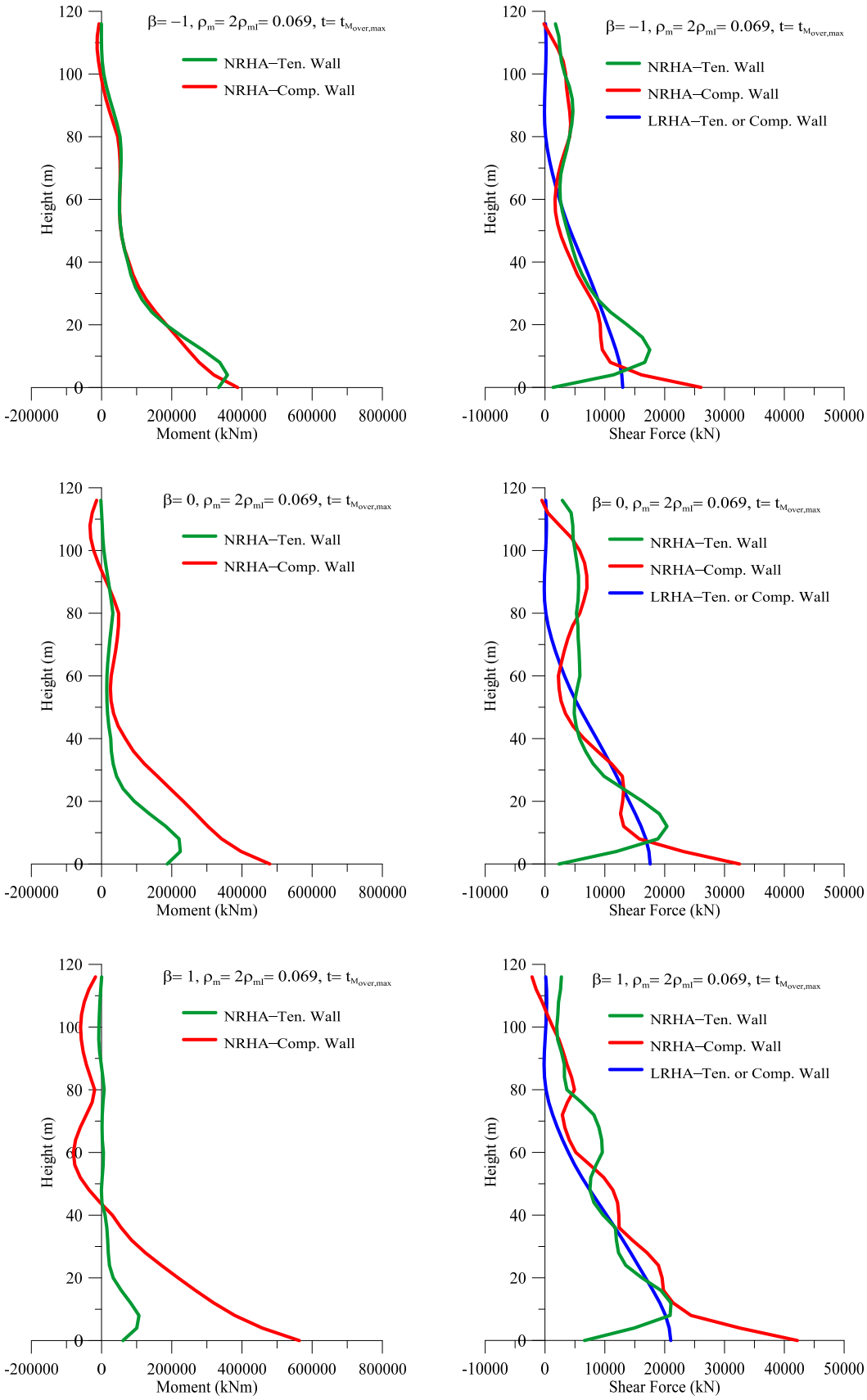

Figure 8.2. Moment and shear demands of walls for three levels of relative yield parameter β_1 and $\rho_m = 2\rho_{ml} = 0.069$ at $t = t_{M_{o,max}}$ (CW12, $n_0 = 0.125$, Chi-Chi earthquake).

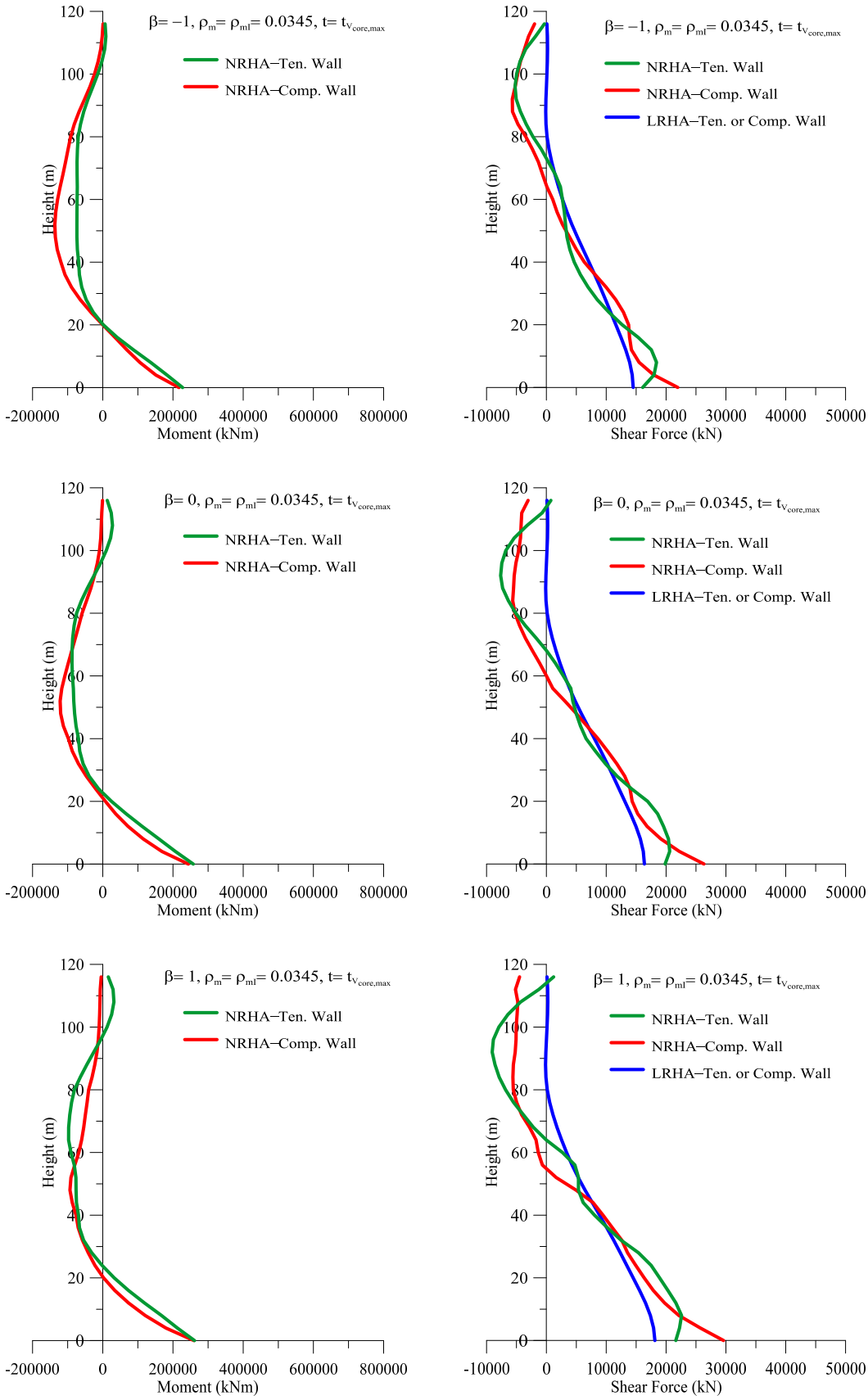

Figure 8.3. Moment and shear demands of walls for three levels of relative yield parameter β_1 and $\rho_m = \rho_{ml} = 0.0345$ at $t = t_{V_{core,max}}$ (CW12, $n_0 = 0.125$, Chi-Chi earthquake).

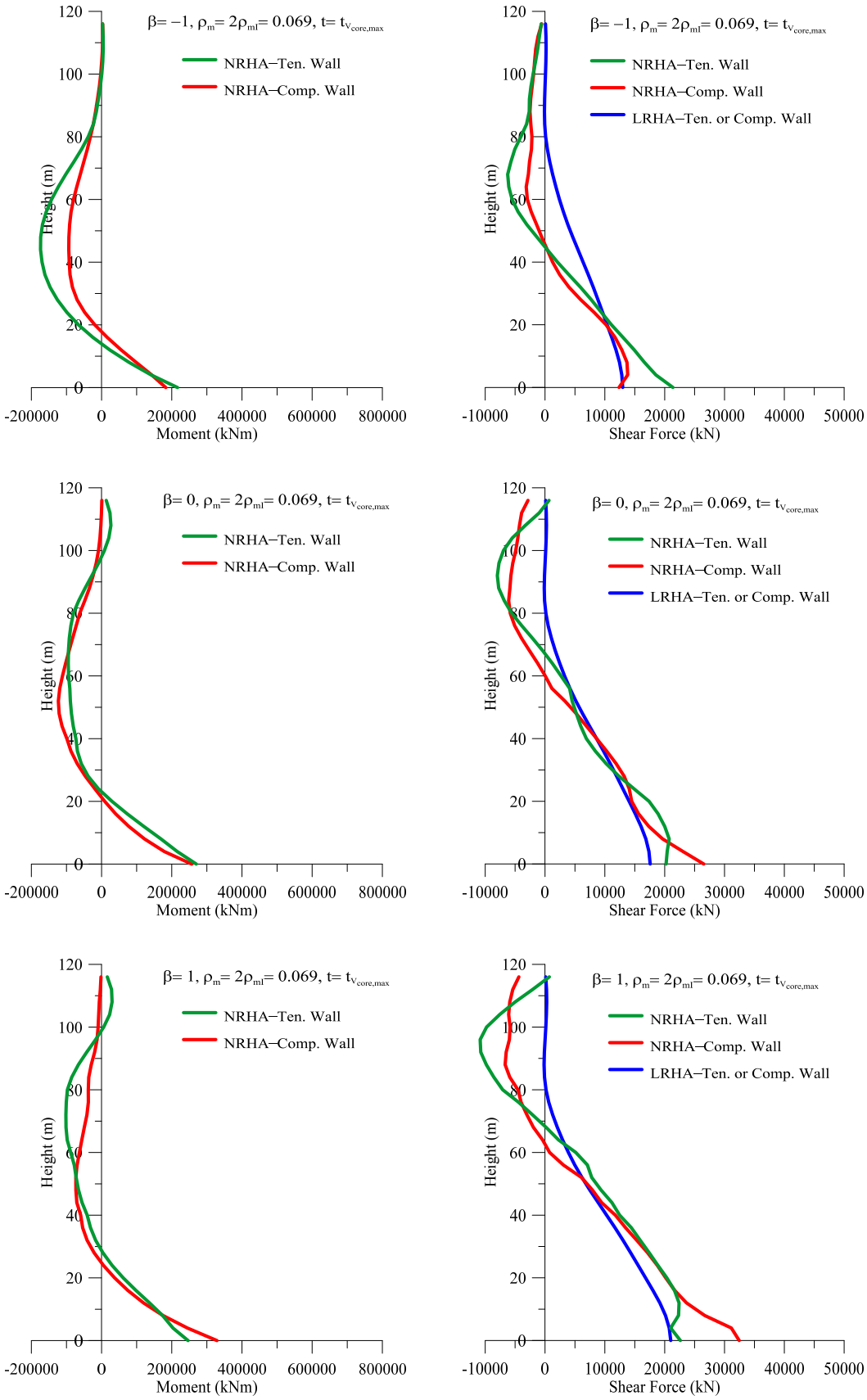

Figure 8.4. Moment and shear demands of walls for three levels of relative yield parameter β_1 and $\rho_m=2\rho_{ml}=0.069$ at $t = t_{V_{core,max}}$ (CW12, $n_0 = 0.125$, Chi-Chi earthquake).

9. CONCLUSIONS

Contemporary design guidelines for performance-based seismic design of tall buildings generally apply a two-stage performance evaluation process following the preliminary design. The two-stage performance evaluation includes a serviceability evaluation stage under the so-called service earthquake and a collapse level evaluation stage under the so-called maximum credible earthquake. In this methodology, preliminary design represents the critical phase of the tall building design in order to achieve acceptable performance levels in the subsequent performance evaluation stages. Therefore, preliminary sizing and reinforcing of structural elements are of major importance to limit the number of trial and errors that may be necessary in order to fulfill nonlinear deformation requirements. However, the guidelines recommend linear analysis methods for preliminary design stage, which may not correctly predict the internal force demands on structural members that would be developed during the nonlinear behavior. Although application of capacity design principles are suggested and ductile or capacity protected members are clearly defined, required strength for yielding actions cannot be correctly estimated by linear analysis.

Coupled core wall systems are one of the most commonly used structural systems in tall buildings. Linear analysis methods would most likely lead to an overdesign of coupling beams with inappropriate and heavily congested reinforcement requirements, which consequently may cause unacceptable level of nonlinear deformations in the coupled walls. In order to control the level of nonlinear deformations of walls, their dimensions and reinforcement may need to be increased. Eventually, design of the entire coupled core wall system may become unnecessarily conservative for deformation-controlled behavior. Moreover, linear analysis may result in underestimated shear demands for coupled walls by neglecting the internal force redistribution during nonlinear behavior, thus leading to under-design of coupled walls for force-controlled actions such as shear.

In an attempt to fill the gap in the preliminary design phase of the tall building design methodology, a simple but rational capacity estimation procedure is developed for coupled core wall systems as an alternative. The capacity estimation procedure is based on a simple

strength of materials approach and defines only three independent parameters to control the capacities of the individual walls and the coupling beams. These parameters are; the normalized gravity load of tension wall (n_0), the mechanical reinforcement ratio of tension wall (ρ_m) and the relative yield parameter of tension wall (β).

A parametric analysis is performed for the evaluation of effects of these three independent parameters. It is observed that for coupled core wall systems with $\supset$ shaped walls, higher values of wall gravity loads are found to be beneficial as long as concrete crushing is avoided. Note that axial load carrying capacity of flanged walls is very high when the flange is in compression and brittle compression failure cannot be developed unless extremely high levels of axial load act on compression wall. The parameters ρ_m and β affect the amount of total coupling shear, hence the total base overturning moment capacity of the coupled core wall system. Relative yield parameter is the measure of yielding of reinforcement in the tension wall. As an extreme limit, β can be equal to unity, which may not be a favorable case, since it corresponds to the full yielding of tension wall, resisting only tension forces with almost no moment capacity. Therefore, β must be smaller than unity, so that both the amount of tensile strains and the extent of yielding along the wall would be reduced. Note that the same amount of contribution to total coupling shear can be obtained by decreasing β and increasing ρ_m such that the amount of $\beta\rho_m$ is kept constant. Another important observation is that the contribution of $\beta\rho_m$ on total coupling shear is more pronounced for low axial gravity load levels.

Following the estimation of total base overturning moment by such a simple capacity estimation procedure, it needs to be checked whether it would be sufficient for the purpose of preliminary design. In order to achieve this, a ductility demand estimation procedure is developed, which is based on a novel application of the well-known pushover concept. This procedure allows the design engineer to easily estimate the overall ductility demand (μ) under the maximum considered earthquake and check whether it was acceptable for a viable design. Nonlinear response history analyses are performed for a typical maximum considered earthquake record in order to estimate the acceptable levels of ductility demands by controlling the acceptable strain capacities of walls and coupling beams.

Nonlinear response history analyses results showed that the walls tend to become uncoupled by decreasing the strength of coupling beams and tend to behave as two single cantilevers. Thus, tensile strain of walls at upper stories may increase beyond yield level, as well as the weak coupling beams are exposed to unacceptable level of tensile strains. Therefore, very low total base overturning moment capacity would be developed leading to an unacceptably high overall ductility demand. On the contrary, very strong coupling beams would lead to increasing tension strains in the tension wall, i.e., spreading of the yielding from the base to the upper parts and hence larger concrete cracking along the wall. It means that excessively high total base overturning moment capacity leading to very low overall ductility demand should also avoided as well. The nonlinear analyses showed that overall ductility demand of a typical coupled core wall system should be bounded within the limits of $2.5 \leq \mu \leq 3.5$.

In conclusion, total coupling shear capacity and total base overturning moment capacity of a coupled core wall system can be successfully estimated by the proposed capacity estimation procedure. The overall ductility demand can further be estimated by the proposed ductility demand estimation procedure in order to assess the adequacy of total base overturning moment capacity. Since capacity and ductility demand estimation procedures are very easy to implement and not time consuming, several trials can be made by changing the independent variables to reach an acceptable overall ductility level. In collapse level evaluation stage, designer may only need to fine-tune the reinforcement of walls and coupling beams based on nonlinear analysis results, in order to improve the inelastic behavior of walls and coupling beams. Nevertheless, the dimensions of coupling beams and walls would most likely need not to be revised.

Finally caution is expressed for the unique shear response characteristics of the structural walls in terms of dynamic shear amplification and dynamic shear migration, the latter of which is proved to be very critical for coupled core wall systems regarding the significant shear transfer (migration) from the yielding tension wall to the compression wall. The nonlinear analyses showed that shear demand on coupled walls calculated by linear mode-combination or mode-superposition methods needs to be amplified approximately by a factor of two because of dynamic shear migration effects. Effects of dynamic shear amplification due to higher mode effects remain limited compared to the

effects of dynamic shear migration. A preliminary estimation may also be made for the base shear demands of tension and compression walls by amplifying the first-mode base shear, which can be approximately calculated by the proposed capacity estimation procedure in terms of total base overturning moment. The approximate amplification factor accounting for the shear migration from the tension wall to the compression wall and the one for higher mode effects can be taken as 2 and 1.5, respectively.

Few suggestions can be made for future research on coupled core wall systems. In this study, the capacity and ductility demand estimation procedures are developed for the preliminary design of single-cell coupled core wall systems only. The same procedures can be extended to more complex systems, such as two-cell or three-cell coupled core wall systems, by appropriate modifications of equilibrium equations. Additionally, a more comprehensive parametric nonlinear response history analyses under a wider range of earthquake records can be performed for different types of coupled core wall systems.

REFERENCES

1. *Concrete Structures Standard, Part 1 – The Design of Concrete Structures, Part 2 – Commentary on the Design of Concrete Structures*, *NZS.3101*, Standards New Zealand, Wellington, New Zealand, 2006.

2. *National Building Code of Canada, Volume 1, Division B, Part 4: Structural Design*, Canadian Commission on Building and Fire Codes, National Research Council of Canada, Ottawa, Canada, 2005.

3. *Design of Concrete Structures, CSA A23.3-04*, Canadian Standards Association, Ontario, Canada, 2004.

4. *Eurocode 8: Design of Structures for Earthquake Resistance – Part 1: General Rules Seismic Actions and Rules for Buildings (EN1998-1)*, European Committee for Standardization, Brussels, Belgium, 2004.

5. *Deprem Bölgelerinde Yapılacak Binalar Hakkında Yönetmelik*, Ministry of Public Works and Settlement, Government of Republic of Turkey, 2007.

6. *FEMA P695: Quantification of Building Seismic Performance Factors,* prepared by Applied Technology Council (ATC), prepared for Federal Emergency Management Agency (FEMA), Washington, D.C., USA, 2009.

7. *Recommendations for the Seismic Design of Tall Buildings – A Consensus Document,* Council on Tall Buildings and Urban Habitat (CTBUH), Seismic Working Group, Illinois Institute of Technology, Chicago, USA, 2008.

8. *An Alternative Procedure for Seismic Analysis and Design of Tall Buildings Located in the Los Angeles Region,* Los Angeles Tall Buildings Structural Design Council (LATBSDC), Los Angeles, CA, USA, 2014.

9. *Recommended Administrative Bulletin on the Seismic Design and Review of Tall Buildings using Non-Prescriptive Procedures*, Structural Engineers Association of Northern California (SEAONC), Tall Buildings Task Group, San Francisco, CA, USA, 2007.

10. *Guidelines for Performance-Based Seismic Design of Tall Buildings*, Version 1.0. Pacific Earthquake Engineering Research Center, PEER Report 2010/05, Tall Buildings Initiative (TBI) Guidelines Working Group, Berkeley, CA, USA, 2010.

11. *PEER/ATC 72-1: Modeling and Acceptance Criteria for Seismic Design and Analysis of Tall Buildings,* Applied Technology Council (ATC), Building Seismic Safety Council (BSSC), National Institute of Building Sciences (NIBS), Federal Emergency Management Agency (FEMA), Pacific Earthquake Engineering Research Center (PEER), University of California, Berkeley, 2010.

12. *Requirements and Guidelines for the Seismic Design of New Tall Buildings using Non-Prescriptive Seismic-Design Procedures – Administrative Bulletin No. AB-083*, San Francisco Department of Building Inspection (SFDBI), San Francisco, CA, USA, 2014.

13. *Istanbul Seismic Design Code For Tall Buildings – Draft Version IV*, Istanbul Metropolitan Municipality (IMM), Istanbul, Turkey, 2008.

14. Aydınoğlu, M. N., "Draft Seismic Design Code for Tall Buildings in Istanbul Metropolitan Area", *U.S.-Iran-Turkey Seismic Workshop on Seismic Risk Management in Urban Areas – December 14-16, 2010*, İstanbul, Turkey, PEER Report 2011/07, pp.55-63, 2011.

15. Aydınoğlu, M. N., "Challenges and Problems in Performance – Based Design of Tall Buildings", *Performance-Based Seismic Engineering: Vision for an Earthquake Resilient Society , Proc. International Workshop in Bled, Slovenia, 2011,* Chapter 20, pp. 279-300, Springer, 2014.

16. Aydınoğlu, M. N., "An Incremental Response Spectrum Analysis Based on Inelastic Spectral Displacement for Multi-mode Seismic Performance Evaluation." *Bulletin of Earthquake Engineering*, Vol 1, pp. 3-36, 2003.

17. Aydınoğlu, M. N., "An Improved Pushover Procedure for Engineering Practice: Incremental Response Spectrum Analysis (IRSA)", *International Workshop on "Performance-based Seismic Design: Concepts and Implementation"*, Bled, Slovenia, PEER Report 2004/05 , pp. 345-356, 2004.

18. Aydınoğlu, M. N. and G. Önem, "Evaluation of Analysis Procedures for Seismic Assessment and Retrofit Design", *Earthquake Engineering in Europe,* Chapter 8, Springer, 2010.

19. Rutenberg, A, "Seismic Shear Forces on RC Walls: Review and Bibliography" *Bulletin of Earthquake Engineering*, Vol 11, pp. 1727-1751, 2013.

20. Paulay, T., *Coupling Beams of Reinforced Concrete Shear Walls*, Ph. D. Thesis, University of Canterbury, 1969.

21. Paulay, T. and M. J. N. Priestley, *Seismic Design of Reinforced Concrete and Masonry Buildings*, John Wiley and Sons, Inc., New York, USA, 1992.

22. Celep, U., *Dynamic Shear Amplification in Seismic Response of Structural Wall Systems*, Ph. D. Thesis, Boğaziçi University, Kandilli Observatory and Earthquake Research Institute, 2008.

23. Coull, A. and S. B. Stafford, "Analysis of Shear Wall Structures", *Symposium on Tall Buildings with Particular Reference to Shear Wall Structures*, *University of Southampton, April 1966*, Oxford, Pergamon Press, pp. 139-155, 1967.

24. Barnard, P. R. and J. Schwaighofer, "The Interaction of Shear Walls Connected Solely Through Slabs", *Symposium on Tall Buildings with Particular Reference to Shear*

Wall Structures, University of Southampton, April 1966, Oxford, Pergamon Press, pp. 157-173, 1967.

25. Macleod, I. A., "Lateral Stiffness of Shear Walls with Openings", *Symposium on Tall Buildings with Particular Reference to Shear Wall Structures*, *University of Southampton, April 1966*, Oxford, Pergamon Press, pp. 223-244, 1967.

26. Binney, J. R., *Diagonally Reinforced Coupling Beams*, Ph. D. Thesis, University of Canterbury, 1972.

27. Paulay, T. and J. R. Binney, "Diagonally Reinforced Coupling Beams", *Shear in Reinforced Concrete, American Concrete Institute (ACI)*, Publication No: SP-42, pp. 579-598, 1974.

28. Santhakumar, A. R., *Ductility of Coupled Shear Walls*, Ph. D. Thesis, University of Canterbury, 1974.

29. Paulay, T. and A. R. Santhakumar, "Ductile Behavior of Coupled Shear Walls", *Journal of Structural Division, American Society of Civil Engineers (ASCE)*, Vol.102 (ST1), pp. 93-108, 1976.

30. Mahin, S. A. and V. V. Bertero, "Nonlinear Seismic Response of Coupled Wall System", *Journal of Structural Division, American Society of Civil Engineers (ASCE)*, Vol.102 (ST9), pp. 1759-1780, 1976.

31. Aristizabal-Ochoa, J. D. and M. A. Sozen, "Behavior of Ten-Story Reinforced Concrete Walls Subjected to Earthquake Motions", *Civil Engineering Studies*, SRS No. 431, University of Illinois, Urbana Champaign, 1976.

32. Takayanagi, T., *Computed Behavior of Coupled Shear Walls*, Ph. D. Thesis, University of Illinois, Urbana Champaign, 1977.

33. Takayanagi, T. and W. C. Schnobrich, "Nonlinear Analysis of Coupled Wall Systems", *Earthquake Engineering and Structural Dynamics*, Vol. 7, pp. 1-22, 1979.

34. Takayanagi, T., A. T. Derecho, and W. G. Corley, "Analysis of Inelastic Shear Deformation Effects in Reinforced Concrete Structural Wall Systems", *CSCE-ASCE-ACI-CEB, International Symposium on Nonlinear Design of Concrete Structures*, University of Waterloo, Ontario, Canada, 1979.

35. Kanaan, A. E. and G. H. Powell, "DRAIN-2D: A General Purpose Computer Program for Dynamic Analysis of Inelastic Plane Structures", *Earthquake Engineering Research Center,* Report No. UCB/EERC 73-6, University of California, Berkeley, 1975.

36. Lybas, J. M. and M. A. Sozen, "Effect of Beam Strength and Stiffness on Dynamic Behavior of Reinforced Concrete Coupled Walls", *Civil Engineering Studies,* SRS No. 444, University of Illinois, Urbana Champaign, 1977.

37. Saatçioğlu, M, *Inelastic Behavior and Design of Earthquake Resistant Coupled Walls*, Ph. D. Thesis, Northwestern University, 1981.

38. Saatçioğlu, M., A. T. Derecho, and W. G. Corley, "Coupled Walls in Earthquake-Resistant Buildings", *Report to National Science Foundation by Construction Technology Laboratories,* Portland Cement Association, Illinois, USA, 1980.

39. Saatcioglu, M., A. T. Derecho, and W. G. Corley, "Modeling Hysteretic Behavior of Coupled Walls for Dynamic Analysis", *Earthquake Engineering and Structural Dynamics*, Vol. 11, pp. 711-726, 1983.

40. Saatcioglu, M., A. T. Derecho, and W. G. Corley, "Parametric Study of Earthquake-Resistant Coupled Walls", *Journal of Structural Engineering, American Society of Civil Engineers (ASCE)*, Vol.113, No.1, pp. 141-150, 1987.

41. Barney, G. B., K. N. Shiu, B. G. Rabbat, A. E. Fiorato, H. G. Russel, and W. G. Corley, "Behavior of Coupling Beams Under Load Reversals", *Research and Development Bulletin RD068.01B.*, Portland Cement Association, Illinois, USA, 1980.

42. Aktan, A. E. and V. V. Bertero, "The Seismic Resistant Design of RC Coupled Structural Walls", *Earthquake Engineering Research Center*, Report No. UCB/EERC-81/07, University of California, Berkeley, 1981.

43. Aktan, A. E., V. V. Bertero, and M. Piazza, "Prediction of the Seismic Responses of RC Frame-Coupled Wall Structures", *Earthquake Engineering Research Center*, Report No. UCB/EERC-82/06, University of California, Berkeley, 1982.

44. Ozselcuk, A., *Experimental and Analytical Studies of Coupled Wall Structures*, Ph. D. Thesis, University of California, Berkeley, 1990.

45. Shiu, N. K., T. Takayanagi, and W. G. Corley, "Seismic Behavior of Coupled Wall Systems", *Journal of Structural Engineering, American Society of Civil Engineers (ASCE)*, Vol.110, No.5, pp. 1051-1066, 1984.

46. Keshavarzian, M. and W. C. Schnobrich, "Analytical Models for the Nonlinear Seismic Analysis of Reinforced Concrete Structures", *Engineering Structures*, Vol.7, No.2, pp.131-142, 1985.

47. Keshavarzian, M. and W. C. Schnobrich, "Computed Nonlinear Seismic Response of RC Wall-Frame Structures", *Civil Engineering Studies,* SRS No. 515, University of Illinois, Urbana Champaign, 1984.

48. Tassios, T. P., M. Moretti, and A. Bezas, "On the Behavior of Reinforced Concrete Coupling Beams of Shear Walls", *Structural Journal, American Concrete Institute (ACI)*, Vol.93, No.6, pp. 711-720, 1996.

49. Harries, K. A., D. Mitchell, R. G. Redwood, and W. D. Cook, "Seismic Design of Coupling Beams – A Case for Mixed Construction", *Canadian Journal of Civil Engineering*, Vol.24, No.3, pp.448-459, 1997.

50. Harries, K. A., D. Mitchell, R. G. Redwood, and W. D. Cook, "Nonlinear Seismic Response Predictions of Walls Coupled With Steel and Concrete Beams", *Canadian Journal of Civil Engineering*, Vol.25, No.5, pp.803-818, 1998.

51. Galano, L. and A. Vignoli, "Seismic Behavior of Short Coupling Beams with Different Reinforcement Layouts", *Structural Journal, American Concrete Institute (ACI)*, Vol.97, No.6, pp. 876-885, 2000.

52. Shen, Q. and Y. C. Kurama, "Nonlinear Behavior of Posttensioned Hybrid Coupled Wall Subassemblages", *Journal of Structural Engineering, American Society of Civil Engineers (ASCE)*, Vol.128, No.10, pp. 1290-1300, 2002.

53. Hindi, R. and M. Hassan, "Shear Capacity of Diagonally Reinforced Coupling Beams", *Engineering Structures*, Vol.26, No.10, pp.822-826, 2004.

54. Zhao, Z. Z., A. K. H. Kwan, and X. G. He, "Nonlinear Finite Element Analysis of Deep Reinforced Concrete Coupled Beams", *Engineering Structures*, Vol.26, pp. 13-25, 2004.

55. Brena, S., M. F. Ruiz, N. Kostic, and A. Muttoni, "Modeling Techniques to Capture the Backbone Envelope Behavior of Coupling Beams Subjected to Seismic Loading", *Studies and Researches*, Vol. 29, Graduate School in Concrete Structures – Fratelli Pesenti, Politechnico di Milano, Milano, 2009.

56. Mohr, D., D. Lehman, and L. Lowes, "Performance Based Design and Nonlinear Modeling of Coupled Shear Walls and Coupling Beams", *Structures Congress 2007: New Horizons and Better Practices*, *American Society of Civil Engineers (ASCE)*, 2007.

57. Bower, O. J. and G. A. Rassati, "Axial Restraint in Diagonally Reinforced Coupling Beams: An Analytical Investigation", *Structures Congress 2008: Crossing Borders*, *American Society of Civil Engineers (ASCE)*, 2008.

58. El-Tawil, S., C. M. Kuenzli, and M. Hassan, "Pushover of Hybrid Coupled Walls. I: Design and Modeling", *Journal of Structural Engineering, American Society of Civil Engineers (ASCE)*, Vol.128, No.10, pp. 1272-1281, 2002.

59. El-Tawil, S. and C. M. Kuenzli, "Pushover of Hybrid Coupled Walls. II: Analysis and Behavior", *Journal of Structural Engineering, American Society of Civil Engineers (ASCE)*, Vol.128, No.10, pp. 1282-1289, 2002.

60. *User's Manual - DIANA Version 7*, DIANA Analysis, P.O. Box 113, 2600 AC Delft, Netherlands, 2000.

61. Hassan, M. and S. El-Tawil, "Inelastic Dynamic Behavior of Hybrid Coupled Walls", *Journal of Structural Engineering, American Society of Civil Engineers (ASCE)*, Vol.130, No.2, pp. 285-296, 2004.

62. Naish, D., J. A. Fry, R. Klemencic, and J. W. Wallace, "Experimental Evaluation and Analytical Modeling of ACI 318-05/08 Reinforced Concrete Coupling Beams Subjected to Reversed Cyclic Loading", *UCLA-SGEL Report 2009/06*, University of California, Los Angeles, 2009.

63. Barbachyn S. M., Y. C. Kurama, and L. Novak, "Analytical Evaluation of Diagonally Reinforced Concrete Coupling Beams under Lateral Loads", *Structural Journal, American Concrete Institute (ACI)*, Vol.109, No.4, pp. 497-507, 2012.

64. *DRAIN-2DX Base Program Description and User Guide*, Prakash, V., G. A. Powell, and S. Campbell, University of California, Berkeley, California, 1993.

65. Deierlein, G. G., A. M. Reinhorn, and M. R. Willford, "Nonlinear Structural Analysis For Seismic Design – National Earthquake Hazards Reduction Program (NEHRP)

Seismic Design Technical Brief No. 4., NIST GCR 10-917-5", *National Institute of Standards and Technology*, U.S. Department of Commerce, USA, 2010.

66. Taucer, F. F., E. Spacone, and F. C. Filippou, "A Fiber Beam-Column Element for Seismic Response Analysis of Reinforced Concrete Structures", *Earthquake Engineering Research Center*, Report No. UCB/EERC-91/17, University of California, Berkeley, 1991.

67. Orakcal, K., L. M. Massone, and J. W. Wallace, "Analytical Modeling of Reinforced Concrete Walls for Predicting Flexural and Coupled – Shear – Flexural Responses", *Pacific Earthquake Engineering Research Center (PEER)*, PEER Report 2006/07, University of California, Berkeley, 2006.

68. Vulcano, A., "Macroscopic Modeling for Nonlinear Analysis of Reinforced Concrete Structural Walls", In H. Krawinkler and P. Fajfar (eds.): *Nonlinear Seismic Analysis of RC Buildings*, Elsevier, pp. 181-190, 1992.

69. Kabeyasawa, T., H. Shioara, and S. Otani, "U.S. - Japan Cooperative Research on RC Full-scale Building Test – Part 5: Discussion on Dynamic Response of System", *Proceedings of 8th World Conference of Earthquake Engineering (WCEE)*, Vol. 6, 1984.

70. Menegotto, M. and E. Pinto, "Method of Analysis for Cyclically Loaded Reinforced Concrete Plane Frames Including Changes in Geometry and Non-elastic Behavior of Elements Under Combined Normal Force and Bending", *Proceedings of International Association of Bridge and Structural Engineering (IABSE) Symposium*, Vol. 13, pp. 15-22, Lisbon, Portugal, 1973.

71. Chang, G. A. and J. B. Mander, "Seismic Energy Based Fatigue Damage Analysis of Bridge Columns: Part 1 – Evaluation of Seismic Capacity", *NCEER Technical Report No. NCEER-94-0006*, State University of New York, Buffalo, 1994.

72. Massone, L. M. and J. W. Wallace, "Load-Deformation Responses of Slender Reinforced Concrete Walls", *Structural Journal, American Concrete Institute (ACI)*, Vol.101, No.1, pp. 103-113, 2004.

73. Massone, L. M., *RC Wall Shear – Flexure Interaction: Analytical and Experimental Responses*, Ph. D. Thesis, University of California, Los Angeles, 2006.

74. Kolozvari, K., T. Tran, J. W. Wallace, and K. Orakcal, "Modeling of Cyclic Shear-Flexure Interaction in Reinforced Concrete Structural Walls", *Proceedings of 15th World Conference of Earthquake Engineering (WCEE)*, 2012.

75. Fischinger, M., K. Rejec, and T. Isakovic, "Modeling Inelastic Shear Response of RC Walls", *Proceedings of 15th World Conference of Earthquake Engineering (WCEE)*, 2012.

76. Computers and Structures Inc., "Perform 3D, Nonlinear Analysis and Performance Assessment for 3D Structures – Version 5", *Computers and Structures, Inc.*, Berkeley, California, 2011.

77. Thomsen, J. H. and J. W. Wallace, "Displacement-based Design of Reinforced Concrete Structural Walls: An Experimental Investigation of Walls With Rectangular and T-shaped Cross Sections", *Department of Civil Engineering, Clarkson University*, Report No. CU/CEE – 95/06, Postdam, New York, 1995.

78. Powell, G. H. "Detailed Example of a Tall Shear Wall Building, Using CSI's PERFORM-3D Nonlinear Dynamic Analysis", Nonlinear Modeling, Analysis and Performance Assessment for Earthquake Loads, *Computers and Structures Inc.*, Berkeley, California, USA, 2007.

79. Lehman, D. E., J. A. Turgeon, A. C. Birely, C. R. Hart, K. P. Marley, D. A. Kuchma, and L. N. Lowes, "Seismic Behavior of Modern Concrete Coupled Wall", *Journal of Structural Engineering, American Society of Civil Engineers (ASCE)*, Vol.139, Special Issue, pp. 1371-1381, 2013.

80. Turgeon, J. A., *The Seismic Performance of Coupled Reinforced Concrete Walls*, M.S. Thesis, University of Washington, Seattle, 2011.